

STRUCTURE-STUDIES OF VAPOUR PHASE DEPOSITS

BY ELECTRON DIFFRACTION

**COMPUTERISED**

A THESIS  
SUBMITTED TO  
THE UNIVERSITY OF POONA  
FOR THE DEGREE OF  
DOCTOR OF PHILOSOPHY  
IN CHEMISTRY

539.234:621.385.833(043)

TH-318

GAD

by

L. H. GADGIL, M.Sc.,  
National Chemical Laboratory,  
Poona-8, India.

DECEMBER 1968

### ACKNOWLEDGEMENTS

I am highly indebted to Dr. A. Goswami for his keen interest and helpful guidance during the course of the present work.

I feel great pleasure in offering my sincere thanks to the Director, National Chemical Laboratory, Poona-8, for granting me a permission to carry research, as a guest-worker and to submit the work in the form of a thesis.

I am also grateful to the Principal and to the Head of the Chemistry Department, Sir Parshurambhau College, Poona-9, for giving me all possible facilities in my job as a Lecturer, which enabled me to complete this work.

I shall be failing in my duty if I do not thank my colleagues, at the Electron Diffraction Section, National Chemical Laboratory, for their kind and hearty cooperation.

Poona,  
December 1968.

(L.H. GADGIL)

## C O N T E N T S

	Page
<u>CHAPTER I</u> : <u>GENERAL INTRODUCTION</u>	1-11
<u>CHAPTER II</u> : <u>EXPERIMENTAL TECHNIQUE</u>	12-18
<u>CHAPTER III</u> : <u>STRUCTURE AND GROWTH OF BISMUTH AND ANTIMONY FILMS</u>	19-51
A. Introduction	
(a) Bismuth	19
(b) Antimony	21
B. Experimental	23
C. Results	
(a) Deposition of Bismuth	
(i) On collodion and on polycrystalline sodium chloride	24
(ii) On glass	25
(iii) On (100) face of rock salt	25
(iv) On (110) face of rock salt	32
(V) On (111) face of rock salt	34
(vi) On cleaved face of mica	35
(b) Deposition of Antimony	36
(1) On collodion and polycrystalline sodium chloride	37
(ii) On glass	38

continued...

	Page
(iii) On (100) face of rock salt	41
(iv) On (110) face of rock salt	43
(v) On (111) face of rock salt	43
(vi) On cleaved face of mica	44
D. Discussion	44
 <u>CHAPTER IV : STUDIES ON THE SUBOXIDE OF BISMUTH (BiO)</u>	52-61
A. Introduction	52
B. Experimental	53
C. Results	
(a) On Collodion by Fine Powder Method	55
(b) Deposition of Bismuth Suboxide From Vapour Phase	
(1) On collodion	55
(11) On (100) face of rock salt	57
(iii) On (110) face of rock salt	57
(iv) On cleaved face of mica	56
D. Discussion	59

continued...

	Page
<u>CHAPTER V</u> : <u>STRUCTURE AND GROWTH OF OXIDE-FILM- OF BISMUTH</u>	62-86

PART-1 : OXIDATION OF BISMUTH FILMS

A. Introduction	62
B. Experimental	63
C. Results	64
(1) On Collodion	
(a) Oxidation at atmospheric pressure	65
(b) Oxidation under reduced pressure	65
(c) Oxidation at very low pressure	67
(ii) On (100) Face of Rock Salt	
(a) Oxidation at atmospheric pressure	68
(b) Oxidation at reduced pressure	68
(c) Oxidation at very low pressure	69
(iii) On (110) Face of Rock Salt	69
(iv) On (111) Face of Rock Salt	70
(v) Vacuum Treatment of Bi <sub>2</sub> O <sub>3</sub>	70
(vi) Oxidation of bismuth during deposition	71

PART-2 : OXIDATION OF ANTHONY FILMS

A. Introduction	72
B. Experimental	74

continued..

	Page
C. Results	
(i) On Collodion	
(a) Oxidation at atmospheric pressure	75
(b) Oxidation at low pressure	75
(ii) On (100) Face of Rock Salt	
(a) Oxidation at atmospheric pressure	76
(b) Oxidation at reduced pressure	77
(iii) Oxidation of antimony during deposition	
(a) On (100) Face of rock salt	78
(b) On (110) face of rock salt	79
(c) On (111) face of rock salt	80
(iv) Existence of Suboxide of Antimony	80
Discussion	81
<u>CHAPTER VI : BISMUTH-ANTIMONY SYSTEM (Bi-Sb)</u>	87-97
A, Introduction	87
B. Experimental	
(i) Preparation of the alloy	88
(ii) Deposition of the alloy films	89

continued...

	Page
C. Results	
(1) On Collodion and Poly-crystalline sodium chloride	89
(ii) On Glass	90
(iii) On (100) Face of Rock Salt	90
(iv) On (110) Face of Rock Salt	93
(v) On (111) Face of Rock Salt	94
(vi) On Cleaved Face of Mica	95
D. Discussion	95
 <u>CHAPTER VII</u> : <u>STRUCTURE AND CRYSTAL GROWTH OF ANTIMONY TELLURIDE AND ANTIMONY-SELENIDE</u>	98-113
A. Introduction	98
B. Experimental	
(i) Preparation of Sb <sub>2</sub> Te <sub>3</sub> and Sb <sub>2</sub> Se <sub>3</sub>	100
(ii) Deposition of Sb <sub>2</sub> Te <sub>3</sub> and Sb <sub>2</sub> Se <sub>3</sub> films	101
C. Results:	
<u>PART-1</u> : <u>ANTIMONY TELLURIDE</u>	
(i) On Collodion	102
(ii) On Glass	102
(iii) On (100) Face of Rock Salt	103
(iv) On (110) Face of Rock Salt	105
(v) On (111) Face of Rock Salt	106
(vi) On Cleaved Face of Mica	100

continued...

PART-2 : ANTIMONY SELERIDE

(i) On Collodion and on Polycrystalline sodium chloride	108
(ii) On Glass	108
(iii) On (100) Face of Rock Salt	109
(iv) On (110) Face of Rock Salt	111
(v) On (111) Face of Rock Salt	112
(vi) On Cleavage Face of Mica	113
D. Discussion	115
<u>SUMMARY AND CONCLUSIONS</u>	119-123
<u>REFERENCES</u>	124-131



## CHAPTER - I

### GENERAL INTRODUCTION.

The importance of vacuum deposited films in research as well as in industry has been well recognised for some time past. In recent times the applications of these films in diversified fields such as reflectors, antireflection coatings, paper capacitors, solid state devices, printed circuits, microminiaturisation, decorative finishes on plastics and textiles etc. have led to more detailed studies of these films from practical as well as fundamental point of view. Recently these thin film-devices have become essential components in space flight techniques. All these uses of thin films have given a new impetus to the study of their structural properties.

It is well known that the properties of thin films and of surface layers differ considerably from those of the bulk material. Many of the properties such as thermionic emission, adsorption catalysis etc. are characteristic of surface layers. Even a thin metal film can exhibit semi-conducting properties, whereas the bulk is metallic in character. As many of the physical properties are structure sensitive, it is of great importance to study the structure of thin films, development of their orientations, crystal growth process, phase transition etc. to correlate them with optical, electrical and other properties. Further,

it is known that by vacuum deposition a wide variety from disordered or amorphous state to highly ordered single crystal form can be obtained in thin film state by an appropriate control of the substrate temperature, the rate of evaporation, the vacuum conditions etc. Single crystal films of any desired size, shape and orientation can also be prepared by the epitaxial growth, using suitable single crystal substrates and controlling the deposition process under appropriate vacuum conditions.

Most of the solids can be classified into two categories namely crystalline or non-crystalline (amorphous). In the crystalline form a material can also exist in single crystal state or polycrystalline state with or without a preferred orientation. In a single crystal, atoms or ions are arranged regularly in three dimensions. Each repeating unit known as a unit cell, is characterised by three different cell dimensions as well as three angles. Depending on the crystal system these dimensions or angles can be equal or different or partly so thus leading to innumerable unit cells. Despite of these different cell dimensions it has been possible to divide these crystals into definite space groups and point group symmetries, thus leading to a systematisation in the crystal structure. It has been found that elements belonging to a particular group of the periodic table generally have similar structures. Same is the case of binary compounds where the nature of the binding force between the elements are also similar. Amorphous materials

have no such regular arrangement of atoms or ions, and these behave as supercooled liquids, when considered from structural point of view.

A historical outline of the study of crystal structure can broadly be summarized as follows:

- |   |   |  |
|---|---|--|
| 1597 - Libavius                                 | : | Identification of salts in mineral waters by crystal shapes.                           |
| 1669 - Steno                                    | : | Constancy of interfacial angles in crystals of one substance.                          |
| 1670 - Bartholinus                              | : | Cleavage and double refraction of calcite.   |
| 1690 - Huygens                                  | : | Polarisation of light by crystals.   |
| 1772 - de Lisle                                 | : | Accurate measurement of crystal angles and their characteristic values for substances. |
| 1782 - Haüy                                     | : | Constructibility of crystals from elementary building blocks, the six crystal systems. |
| 1803 - Black                                    | : | On latent heat of melting.   |
| 1808 - Widmannstätten                           | : | Etch figures on meteoric iron.   |
| 1811 - Arago                                    | : | Rotation of the plane of polarisation of light in quartz.                              |
| 1818 - Brewster                                 | : | Relation between optical properties and symmetry.                                      |
| 1819 - Mitscherlich                             | : | Isomorphism and polymorphism.  |
| 1830 - Hessel                                   | : | The thirty two crystal classes.  |
| 1880 - Curie                                    | : | Piezoelectric effect.  |
| 1912 - Laue                                     | : | X-ray diffraction by crystals.   |
| 1927 - Davisson &<br>1928 - Germer;<br>Thomson. | : | Electron diffraction by thin films.  |

The discovery of the phenomenon of diffraction of X-rays by crystal lattice (Friedrich, Knipping and Laue 1912), for the first time showed that atoms or ions are regularly arranged in a crystal lattice. Since then X-ray diffraction technique has become an important tool in the hands of scientists to determine the structure of solids, thus leading to the foundation of a new science of X-ray crystallography. Despite of the great advantage of this new technique for bulk structure determination, it has become quite ineffective for structures of thin films as well as of surface layers.

The diffraction of electrons by crystal lattice was observed almost simultaneously both by Davison and Germer (1927) and by Thomson (1928). Since then electron diffraction technique has become a versatile tool and been advantageously used by many workers to elucidate the structures of thin films and of surface layers (Finch and Wilman, 1937; Thomson and Cochrane, 1939; Raether 1951, 1957; Pinsker, 1953; Cowley and Rees, 1958; Vainshtein, 1964).

X-rays are scattered by electron shells of the atoms and a picture of the electron density distribution within the crystal can be obtained by the Fourier analysis of the experimental data, the peak in the electron density map corresponding to the atoms of the crystal lattice. In the Fourier treatment of electron diffraction data also, the maxima in the potential distribution maps coincide with the nuclei. Scattering of X-rays by atoms is approximately

proportional to the atomic number and hence light atoms in the presence of heavy atoms present difficulties in resolving. In the case of electrons the scattering amplitude is less dependent on the atomic number and hence lighter atoms are easily resolved. The average absolute magnitude of the atomic amplitude of scattering for X-rays is about  $10^{-11}$  cm. and that for electrons is about  $10^{-8}$  cm. and hence the intensities of scattered waves of X-rays and of electrons are about  $1:10^6$ . In the case of X-ray comparatively thicker samples of about 0.1 to 1 mm. are necessary to get sharp and clear diffraction patterns, whilst for electron diffraction the thickness of about  $10^{-4}$  to  $10^{-5}$  mm. is sufficient. The thickness is however limited by the increase of effects due to inelastic and incoherent scattering, secondary scattering etc. Electrons with accelerating voltage of about 50 to 65 KV can penetrate films of a few hundred angstroms thickness, depending on the atomic weight of the constituent atoms of the material. During this process electrons do not lose appreciable amount of energy and hence the scattering is elastic and coherent.

Electron diffraction technique can be employed both by transmission as well as by reflection methods. In the case of a study by reflection, a surface layer of a thickness of 5 to  $10 \text{ \AA}$  is good enough to yield sharp patterns. Transmission examination brings forth information which is characteristic of the total thickness and hence provides a

knowledge of the deposit as a whole. Since during the growth of a crystal, often many changes such as phase transformation, orientation and ordered state of the crystal may take place. It is possible to investigate them by using both reflection and transmission techniques. The later method gives the overall picture of the growth state, whereas former only of the surface layers. Temperature sensitiveness of the deposit structure can also be revealed by the electron diffraction studies at different temperatures. Thus electron diffraction technique can be profitably employed for studying any changes associated with the growth process of vacuum deposits, anodic or cathodic deposits, solid-liquid or solid-gas reaction products and in many other wide fields.

### Crystal Growth

In an ideal crystal, atoms or ions occupy the minimum potential energy configuration. Due to the action of the inter atomic forces the atoms or ions are clustered together to pack themselves closely, thus forming a three dimensional pattern. The crystal grows atom by atom, layer by layer, though the growth of succeeding layers may generally start before a layer is completed. Each atom or ion as it deposits on the surface of the crystal, takes up a position comparable in terms of potential energy, with the surrounding conditions. The sites of the deposited atoms or ions are then principally determined by the positions of atoms or ions in the initial surface and subsequently by the positions of the atoms or ions in the surface of the crystal. The nuclei thus formed over the substrate surface begin to grow and the further growth of the film, in general, is no longer

directly influenced by the substrate. Since the growth takes place simultaneously either on the same or different layers, the atoms at the junction are not in their maximum stability conditions, thus giving rise to crystal defects such as dislocations, stacking faults, twinning and rotational slip etc.

Gibbs (1878) on thermodynamical ground suggested the first quantitative theory of the crystal growth process. Curie (1885) and Wulff and others followed it. The atomic theory of crystal growth has been developed by many workers (Kossel, 1927, 1928; Volmer, 1939; Stranski, 1928, 1949; Beker and Doring, 1935, 1949; and Frenkel, 1945, 1946). Later on by taking into consideration the presence of imperfections and dislocations, Burton and Cabrera (1949), Burton, Cabrera and Frank (1951) developed the dislocation theory of crystal growth. Most recently Hirth, Hruska and Pounds (1964), Rhodin and Walton (1964), Bauer (1964) and van der Merwe (1964) and others have discussed the theories for vapour phase deposits of thin films, their initial nucleation, growth process and effects of interfacial misfits etc.

The presence of impurities during the growth of a crystal may considerably modify the morphology of it. This is illustrated by the growth of sodium chloride crystals which are cubic in nature if grown from a neutral solution.

But in the presence of a little urea octahedral crystals are formed whilst a little of gum-arabic causes dendritic growth of crystals. In all these cases, however, the atomic arrangement in the crystals remains the same.

### Epitaxy

The term epitaxy was used first by Royer (1928) to signify the oriented over-growth of a crystal over another. An epitaxial growth on a crystalline substrate means the formation of a single crystal film, the crystal lattice of which has a definite orientation relationship with respect to that of the substrate. Such a growth of films over another substance is known as oriented over-growth or epitaxy (epitaxy-arrangement on). A comprehensive review of the epitaxial growth of crystals observed in nature was given by Wallerant (1902) and by Mugge (1903). Royer studied a number of cases of epitaxial growth; his conclusions can be summarized as follows:

The deposit atoms or ions took up orientation as to follow the substrate structure such that there was a close fit between the two dimensional network at the interface of the deposit-atoms and the atoms of the substrate. In the cases of epitaxy there was a densely populated lattice row in the deposit parallel to one of the substrate rows, provided their relative identity spacings did not differ by more than 15%. This view was supported by the work of Frank and van der Merwe (1949) who found a similar limit, for the formation of



epitaxial layers, by treating the substrate surface as a two dimensional network. The difference between the network spacing of the substrate and the deposit layer of atoms is generally expressed in terms of percentage misfit. Thus if  $a$  and  $b$  are the corresponding network spacings in the substrate and overgrowth respectively, then the percentage misfit is given by  $100(b-a)/a$ . From the vast experiences in the study of epitaxy, it can be said that epitaxy of a given deposit can occur on a variety of substrates and it does not necessarily depend on a close crystallography registry between the substrate and the deposit. The epitaxial growth of a crystal can take place even if the lattice misfit is as high as 50% or more (Goswami, 1954; Pashley, 1956) suggesting that van der Merwe's ideas are not strictly fitting to the experimental evidence. General understanding of epitaxial growth in the case of vacuum deposits depends on a detailed knowledge of the mode of nucleation and growth characteristic of each vapour-solid combination. Further other factors such as the substrate-temperature, rate of deposition etc. have great influence on the growth process of the crystal.

#### Phase Transition and Polymorphism

A material in bulk form may not show any polymorphism but this phenomenon is often observed when it is in the thin film state. Thus in electrodeposited nickel a hexagonal

phase often along with f.c.c. has been observed (Finch, Wilman, Yang, 1947). A new b.c.c. form has also been reported in vacuum deposited nickel on rock salt under suitable conditions (Finch, Sinha and Goswami, 1955). Rubidium bromide which has normally NaCl type of structure was found to have CsCl type structure when deposited on silver substrate (Schulz, 1951a) the misfit being zero, while cesium and thallium halides in the thin film form often possessed NaCl type of structure (Schulz, 1951b). Bublik (1952) studied the structures of thin films of chromium, nickel, beryllium and cobalt by electron diffraction and found that these structures were dependent on the thickness of the films. Piggott and Wilman (1958) observed some super structures of sulphides. Goswami and Trehan (1959) observed polymorphism in  $Cu_2S$  during their study of the reaction of sulphur vapour on copper single crystals. Aggarwal and Goswami (1963) observed that cubic ZnS or CdS, when vacuum deposited, transformed into a hexagonal phase depending on the substrate temperature.

#### Present Work

In recent times antimony bismuth and their compounds such as selenides and tellurides as well as the Bi-Sb alloys have gained much importance because of their thermoelectric and semiconducting properties. There is a considerable interest in the growth of epitaxial films of semiconducting

materials, due to the application of these techniques in the manufacture of multilayer devices and various types of microcircuits. But as yet there is very little work carried out on the orientations and epitaxy of rhombohedral systems. Since most of these elements and compounds belong to the rhombohedral system, it would be of great interest to study the epitaxy on rock salt substrates, since the lattice fit would not likely to be so simple. Further the existence of some of these compounds have not yet been proved beyond doubt. With this idea in view, the following studies on the structure and orientations of the vapour phase deposits of antimony, bismuth, the Bi-Sb system, oxides of bismuth and antimony as well as selenide and telluride of antimony have been undertaken. A detailed study has also been made on the oxidation of epitaxially grown bismuth and antimony films, under various conditions of pressures so as to reveal the existence of suboxide and other oxidation states of bismuth and antimony films and also to study their growth process.

.....

## CHAPTER - II

### EXPERIMENTAL TECHNIQUE

#### (a) Materials deposited

Bismuth and antimony metals of analytical grade (A.R.) were used for vacuum deposition. The compounds such as bismuth suboxide, antimony selenide, antimony telluride and the alloy Bi-Sb, were prepared in the laboratory. The details of the methods are described in later chapters in the corresponding experimental parts.

#### (b) Substrates

Both crystalline as well as amorphous materials were used as substrates for deposition. Crystalline substrates used were different faces of rock salt, cleavage faces of mica and polycrystalline sodium chloride tablets. Collodion films and glass pieces were used as amorphous substrates.

#### (c) Preparation of substrates

##### (1) Rock salt

(100) faces of rock salt were obtained by cleaving the crystal with a razor-blade or a clean knife edge by applying slight pressure. (110) and (111) faces of

rock salt were obtained by careful grinding of the crystals in presence of benzene, at appropriate angles with emery papers upto 0000 grade. The faces were then cleaned by a camel hair brush, etched with running distilled water and finally dried by pressing immediately between clean filter papers. The faces thus prepared were examined by electron diffraction methods, and if necessary were reground to get appropriate faces.

(ii) Polycrystalline sodium chloride

Sodium chloride tablets were ground with emery papers successively upto 0000 grade in the presence of benzene. The surfaces were then cleaned by a camel hair brush followed by an etch in running distilled water. These were then dried by pressing between filter papers in the usual way.

(iii) Mica

(0001) face of mica was prepared by cleaving good quality mica sheets. Freshly cleaved faces were used for deposition.

(iv) Collodion

Thin films of collodion were prepared by adding drops of 0.25% solution of collodion (in amyl acetate), on the surface of distilled water in a petri dish. The films floating on water were then picked up on clean wire

gauzes with the help of tweezers. These were then dried in a hot oven for about half an hour and preserved in a desiccator.

(v) Glass

Microscope slides of good quality were cut so as to give small plates of a size of about 1 cm. x 2 cm. They were then cleaned in chromic acid solution, washed successively with distilled water, alcohol and finally dried in an oven at about 80-100°C.

(d) Method of deposition

In most of the cases the specimens were prepared by the deposition of the materials from the vapour phase on the different substrates.

Filaments used were either of Kanthol or of Tungsten wire of appropriate sizes. Conical baskets of these wires were initially made and then they were flashed in vacuo with high current to remove the surface impurities. Materials were then put in these baskets and evaporated in vacuo (better than  $10^{-4}$  mm of Hg), on different substrates at different temperatures.

The evaporation chamber consisted of a pyrex glass tube, having rubber stoppers at the two ends. Four terminals, two for filament and two for a thermocouple,

were put through one of the rubber bungs. The whole chamber was evacuated from the other end by means of rotary and diffusion pumps. A Pirani gauge and an ionisation gauge were also included in the system for measuring the vacuum. In order to heat the evaporation chamber a tubular furnace was placed around the pyrex tube, so that the temperature of the pyrex tube could be raised to about  $500^{\circ}\text{C}$  by controlling the heating of the tubular furnace.

Before deposition, the whole chamber along with the substrates as well as the charge inside the basket, was evacuated and then the temperature of the furnace was slowly raised to the appropriate value. When equilibrium was established, the deposition was carried out at an appropriate rate for a few seconds or more. The temperature of the chamber was maintained for some time more, before it was cooled to room temperature. The specimens were then taken out and immediately examined by reflection or transmission or by both the methods, for the nature of the surface layers as well as their orientations etc.

(e) Removal of deposit films from the substrate

For transmission, the films deposited on the substrate surface were normally removed by slowly dipping the substrate in distilled water in such a way that the

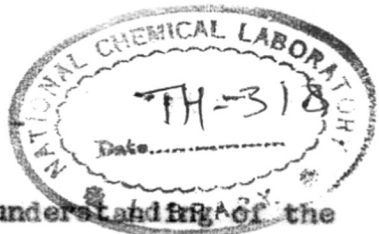
substrate surface layers underneath the deposit films were dissolved and the film could float on water surface. The films were then washed very carefully with distilled water several times, before examining by electron diffraction. Often it was found that due to the rapid dissolution of the rock salt substrate the films broke into pieces. In order to avoid this a special technique was evolved.

A nearly saturated solution of sodium chloride was prepared and put in the petri dish instead of pure distilled water. It was found that because of low dissolution rate of the substrate due to the nearly saturated condition of the solution very thin films of the deposit could also be removed from the substrate without much difficulty. These films were then washed carefully, several times with distilled water as mentioned before and further examined in the camera.

(f) Examination of specimens by electron diffraction

The specimens were examined by using a Finch type (cold cathode) electron diffraction camera, fabricated at the National Chemical Laboratory, the accelerating potential being 45 to 60 KV. The specimens were examined by transmission as well as by reflection methods. In order to measure the d-values accurately, graphite ring ( $11\bar{2}0 = 1.23 \overset{0}{\text{Å}}$ ) was used as standard.





Further to facilitate the understanding of the orientation relationship between the substrate and the deposits especially in transmission patterns, the detached films of the deposits were placed in the camera in such a way that one of the edges of the deposited film, corresponding to one of the principal axis of the substrate, was kept parallel to one of the sides of the photographic plate. In this way it was possible to correlate the diffraction patterns with respect to the substrate.

(g) Methods of interpretation of Electron Diffraction Patterns

The patterns obtained were interpreted by the methods described by previous workers (Finch and Wilman, 1937; Beeching, 1936; Thomson and Cochrane, 1939; Wilman, 1948a & b, 1949, 1952; Raether, 1951; Pinsker, 1953; Cowley, 1953, 1956; Vainshtein, 1964). The use of charts for hexagonal and rhombohedral lattices and other systems was made to identify the indices of different planes.

The diffraction patterns can be conveniently classified into three categories i.e. (1) single crystal or two degree (2-d) oriented patterns consisting of spots which changed with the azimuthal direction of electron beam. Sometimes the spots showed a slight elongation,

539.234; 621.385; 833(043)

GAD

spreading etc. depending on the degree of perfection of a single crystal or of the orientation etc. of the deposit film. (ii) Ring patterns indicating the polycrystalline nature of deposits. The rings not showing any change of intensity on changing the beam direction were characteristic of a random disposition of crystallites. (iii) Patterns consisting of arcs which did not change on changing the beam direction. These were due to the polycrystalline deposits with a preferred orientation. Sometimes ring patterns with a few rings of unusual intensity were observed in transmission method. These however broke into arcs by tilting the specimen. The above features suggested that the deposits had developed a one degree (1-d) orientation sometimes referred as deposits having "textured structure" or "fibre axis".

-----

## CHAPTER - III

### STRUCTURE AND GROWTH OF BISMUTH AND ANTIMONY FILMS

#### A. INTRODUCTION

##### (a) Bismuth

Structure of bismuth was first studied by Kahler (1921) by X-ray diffraction of sputtered films and found them to consist of crystalline bismuth, mixed with a little of amorphous variety of bismuth and a small amount of the oxide of bismuth. He also evaporated the metal in an evacuated pyrex tube and found that the films deposited on the colder parts of the tube were amorphous in nature. Gross (1930) studied the resistance of thin bismuth films in a magnetic field. Bunsen and Gross (1930) studied the structure of thin films of bismuth and found two modifications to be present, namely, a grey modification with randomly deposited crystals and another, a bright thin layer deposition with one degree orientation. Goetz and Dodd (1935) evaporated bismuth in vacuo and deposited it on a water cooled pyrex surface. The initial deposit of about  $10^{-2}$  mm thickness had a microcrystalline structure and with an increase of thickness these suddenly changed to macrocrystalline form with a fibre texture. This they claimed to be due to less efficient cooling with the increase in the thickness of deposit. Bound and Richards (1939) prepared

thin films of bismuth by evaporation on collodion and glass and found that the deposits developed a  $\{111\}$  orientation, presumably 1-d, of the rhombohedral structure. A similar observation was also made by Kirchner (1932). Hume-Rothery (1945) reported a rhombohedral cell for bismuth, the lattice parameters being  $a_0 = 4.7364 \text{ \AA}$  and  $\alpha = 57^\circ 14' 13''$ . Acharya (1948) assumed a pseudo cubic structure of bismuth for the ease of interpretation of the spots obtained in electron diffraction patterns. Bryant (1954) suggested that the action of an electron beam on bismuth films was to enhance the aggregation of crystallites by extremely localised melting, evaporation and recrystallisation. Takagi (1956) and Eublik (1957) worked on the structure of liquid bismuth films near the melting point and showed that there was a tendency of close packing in the liquid state but at higher temperatures the packing became more dense. Aggarwal and Goswami (1958) studied the oxidation of bismuth films and observed 1-d  $\{01.1\}$  and 1-d  $\{10.2\}$  orientations of Bi films. Most of the recent work on bismuth concerns with the structure study at low temperatures upto  $4^\circ\text{K}$ . Capella (1962) has studied the epitaxy of As, Sb and Bi on  $\text{PbS}$ ,  $\text{CaF}_2$  and on (100) faces of five alkali halides, and found that 11.0 face of bismuth grew on a (100) face of support. A new cubic phase of bismuth with  $a_0 = 3.177 \text{ \AA}$  has been observed by Jaggi (1964) by subjecting bismuth to a very high pressure of about 25,000 atmospheres.

(b) Antimony

Kirchner (1932) studied evaporated films of antimony on collodion but obtained diffuse ring patterns while Dixit (1933) obtained 1-d oriented patterns. Jette and Foote (1935) reported antimony to have a rhombohedral A7 type structure with  $a_0 = 4.4976 \text{ \AA}$  and  $\alpha = 57^\circ 6' 27''$ . Practically the same values of parameters were also reported by Trzebiatowski (1938) and Lu and Chang (1941). Bound and Richards (1939) however treated the oriented ring patterns obtained, on the basis of a deformed face centred cubic lattice with  $a_0 = 6.23 \text{ \AA}$  and  $\alpha = 87^\circ 24'$ . Wilman (1952) studied the orientations of antimony deposits formed from vapour phase and found that these corresponded to 1-d  $\{21\bar{1}\}$  and  $\{1\bar{1}\bar{1}\}$  orientations of the pseudo cubic phase of antimony. Zorll (1954) studied the films of antimony formed on collodion and found that their (111) planes were parallel to the substrate. The films were textured and reflections were arranged on a system of straight lines, ellipses or hyperbolae. Krebs et al. (1955) studied mainly the structure of explosive antimony and suggested on the basis of chemical arguments that it was a mixed polymer. He also studied the structure of antimony films by electron diffraction and found that antimony has a hexagonal (rhombohedral) structure with  $a_0 = 4.296 \text{ \AA}$ ,  $c_0 = 11.26 \text{ \AA}$ . Stoyanova (1956) has shown by electron diffraction that the so called amorphous films of antimony contain fine crystals of size 30 to 35  $\text{\AA}$ . A number of workers have studied the other properties of antimony

such as, use of amorphous antimony films as semiconductors (Mooser, 1957), relation between phase change and electrical properties (Kurov, 1956), electric and magnetic properties (Colombani, 1958), conductivity of antimony films (Bonfiglioli, 1959) etc. The electron microscopic and X-ray studies of the dislocations on the (111) cleavage planes by etching were carried out by Soifer (1960), Lavrentev (1960) and Kosevich (1961). The crystallisation process of antimony has also been studied by many workers such as Palatnik (1960A) who showed two types of transformations in antimony films. The first is a slow change from amorphous to crystalline ( $\alpha$ ) and the second a sudden change from amorphous to crystalline ( $\beta$ ). He has also shown that addition of Al, Cr, Be increases stability of amorphous phase (1960B) Ruedl (1959) has found that very thin films of antimony are amorphous, but as the thickness increases they become crystalline, apart from these, some films are also heterogeneous. Capella (1962) has worked on the epitaxy of Sb films on PbS, CaF<sub>2</sub> and alkali halides as substrates but he has obtained the films by the reduction of the vapours of Sb<sub>2</sub>S<sub>3</sub> and not by direct evaporation of the metal. Baux (1963) deposited Sb from vapour phase on freshly cleaved Sb and found that the films are  $\{\bar{1}11\}$  oriented and this rearranged to  $\{111\}$  orientation by electron bombardment. Electron microscopic studies of the growth of Sb crystals have been done by Pandya (1963) and Bolotov (1965) and they have noted various types of growth triangles and spherulites and the triangular faces are (111) faces of antimony.

Bacon (1964) calculated the crystallographic angles for Bi as  $87^{\circ}32'$ , Sb as  $87^{\circ}25'$ . Mesnard (1964) described an equipment for simultaneous deposition of several layers of varying thickness and has shown that in case of antimony various structures are possible by changing the evaporation technique.

From the above study it is seen that no systematic work has yet been carried out on the epitaxial growth, orientation relationship, phase changes if at all, etc. of bismuth and antimony films on different single crystal substrates. Further whatever work has been done on thin films by electron diffraction, the interpretation was generally done on the basis of a pseudocubic structure. This is not likely to give a clear information about the crystal growth process as well as the orientation relationships. In the following work a detailed study has been made on the crystal growth process, epitaxy, orientation etc. of their deposits on different faces of rock salt, (0001) face of mica and also on amorphous as well as polycrystalline substrates.

#### B. EXPERIMENTAL

Bismuth and antimony metals of analytical grade (A.R.) were vacuum deposited separately on the different substrates such as collodion, glass, (100), (110) and (111) faces of rock salt as well as on cleavage faces of mica in vacuo ( $\approx 10^{-4}$  mm of Hg) at various substrate temperatures. The

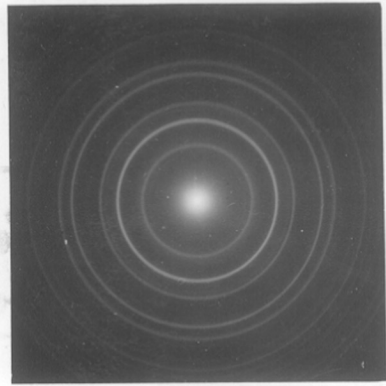


(Fig 1) Bismuth on collodion  
at Room temperature.

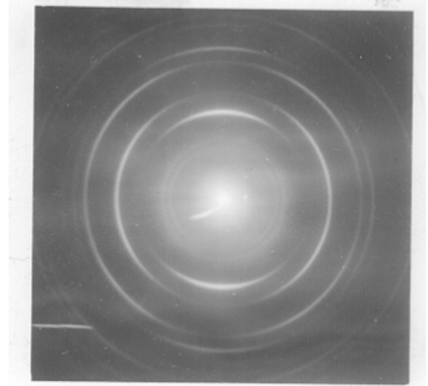


(Fig 2) Specimen in Fig 1  
Tilted by  $30^\circ$ .

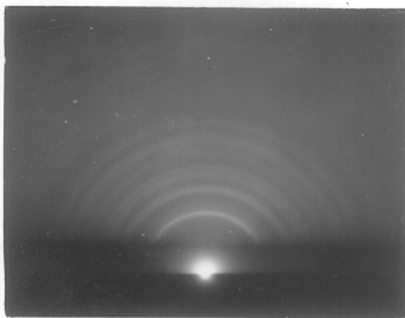


(Fig 3) Bismuth on glass  
at Room temperature.

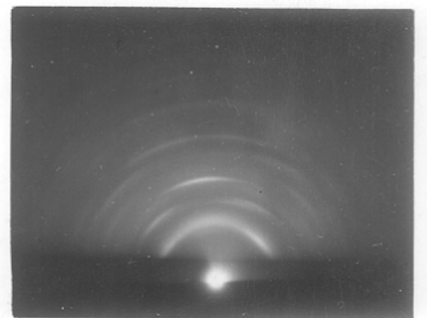


(Fig 4) Bismuth on glass  
at Room temp. Thick deposit  
1-d {01.1}



BISMUTHTABLE - 1

(Ref. page 24)

Analysis of the patternFigure-1

$I/I_0$ observed	d	hkl	$I/I_0$ X-ray A.S.T.M. Card No. 5-0519
vvf	3.71	01.1	3
ms	3.26	10.2	100
vs	2.28	11.0	41
f	1.94	20.1	23
m	1.86	02.2	23
vf	1.62	20.4	9
s	1.43	21.2	16
ms	1.32	12.4	11
vvf	1.25	21.5	2
vf	1.13	22.0	4
f	1.07	30.6	2

$$a_0 = 4.53 \text{ \AA}, \quad c_0 = 11.85 \text{ \AA}$$

s - strong  
m - medium  
f - faint

ms - medium strong  
vf - very faint  
vvf - very very faint

detailed method of deposition has already been discussed in the Chapter II. The deposits were then examined both by reflection and transmission methods in the usual way as mentioned before.

### C. RESULTS

#### (a) Deposition of Bismuth

##### (1) On collodion and on polycrystalline sodium chloride

Bismuth films deposited on collodion as well as on polycrystalline sodium chloride at room temperature yielded patterns (Fig.1) consisting of continuous rings due to the polycrystalline nature of the deposits. On analysis of these patterns (Table 1), it was found that the d-values for the various reflections agree with those given in the X-ray data (A.S.T.M. Card No.5-0519), corresponding to a (modified) hexagonal structure for bismuth ( $a_0 = 4.5464 \text{ \AA}$ ,  $c_0 = 11.86 \text{ \AA}$ ), having a basic rhombohedral unit cell ( $a_0 = 4.736 \text{ \AA}$ ,  $\alpha = 57^\circ 14' 13''$ ). It was, however, found that the intensities of the different reflections of electron diffraction patterns differed considerably from those of X-ray data. On tilting the specimens say by about  $30^\circ$ , it was observed that the new diffraction pattern (Fig.2) now consisted of broken arcs and rings, thus suggesting that the deposits had developed a preferred orientation. Such an orientation was also observed even when the deposition

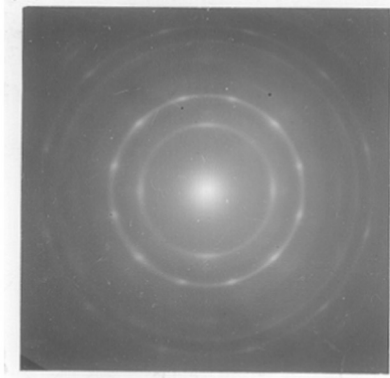


(Fig 5) Bismuth on (100) of  
Rock salt at 100°C.  
PseudoCubic 2-d {100} + 2-d {111} rotated by 30°

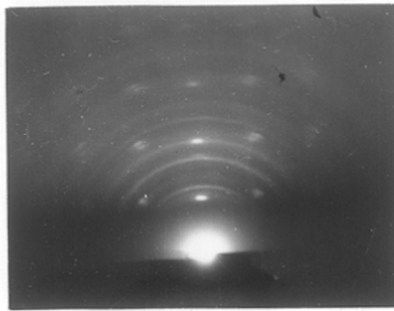


(Fig 6) Bismuth on (100) of  
Rocksalt at 150°C. beam <100> of Rocksalt  
2-d {10,2} Hexagonal  
or 2-d {100} Pseudocubic

was made only for a few seconds. Patterns from deposits formed on collodion and also on polycrystalline sodium chloride at 100°C or slightly higher temperatures were similar in nature, except that the rings were sharper, thereby indicating an increase in grain size of the crystallites.

(ii) On glass

Deposits of bismuth formed on glass at room temperature or at higher temperatures had a blackish-red metallic lustre. These specimens when examined by electron diffraction produced ring patterns (Fig. 3) characteristic of the hexagonal (rhombohedral) structure. Thicker deposits obtained at room temperature, however, produced arc patterns, which did not change even on rotating the specimen with respect to the beam direction. It can be seen from the pattern (Fig. 4) that reflections such as 01.1, 02.2 are in the plane of incidence, thus suggesting the development of 1-d {01.1} orientation of the deposit films.

(iii) On (100) face of rock salt

Deposits formed on this face at room temperature were polycrystalline in nature. At a higher temperature of about 100°C, deposits yielded patterns (Fig. 5) consisting of spots lying on various rings when examined by transmission. A careful examination showed that the spot patterns arose from two basic units namely (a) approximate square network of spots and (b) centred rectangular

network of spots with the sides of the rectangles nearly in the ratio  $\sqrt{3}:\sqrt{24}$ , suggesting 2-d  $\{100\}$  + 2-d  $\{111\}$  orientations of a pseudo-cubic structure of the deposits. It was also found that the spot patterns due to  $\{111\}$  orientation were rotated by  $30^\circ$ , no doubt, due to the rotation of the crystallites.

It may be mentioned here that even though bismuth films have a hexagonal cell ( $a_0 = 4.5464 \text{ \AA}$ ,  $c_0 = 11.86 \text{ \AA}$ ), it is possible to make an approximate analysis of the diffraction patterns, especially the single crystal patterns assuming a pseudo-cubic structure with  $a_0 = 6.54 \text{ \AA}$  and  $\alpha = 87^\circ 48'$ .

The deposits formed at about  $150^\circ\text{C}$  and  $200^\circ\text{C}$ , when examined by reflection yielded patterns (Fig. 6), when beam was along  $\langle 100 \rangle$  of rocksalt. These patterns, at first sight appear to consist of a square type of network with 10.2 and its higher order reflections in the plane of incidence thus suggesting a 2-d  $\{10.2\}$  of the hexagonal or a 2-d  $\{100\}$  orientation of the pseudo-cubic structure of the deposits. A closer examination of the patterns, however, revealed that the simple interpretation, on the basis of a pseudocubic structure, cannot account for the existence of many other spots which are lying close to one another. For a complete understanding of these patterns, it was found essential to interpret them from the hexagonal

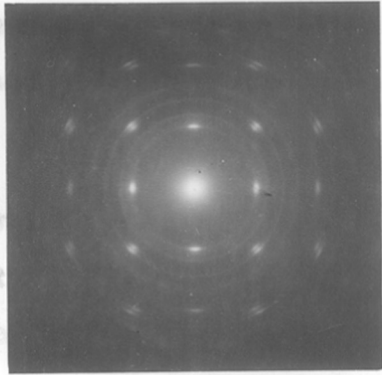


(Fig 7) Biomuth on (100) of  
Rock salt. 2-d {30.7} orientation.  
normal and anti

HEXAGONAL (RHOMBOHEDRAL)  
TRANSMISSION  
2-d {30.7} ORN.

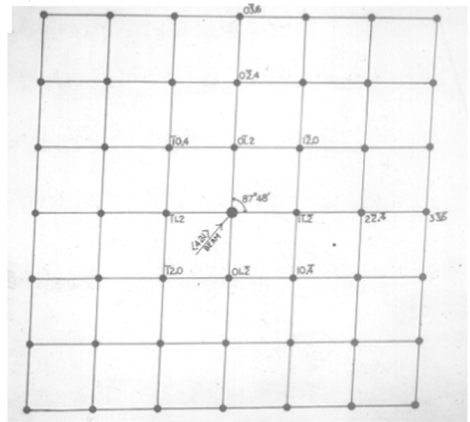


(Fig 8)

HEXAGONAL (RHOMBOHEDRAL)  
TRANSMISSION  
2-d {30.7} ORN.  
NORMAL & ANTI

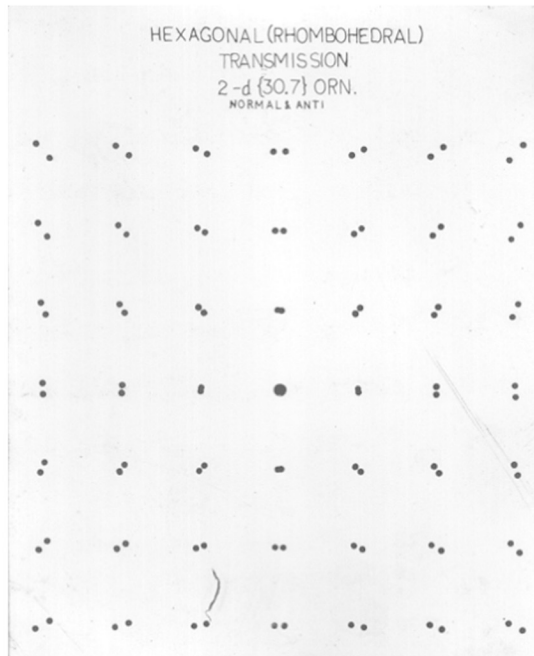


(Fig 9)

(rhombohedral) structure, rather than the simplified pseudocubic lattice.

The same specimen (cf. Fig.6) when examined by transmission yielded patterns (Fig.7) which consisted of a nearly square network of spots as was observed in the reflection pattern.

From the considerations of the  $d$ -values of the hexagonal structure, the above square network is formed by  $000$ ,  $1\bar{1}.2$ ,  $1\bar{2}.0$  and  $0\bar{1}.2$  reflections. It is also seen that there is another spot just inside the  $1\bar{2}.0$  reflection with a ' $d$ ' value =  $2.39 \text{ \AA}$ , corresponding to  $01.4$  reflection. Such a disposition of spots cannot be expected from a pseudocubic structure. In order to have a better understanding of the patterns, a detailed analysis was carried out from the reciprocal lattice consideration of hexagonal structure, conforming to the basic rhombohedral cell.

For the interpretation of spot patterns of bismuth as obtained by the transmission method, it is necessary to identify first the reciprocal lattice rows  $[h_1 k_1 . l_1]^*$  and  $[h_2 k_2 . l_2]^*$  in two different directions, preferably at right angles to each other.

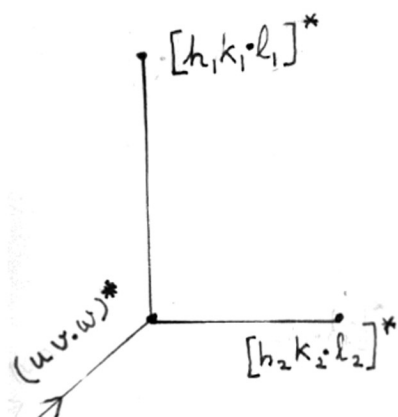
The condition for the normality for a hexagonal system that the value of  $\cos\theta$ , given by the following equation:

$$\cos \theta = \frac{h_1 h_2 + k_1 k_2 + \frac{1}{2} (h_1 k_2 + h_2 k_1) + \frac{3}{4} \cdot \frac{a^2}{c^2} \cdot l_1 l_2}{\sqrt{(h_1^2 + h_1 k_1 + k_1^2 + \frac{3}{4} \frac{a^2}{c^2} l_1^2) (h_2^2 + h_2 k_2 + k_2^2 + \frac{3}{4} \frac{a^2}{c^2} l_2^2)}}$$

$$= 0 \quad \dots (I)$$

Thus the condition for perpendicularity of the reciprocal lattice rows  $[h_1 k_1 \cdot l_1]^*$  and  $[h_2 k_2 \cdot l_2]^*$  is that

$$h_1 h_2 + k_1 k_2 + \frac{1}{2} (h_1 k_2 + h_2 k_1) + \frac{3}{4} \cdot \frac{a^2}{c^2} \cdot l_1 l_2 = 0 \quad \dots (II)$$



Now knowing  $[h_1 k_1 \cdot l_1]^*$  and  $[h_2 k_2 \cdot l_2]^*$  with their appropriate signs it is possible to find out the reciprocal lattice plane  $(uvw)^*$ , by the general condition true for all systems viz.

$$u:v:w = \begin{vmatrix} h_1 & k_1 & l_1 & h_1 & k_1 & l_1 \\ & \swarrow & \searrow & \swarrow & \searrow & \\ h_2 & k_2 & l_2 & h_2 & k_2 & l_2 \end{vmatrix}$$

i.e.

$$u:v:w = (k_1 l_2 - l_1 k_2) : (l_1 h_2 - h_1 l_2) : (h_1 k_2 - k_1 h_2) \quad \dots (III)$$

Thus the patterns corresponding to  $(uvw)^*$  reciprocal lattice plane is due to beam along  $\langle u v w \rangle$  of the real axis which has  $\{hk.l\}$  plane normal to it.



Having found out the beam direction  $\langle uv.w \rangle$ , the orientation plane (hk.l) is found out by the expression

$$h:k:l = \left( u - \frac{v}{2} \right) : \left( v - \frac{u}{2} \right) : \left( w \cdot \frac{c^2}{a^2} \right) \dots (IV)$$

In the case of a basic rhombohedral cell expressed in the hexagonal notation the criteria for reinforcement of diffraction are given by

$$\left. \begin{aligned} h - k + l &= 3n \\ h + 2k + l &= 3n \\ -2h - k + l &= 3n \end{aligned} \right\} \dots (V)$$

where n is a whole number including zero.

In order to interpret the transmission pattern (Fig.7) we have to satisfy the different conditions as already mentioned above. Taking this spot pattern into consideration, it is seen that spot rows containing  $1\bar{1}.2$  and  $0\bar{1}.2$  reflections but passing through the central undeflected spot, appear to be at right angles. These hk.l reflections also satisfied the rhombohedral conditions given above by the equation (V). The actual angle calculated with the help of equation (I) was found to be  $87^{\circ}48'$ .

Now with the help of the relation (III) the reciprocal lattice plane (uv.w)\* becomes,

$$u:v:w = \begin{array}{c} 1 \\ 0 \end{array} \left| \begin{array}{cc} \bar{1} \bar{2} & 1 \bar{1} \\ \swarrow \quad \searrow & \swarrow \quad \searrow \\ 1 \bar{2} & 0 1 \end{array} \right| \begin{array}{c} \bar{2} \\ \bar{2} \end{array} = 4:2:1$$

i.e.  $(uv.w)^* = (42.1)^*$ .

With the help of equation (IV) and also knowing  $c/a$  for bismuth  $\simeq 2.61$ , the plane  $(hk.l)$  normal to the above direction  $\langle 42.1 \rangle$  can be calculated as below:

$$\begin{aligned} h:k:l &= (4 - \frac{2}{2}) : (2 - \frac{4}{2}) : 1(2.61)^2 \\ &= 3:0:6.8 \end{aligned}$$

Hence  $hk.l = 30.6.8 \simeq 30.7$

Thus the deposits developed a 2-d  $\{30.7\}$  orientation on a cube face of rock salt. As mentioned earlier the angle between  $[\bar{1}\bar{1}.2]^*$  and  $[0\bar{1}.2]^*$  was  $87^\circ 48'$  and a reciprocal lattice was constructed as in Fig.8 to verify the disposition of spots with respect to the theoretical diagram. It can be seen that such a lattice is unsymmetrical while the actual pattern was symmetrically disposed. It can further be seen that by interchanging the positions of  $1\bar{1}.2$  and  $\bar{1}\bar{1}.2$  reflections another unsymmetrical reciprocal lattice is produced. When these two reciprocal lattices are superimposed, the mixed reciprocal lattices formed (Fig.9) conform in all respects to the electron diffraction patterns observed. Thus it appears that the deposits developed both normal and anti 2-d  $\{30.7\}$  orientation. With the above

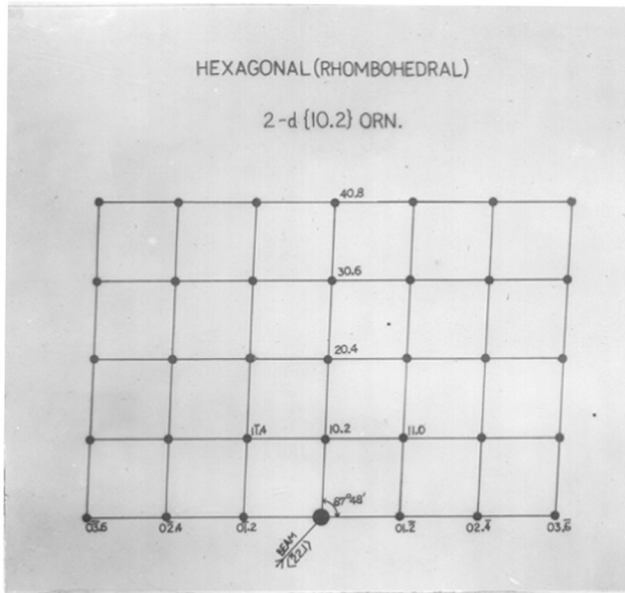


(Fig 10)

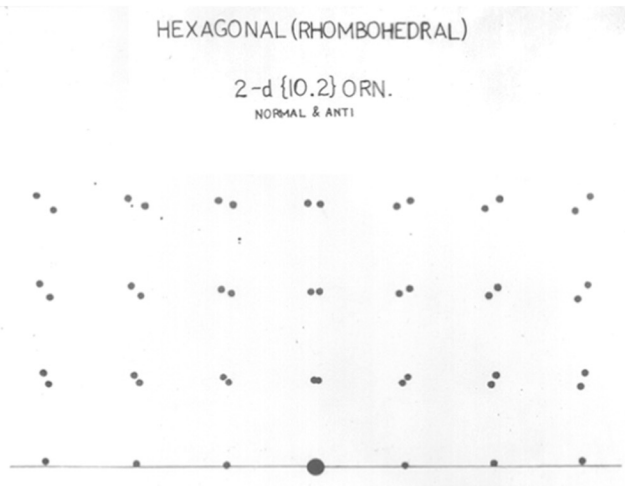


(Fig 11)

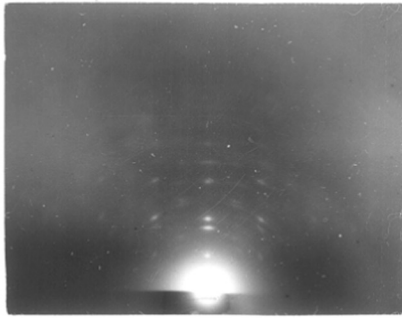


(Fig 12)  
 Bismuth on (100) of Rock salt at 150°C.  
 Beam  $\langle 110 \rangle$  of Rock salt  
 2-d  $\{10, 2\} + \{0, 1\}$  orientations

HEXAGONAL (RHOMBOHEDRAL)

2-d  $\{10, 2\}$  ORN.

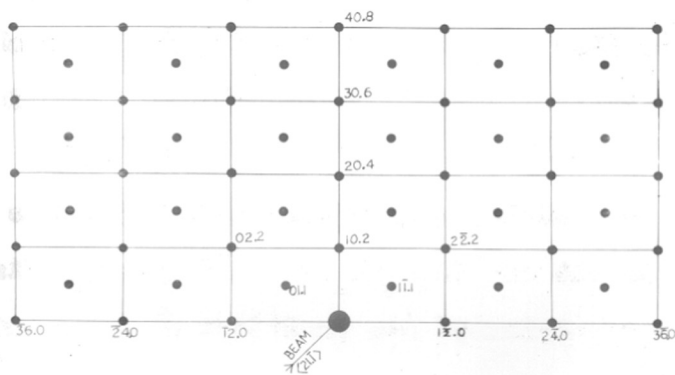


(Fig 13)

interpretation the appearance of the 01.4 as well as 11.0 reflections in the pattern (Fig.7) as doubled spots is also well explained.

In the light of the above treatment it is now possible to interpret fully the disposition of spots even in the reflection pattern (Fig.6), when beam was along  $\langle 100 \rangle$  of rock salt by drawing a reciprocal lattice (Fig.10) for a 2-d  $\{10.2\}$  orientation of the hexagonal structure. The double spots due to 01.4 and 11.0 appearing very near each other can be explained on the basis of normal and anti orientations of the deposit crystals (Fig.11).

When the beam was along  $\langle 110 \rangle$  of rock salt the patterns (Fig.12) obtained consisted of rectangular network due to 000, 10.2, 02.2 and 11.0 reflections. The 10.2 and 11.0 reciprocal points after giving appropriate signs as 10.2 and  $\bar{1}\bar{2}.0$  and testing for rhombohedral conditions (Equation (V)), were found to satisfy the condition for normality as in equation (II). The reciprocal lattice constructed (Fig.13) shows that as the angle between  $(h_1k_1.l_1)^*$  and  $(h_2k_2.l_2)^*$  is  $90^\circ$ , so the interchanging of the positions of 10.2 and  $\bar{1}\bar{0}.\bar{2}$  will cause no change in the disposition of spots, and hence doubling of spots is not possible at 11.0 reflection. This is also confirmed from the actual pattern (Fig.12). The presence of 10.2 reflection in



(Fig 14)

Bismuth on (110) of Rock salt at 150°C.  
Beam  $\langle 100 \rangle$  of Rock salt.  $2\text{-}d\{11.0\}$  ORN.

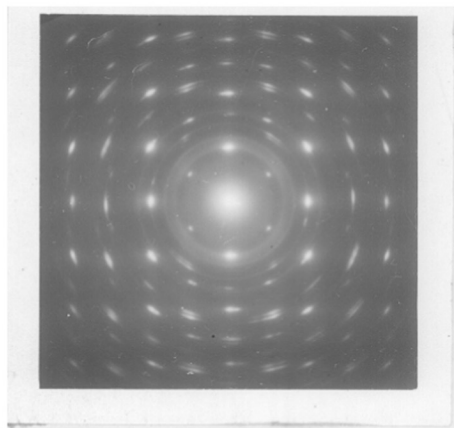


(Fig 15)

Specimen in Fig 14, Seen by  
Transmission  
 $2\text{-}d\{11.0\} + 2\text{-}d\{30.\bar{1}4\} + 2\text{-}d\{11.\bar{7}\}$  normal  
and anti

HEXAGONAL (RHOMBOHEDRAL)  
TRANSMISSION  
 $2\text{-}d\{30.\bar{1}4\}$  ORN.

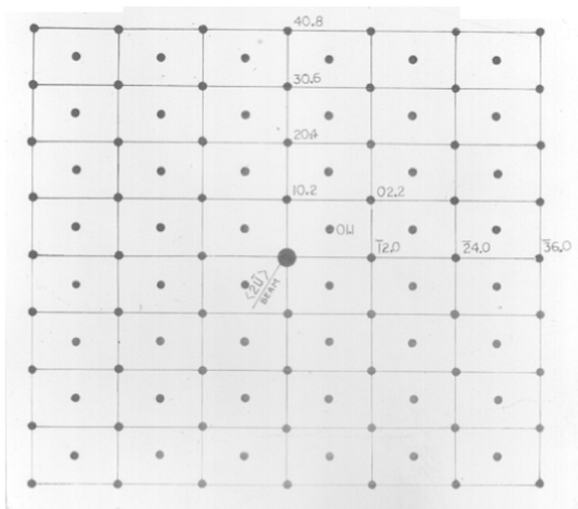


(Fig 16)

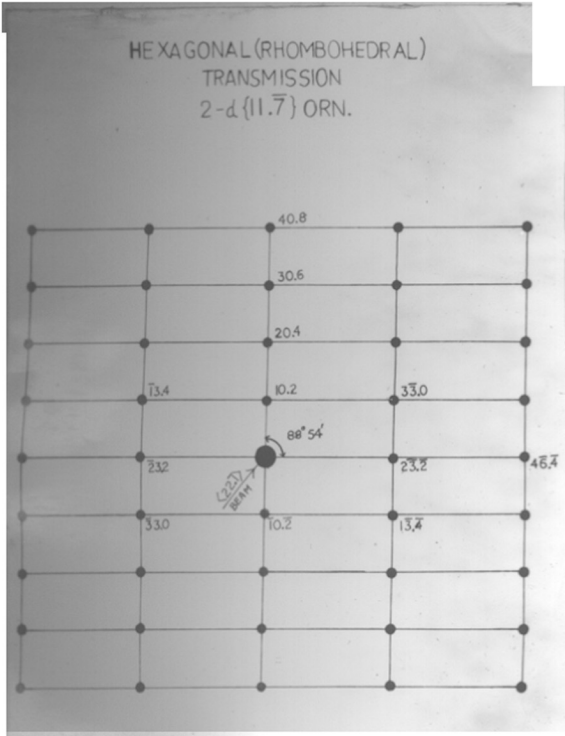


(Fig 18)

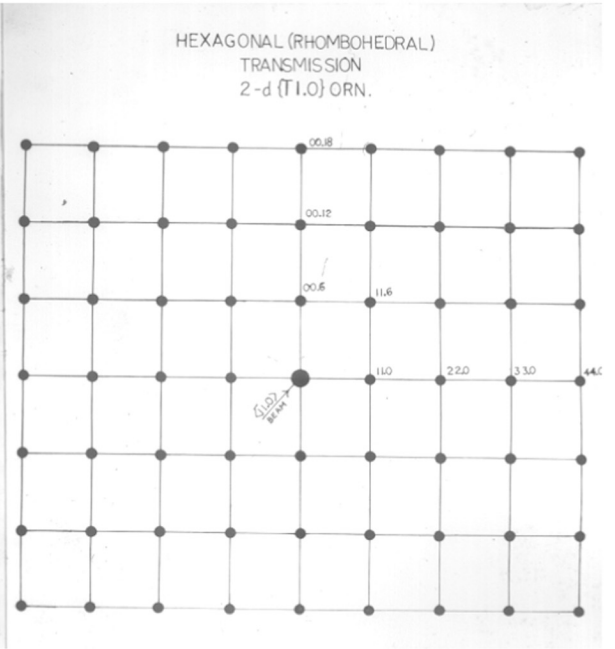


(Fig 17)

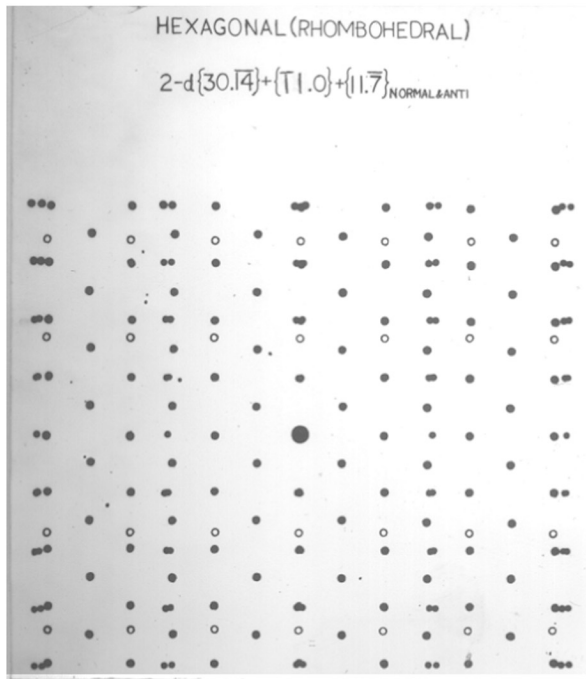


(Fig 19)

the plane of incidence also shows the formation of a 2-d  $\{10.2\}$  orientation of the deposits. However a faint spot in the plane of incidence due to 01.1 reflection shows that the deposits also developed a 2-d  $\{01.1\}$  orientation.

(iv) On (110) face of rock salt

The deposits formed at room temperature and also at about  $50^{\circ}\text{C}$  were polycrystalline in nature. The deposits formed at  $100^{\circ}\text{C}$  were partly polycrystalline and partly single crystal type. The disposition of strong spots can roughly be explained on the basis of a 2-d  $\{110\}$  orientation of the pseudocubic structure of the deposit films.

The deposits formed at about  $150^{\circ}$  and  $200^{\circ}\text{C}$  when examined by reflection with beam along  $\langle 100 \rangle$  of rock salt produced patterns (Fig. 14) with 11.0 reflection in the plane of incidence thus suggesting a 2-d  $\{11.0\}$  orientation of the hexagonal structure. The same specimen when examined by transmission yielded patterns (Fig.15) consisting of nearly  $\sqrt{2}$  type rectangles formed by the arrays of spots, thus suggesting a 2-d  $\{110\}$  orientation of the pseudocubic structure. However it is not possible to explain all the reflection spots merely with the help of a pseudocubic structure.



The main pattern (nearly  $\sqrt{2}$  type of rectangles) is formed by 000, 10.2, 02.2 and 11.0 reflections. With appropriate signs of  $hk.l$  permissible by rhombohedral conditions, the network has the following indices 000, 10.2, 02.2 and  $\bar{1}2.0$  such that the spot rows containing 10.2 and  $\bar{1}2.0$  reflections passing through the central undeflected <sup>spot</sup> are at right angles to each other. The beam direction as calculated by applying the expression (III) comes out to be  $\langle 21.\bar{1} \rangle$ , and the plane perpendicular to this becomes  $(30.\bar{1}4)$  i.e. nearly  $(10.\bar{5})$ . Thus the bismuth films developed a 2-d  $\{10.\bar{5}\}$  orientation on a (110) face of rocksalt. The reciprocal lattice diagram (Fig.16) constructed for this orientation shows that there are still many more spots in Fig.15, which remain unidentified. A closer examination shows that there are two more orientations. One of these is represented by rectangles formed by reflections such as 000, 00.6, 11.6 and 11.0. The calculations show that the beam direction for such disposition of spots is  $\langle \bar{1}1.0 \rangle$  and hence the plane of orientation is  $(\bar{3}3.0)$  i.e.  $(\bar{1}1.0)$ . Thus the deposit also developed a 2-d  $\{\bar{1}1.0\}$  orientation. The other was revealed by the rectangles formed by the reflections such as 000, 10.2, 30.0 and 21.2. These with appropriate signs become 000, 10.2,  $\bar{3}\bar{3}.0$  and  $2\bar{3}.\bar{2}$ . The angle between 10.2 and  $2\bar{3}.\bar{2}$  reflections is  $88^{\circ}54'$ . The beam direction then comes out as  $\langle 22.\bar{1} \rangle$  and then the plane of orientation as  $(11.\bar{7})$ . Figures 17

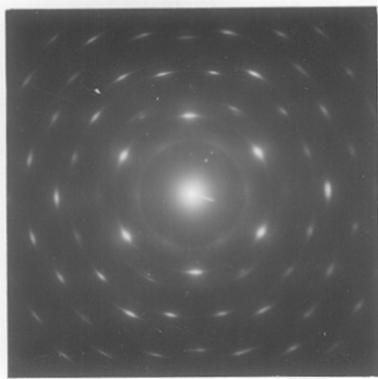


(Fig 20)  
 Bismuth on (111) of Rocksalt at 100°C.  
 2-d {00.1} + 2-d {1T.9} ORN rotated by 60°

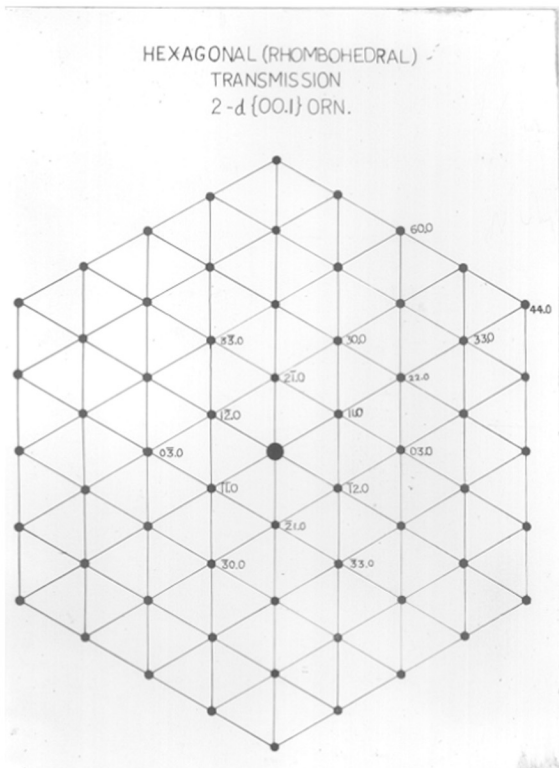


(Fig 21)

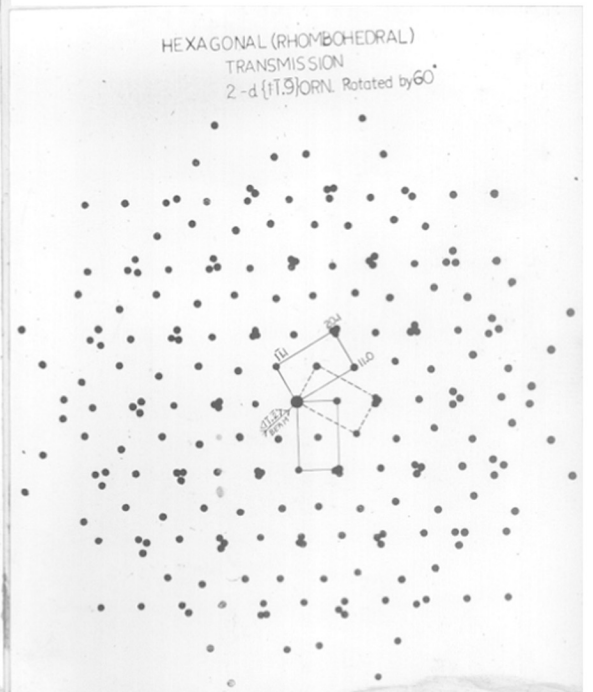


(Fig 22)

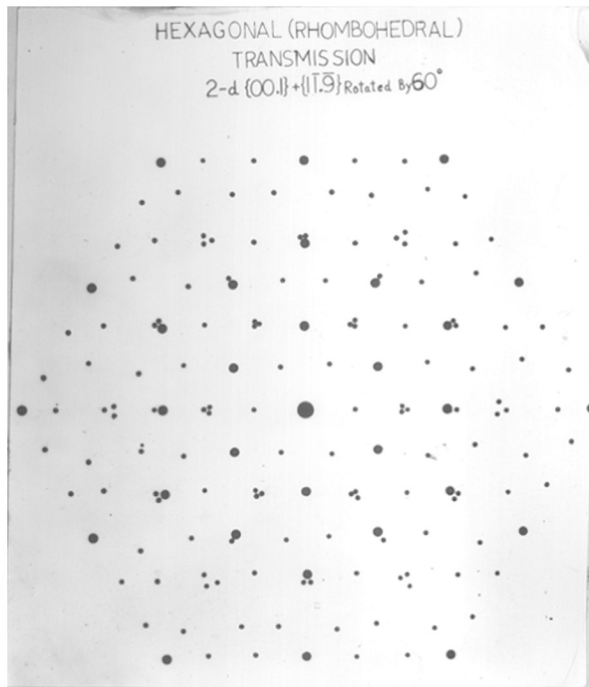


(Fig 23)

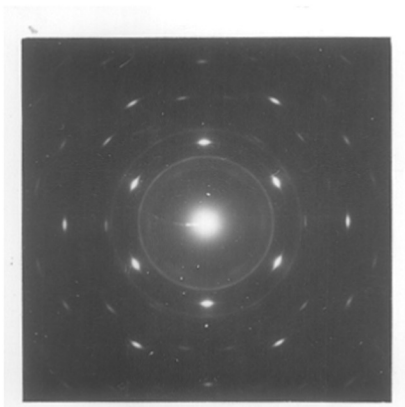


(Fig 24)

Bismuth on Rocksalt (111) at  $150^\circ\text{C}$ .

and 18 respectively show the reciprocal lattice diagrams for 2-d  $\{\bar{1}1.0\}$  and  $\{11.\bar{7}\}$  orientations. It may be mentioned that the pattern in Fig.18 is unsymmetrical, whilst those obtained in the diffraction were symmetrical. This could be explained by the normal and anti development of the crystallites with  $\{11.\bar{7}\}$  orientation. The Fig.19 showing all these orientations together, resembles the actual patterns. Still then a few reflections remain unidentified which may be due to the double scattering. Thus bismuth film developed a mixture of two degree  $\{10.\bar{5}\} + \{\bar{1}1.0\} + \{11.\bar{7}\}$  orientations on (110) face of rocksalt. In the last case both normal and anti type crystals were present.

(v) On (111) face of rock salt

The deposits on a (111) face did not yield any patterns by reflection. When examined by transmission the deposits formed at 100°C and higher temperatures yielded sharp spot patterns (Fig.20). It is seen that there is a hexagonal network of strong spots, such that six 11.0 type of reflections are closest to the undeflected beam. This arrangement suggests the development of a 2-d  $\{00.1\}$  orientation of the hexagonal structure. It is further seen that there are many other spots which cannot be explained from the 2-d  $\{00.1\}$  orientation alone. These additional spots, which are not so strong as those from  $\{00.1\}$  orientated crystallites form a rectangular network by means of 000, 11.0,

20.1 and  $1\bar{1}1$  reflections. On further considerations it was found that the beam direction normal to the reciprocal lattice was  $\langle 1\bar{1}.2 \rangle$  and hence the deposits developed a 2-d  $\{1\bar{1}.9\}$  orientation. Figures 21 and 22 respectively show the reciprocal lattices for 2-d  $\{00.1\}$  orientation and 2-d  $\{1\bar{1}.9\}$  orientation with crystallites rotated by  $60^\circ$ . When a combined reciprocal lattice diagram (Fig.23) is constructed and the patterns compared, it is seen that practically all the reflections can be explained by rotation of this  $\{1\bar{1}.9\}$  orientated crystallites through  $60^\circ$ . Thus the deposits developed two degree  $\{00.1\} + \{1\bar{1}.9\}$  orientated crystallites rotated through  $60^\circ$ .

The patterns (Fig.24) obtained from deposits formed at about  $150^\circ\text{C}$  also revealed the presence of both these orientations. But in this case the reflections due to  $\{00.1\}$  orientation were more prominent while reflections due to  $\{1\bar{1}.9\}$  orientation were fainter. The patterns yielded by deposits formed at about  $200^\circ\text{C}$ - $250^\circ\text{C}$  consisted only of a 2-d  $\{00.1\}$  orientation. It thus seems that at higher temperature only a 2-d  $\{00.1\}$  orientation was favoured.

(vi) On cleaved face of mica

The deposits of bismuth formed at room temperature on cleaved faces of mica yielded diffuse ring patterns. The deposits formed at about  $100^\circ\text{C}$  produced faint arc

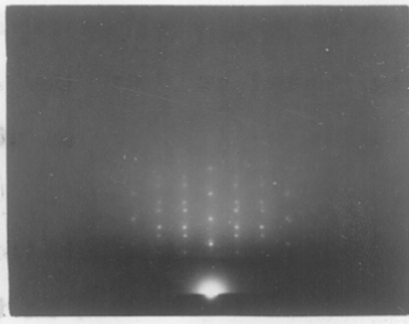


(Fig 25)  
Bismuth on mica at 200°C.  
2-d {00.1} ORN.

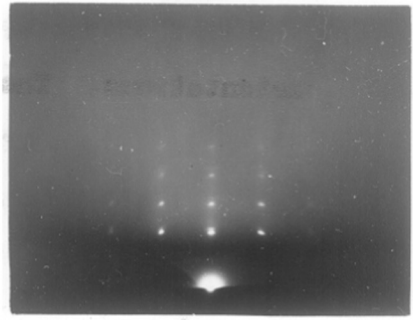


(Fig 26)  
Bismuth on mica at 200°C.  
Beam at 30° to in Fig 25, 2-d {00.1} ORN

HEXAGONAL (RHOMBOHEDRAL)

Normal to anti  
2-d {00.1} ORN.

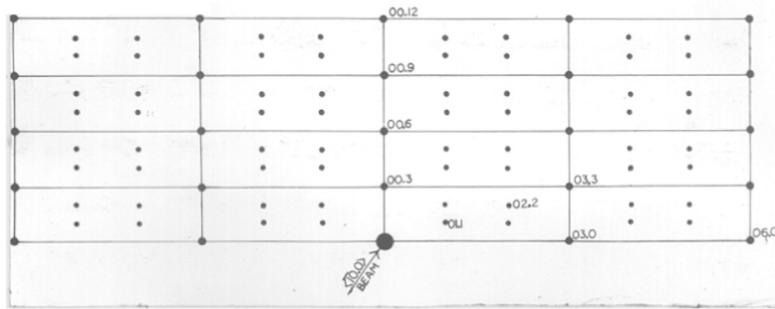


(Fig 27)

HEXAGONAL (RHOMBOHEDRAL)

2-d {00.1} ORN.

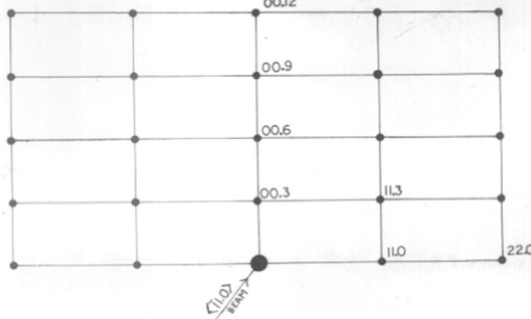


(Fig 28)

patterns characteristic of a 1-d  $\{10.2\}$  and  $\{01.1\}$  orientations. The deposits formed at about  $150^{\circ}\text{C}$  and  $200^{\circ}\text{C}$  yielded patterns (Figs. 25 and 26) taken at azimuths of  $30^{\circ}$  to each other, show a change in the disposition of spots, suggesting a 2-d orientation of the deposits. From the disposition of spots in the patterns, apparently a 2-d  $\{111\}$  orientation of the pseudocubic can be suggested.

A closer study of the patterns showed that rectangles were formed by 000, 00.3, 03.3, 03.0 reflections of the hexagonal structure with spots at  $1/3^{\text{rd}}$  distance along the diagonal corresponding to 01.1 and 02.2 directions. This showed that the deposits developed a 2-d  $\{00.3\}$  i.e.  $\{00.1\}$  orientation of the hexagonal structure with the beam along  $\langle \bar{1}0.0 \rangle$  with respect to the deposit. The pattern at  $30^{\circ}$  azimuth also consisted 00.3 reflection in the plane of incidence, and rectangles were formed by 000, 00.3, 11.3 and 11.0 reflections confirming the 2-d  $\{00.1\}$  orientation. Reciprocal lattice diagrams for 2-d  $\{00.1\}$  orientation corresponding the beam directions  $\langle \bar{1}0.0 \rangle$  and  $\langle \bar{1}1.0 \rangle$  respectively are shown in Figures 27 and 28.

#### (b) Deposition of Antimony

Deposition of antimony was in general very difficult, especially when the epitaxial growth was desired. At a slow rate of deposition the deposits were found to be

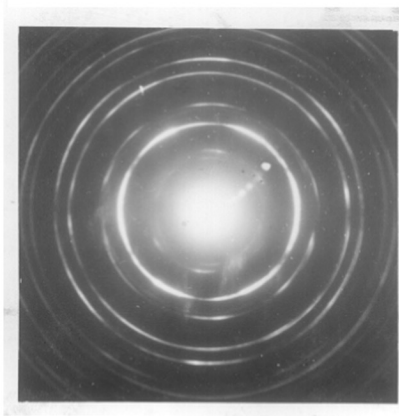


(Fig 29)  
Antimony on collodion at room  
Temp. Thick films.

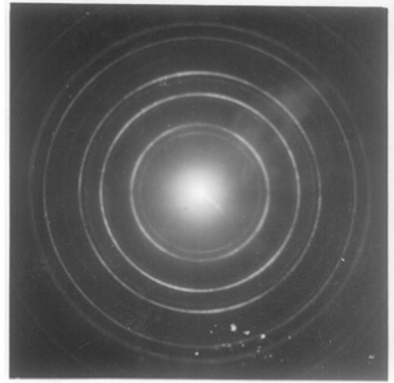


(Fig 30)  
Specimen in Fig 29 Heated at 200°C  
in vacuo for about an hour.

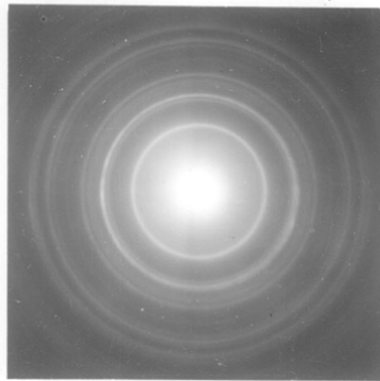


(Fig 31)  
Antimony on Collodion  
at Room Temperature  
Thin Films.



ANTIMONYTABLE - 2

(Ref. page 33)

Analysis of the patternFigure-31

$I/I_0$ observed	d	hkl	$I/I_0$ X-ray A.S.T.M. Card No. 5-0562
vvf	3.55	01.1	47
s	3.12	10.2	100
vf	2.26	01.4	70
s	2.16	11.0	56
vvf	1.92	10.5	12
vf	1.87	00.6	35
m	1.77	02.2	26
vvf	1.57	20.4	15
f	1.41	11.6	63
m	1.38	21.2	67
f	1.32	10.8	40
f	1.27	12.4	30

$$a_0 = 4.29 \text{ \AA}, \quad c_0 = 11.26 \text{ \AA}$$

s - strong  
m - medium  
f - faint

vf - very faint  
vvf - very very faint

patchy and often so thick that the electron beam could not pass through. At a high rate of deposition, the films were normally polycrystalline even at 200°C. It was, however, observed that with a flash evaporation under appropriate conditions, it was possible to get epitaxial growth only at a temperature of about 200°C. Further, because of high rate of re-evaporation of Sb at higher substrate temperature the deposition above 250°C was not possible and in some cases the deposits initially formed on substrates were re-evaporated during cooling in vacuo.

(1) On collodion and polycrystalline sodium chloride

When the deposition was carried out at room temperature on collodion or on polycrystalline sodium chloride the deposit films showed a considerable variation of intensity for different rings when seen by transmission (Fig. 29) and the effect was more pronounced when the specimen was tilted. These features are, no doubt, due to the development of a one degree orientation of the deposits. When the same film was subsequently heated at 200°C for about an hour in a vacuum of about  $10^{-4}$  mm Hg the arcing effects were reduced and the films showed a tendency to form continuous rings (Fig. 30), presumably, due to the rearrangement of the deposits due to heating in vacuo.

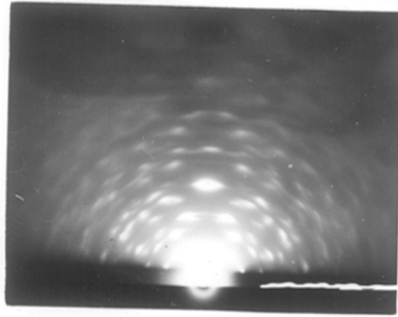


(Fig 32)  
 Thick Sb deposits on glass at  
 Room temperature  $1-d \{12.4\}02n$ .

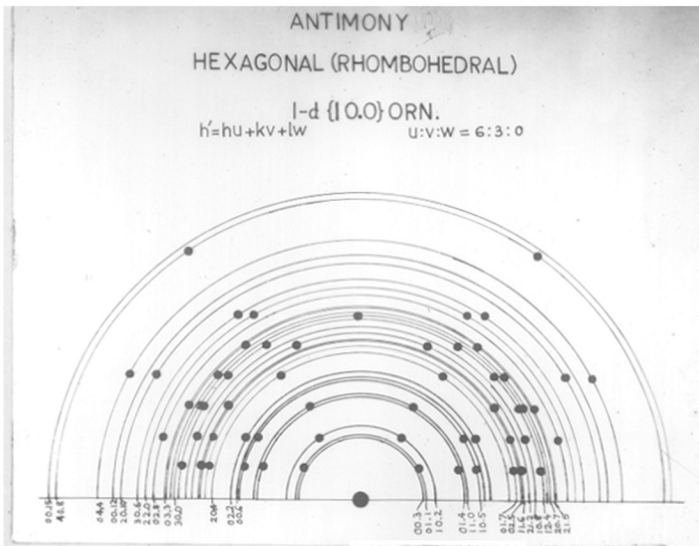


(Fig 33)

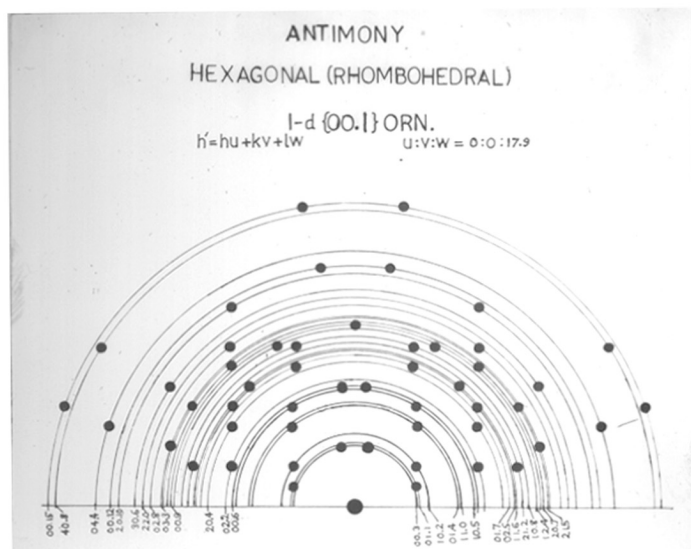


(Fig 34)

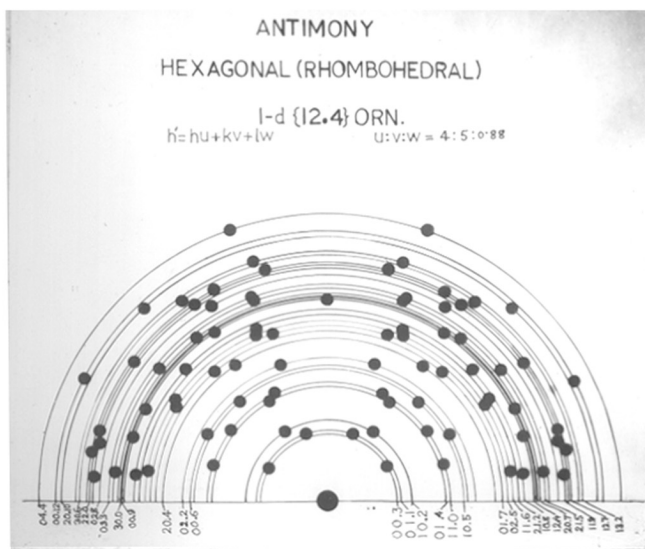


(Fig 35)

Even a very thin film formed at room temperature yielded continuous ring patterns by transmission (Fig.31) but showed arcing of rings on tilting the specimen, thus suggesting the development of a 1-d orientation. Deposits formed at higher temperatures say at about 100°C or 200°C, also had similar features. Analysis (Table-2) of the pattern (Fig.31) shows that the reflections correspond to the hexagonal (rhombohedral) structure of antimony ( $a_0 = 4.307 \text{ \AA}$ ,  $c_0 = 11.273 \text{ \AA}$ ).

(ii) On glass

Deposits formed on glass at room temperature showed some peculiar features, which were not observed so predominantly in the case of bismuth. Figure 32 shows a pattern obtained from antimony formed on glass when deposited at room temperature. The pattern consists of many spots, a little extended, and through which faint rings are passing. This spot type of pattern apparently suggests the development of a 2-d orientation of antimony. It was, however, found that this pattern did not materially change with the change of beam direction with respect to the substrate. These characteristics show that even though the diffraction patterns were of a spot type, these were really due to the development of a 1-d orientation of the deposit crystallites.

It is further seen from the pattern that there can be three strong reflections such as 12.4, 00.9 and 30.0 which

are very near to each other ( $d_{12.4} = 1.261 \text{ \AA}$ ,  $d_{00.9} = 1.252 \text{ \AA}$ ,  $d_{30.0} = 1.243 \text{ \AA}$ ) lying in the plane of incidence, thus suggesting that either one, or two or all of these planes were lying parallel to the substrate surface. In order to decide the orientation and to compare the position of the reflections with the observed ones, theoretical patterns for these three orientations were drawn in the manner described below, keeping in mind that only those reflections which satisfy the rhombohedral conditions given previously (page 29, equation (V)), would appear in the pattern.

Calculations for theoretical patterns with l-d orientation

The theoretical pattern has been calculated by the method developed by Wilman as described below:

For a lattice row  $[uv,w]^*$  to be normal to any plane (hkl) it must have

$$\begin{aligned}
 u:v:w &= \underline{r^*} \cdot \underline{a^*} : \underline{r^*} \cdot \underline{b^*} : \underline{r^*} \cdot \underline{c^*} \\
 &= \frac{1}{a} \left\{ \left( \frac{h}{a} \right) \sin^2 \alpha + \left( \frac{k}{b} \right) (\cos \alpha \cos \beta - \cos \gamma) \right. \\
 &\quad \left. + \frac{l}{c} (\cos \alpha \cos \gamma - \cos \beta) \right\} \\
 &: \frac{1}{b} \left\{ \left( \frac{h}{a} \right) (\cos \alpha \cos \beta - \cos \gamma) + \left( \frac{k}{b} \right) \sin^2 \beta \right. \\
 &\quad \left. + \frac{l}{c} (\cos \beta \cos \gamma - \cos \alpha) \right\} \\
 &: \frac{1}{c} \left\{ \left( \frac{h}{a} \right) (\cos \alpha \cos \gamma - \cos \beta) + \left( \frac{k}{b} \right) \right. \\
 &\quad \left. (\cos \beta \cos \gamma - \cos \alpha) + \left( \frac{l}{c} \right) \sin^2 \gamma \right\} \\
 &\dots (VI)
 \end{aligned}$$

In the case of a hexagonal lattice the above condition reduces to

$$u:v:w = (2h + k) : (h + 2k) : \frac{3}{2} \cdot \frac{l}{(c/a)^2} \quad \dots \text{ (VII)}$$

The diffraction spots, in the case of a 1-d orientation will lie on the layer lines of the order  $h'$ , given by the expression

$$h' = hu + kv + lw \quad \dots \text{ (VIII)}$$

The values of  $h'$  are worked out for each ring, taking into account all the equivalent planes. Ring radii ( $\mathcal{R}$ ) of different reflections can now be calculated from the relation  $\mathcal{R} = \frac{\lambda_L}{d}$ , after assigning any arbitrary value and also knowing 'd' for each hkl reflection. The points of intersection of the rings and layer lines indicate the positions of spots in any 1-d oriented pattern. Thus for a 1-d {10.0} orientation of antimony, which has hexagonal (rhombohedral) structure, 30.0 reflection will be in the plane of incidence.

$$\text{Hence } (hk.l) = (30.0)$$

$$u:v:w = 6:3:0$$

$$h' = 18$$

$$d_{30.0} = 1.243 \text{ \AA} \quad \text{as } \lambda_L = 10 \text{ \AA-cm.}$$

$$\mathcal{R} = 8.04 \text{ cm.}$$

$$\therefore h' \text{ unit} = 0.447 \text{ cm.}$$

Equivalent planes satisfying rhombohedral conditions are  $30.0$ ,  $\bar{3}0.0$ ,  $03.0$ ,  $0\bar{3}.0$ .  $h'$  values are also calculated for all these planes and layer lines are drawn to get the positions of the spots.

Now comparing the position of spots in the theoretical patterns as well as in the obtained pattern, one can see that if both for  $30.0$  and  $00.9$  reflections are to be in the plane of incidence, all the calculated spots will lie on a set of parallel lines, represented by the layer lines (Figs. 33 and 34) which will be quite far off. In the actual pattern these are however very close. When the obtained pattern is compared with the theoretical diagram for  $1-d\{12.4\}$  orientation (Fig. 35), ~~that~~ the disposition of spots in both of them agrees closely. This suggests that the deposits of antimony formed on glass developed a  $1-d\{12.4\}$  orientation.

Patterns produced by films deposited on glass at  $100^{\circ}\text{C}$  or higher temperatures consisted of continuous rings, thus suggesting the polycrystalline nature of the deposits.

(111) On (100) face of rock salt

Deposits of antimony formed on a (100) face of rock salt, between the temperature range of room temperature and about  $150^{\circ}\text{C}$  were polycrystalline in nature.



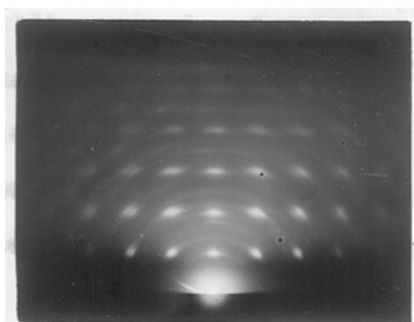


(Fig 36)  
Antimony on (100) Rocksalt at 200c  
Beam  $\langle 100 \rangle$  of Rocksalt. 2-d  $\{10.2\}$  orn.  
normal & anti.

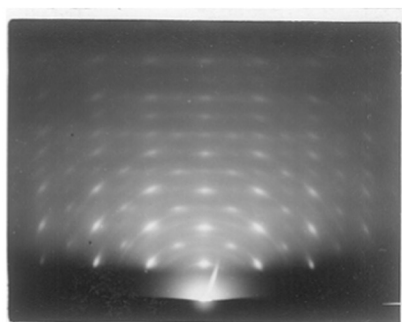


(Fig 37)  
Specimen in Fig 36 Beam  $\langle 110 \rangle$   
of Rocksalt 2-d  $\{10.2\}$  orn.

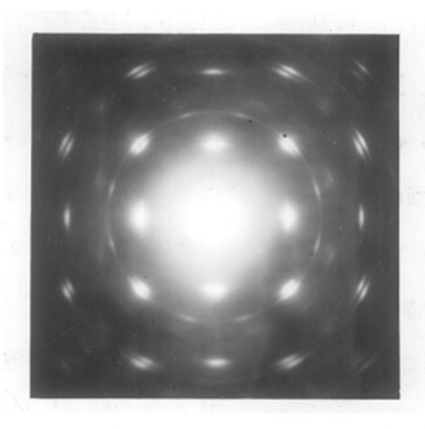


(Fig 38)  
Transmission pattern from  
specimen in Fig 36.  
2-d  $\{30.7\}$  orn.  
normal & anti

The deposits formed at 200°C of the substrate temperature were epitaxial in nature as shown by electron diffraction patterns (Figs. 36 and 37), when the beam was grazing respectively along  $\langle 100 \rangle$  and  $\langle 110 \rangle$  directions of rock salt. The general disposition of the spots suggests a 2-d  $\{100\}$  orientation of the cubic form. A careful measurement of the sides of rectangles in Figure 37 showed that they are in the ratio 1:1.45 instead of  $1:\sqrt{2}$ . Even in Figure 36, it was found neither the sides were exactly in the ratio 1:1 nor the angle between them was exactly 90°. These observations suggest a nearly cubic (pseudo-cubic) structure of antimony as observed before for bismuth.

For a complete analysis hexagonal structure should be taken into consideration. It is seen that in both the patterns, 10.2 reflection and its higher orders are in the plane of incidence, thus indicating that the deposit crystallites developed a 2-d  $\{10.2\}$  orientation of the hexagonal structure. The transmission patterns (Fig.38) from the same specimen were also similar to those of bismuth (cf. Fig.7). In the above the reflections such as  $1\bar{1}.2$  and  $0\bar{1}.2$  which appeared to be at right angles were actually at about  $87^\circ 10'$ . The reciprocal lattice networks were constructed both for reflection and transmission patterns in same way as were in the case of bismuth (cf. Figs. 8 and 9) and the positions of  $(hkl)^*$  corresponded exactly to the observed pattern. It was

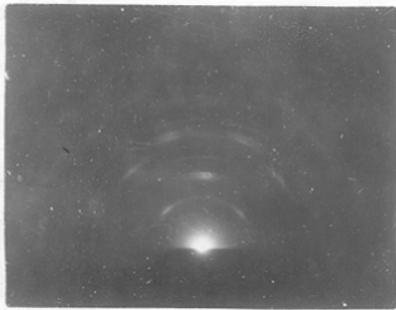


(Fig 39)  
Antimony on (110) of Rocksalt at 200°C.  
Beam  $\langle 100 \rangle$  of Rocksalt  $2-d\{11.0\}$  orn.  
+  $\{01.4\}$  orn.

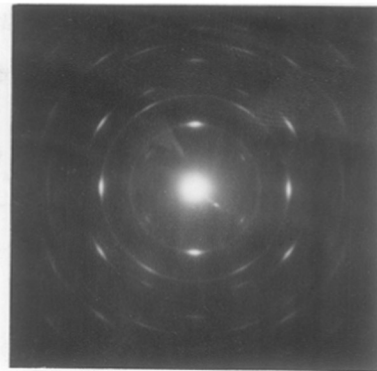


(Fig 40)  
Transmission pattern  
from specimen in fig 39.  
 $2-d\{30.\bar{1}4\}$  orn.

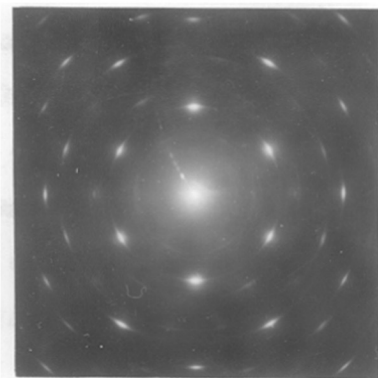


(Fig 41)  
Antimony on Rocksalt (111) at 200°C.  
 $2-d\{00.1\}$  +  $2-d\{1\bar{1}.9\}$  orn. rotated by  $60^\circ$

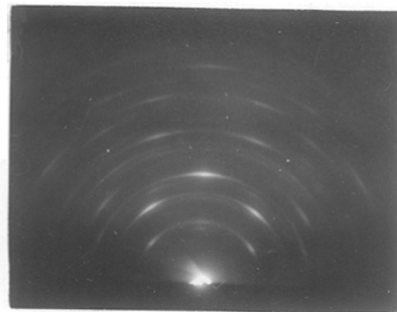


(Fig 42)  
Antimony on mica at 200°C.  
 $1-d\{01.1\}$  orn.

found that the beam direction was  $\langle 42.1 \rangle$  and the deposits had developed a 2-d  $\{10.2\}$  or a 2-d  $\{30.7\}$  orientation.

(iv) On (110) face of rock salt

Deposits of antimony formed upto  $150^{\circ}\text{C}$  on a (110) face of rock salt were polycrystalline in nature. The deposits formed at about  $200^{\circ}\text{C}$  when examined by reflection yielded patterns (Fig. 39) when the beam direction was along  $\langle 100 \rangle$  of rock salt. On rotation of the specimen the pattern changed considerably, but in all cases the 11.0 reflection remained in the plane of incidence, thus suggesting a 2-d  $\{11.0\}$  orientation of the deposit films. Faint spots corresponding to 01.4 reflection are also noted in the plane of incidence which suggest that a few crystallites also developed a 2-d  $\{01.4\}$  orientation of the hexagonal structure. The transmission pattern (Fig. 40) produced by the same specimen showed a network of centred rectangles formed by the 000, 10.2, 02.2,  $\bar{1}2.0$  reflections as in the case of bismuth. From the consideration of a hexagonal structure the beam direction was along  $\langle 21.\bar{1} \rangle$  and the deposit films developed a 2-d  $\{30.\bar{1}4\}$  or nearly a 2-d  $\{10.\bar{5}\}$  orientation. There were a few more reflections in the pattern, thus suggesting an additional orientation.

(v) On (111) face of rocksalt

Films deposited from room temperature to about  $150^{\circ}\text{C}$  on a (111) face of rock salt were polycrystalline in

nature, with or without a preferred orientation. The patterns (Fig. 41) obtained from deposits formed at about 200°C showed an epitaxial growth. The hexagonal disposition of spots corresponds to the reflections such as 11.0 and 30.0 and their higher orders suggest a 2-d  $\{00.1\}$  orientation of the deposits. It may be pointed out that the above orientation alone cannot explain all the spots in the pattern. On a consideration similar to bismuth it was found that 000, 01.1, 20.1 and 11.0 reflections formed rectangular network of spots thus suggesting a 2-d  $\{1\bar{1}.9\}$  orientation of crystallites rotated by 60°. These two orientations fully account for all the reflections observed in the pattern (Fig. 41).

(vi) On cleaved face of mica

The deposition carried out upto 150°C produced polycrystalline films of antimony. Deposits formed at 200°C yielded patterns (Fig. 42) only in one trial out of many. The pattern remained unchanged even on rotating the specimen, while 01.1 reflection and its higher order remained in the plane of incidence thus suggesting a 1-d  $\{01.1\}$  orientation of the antimony deposits.

DISCUSSION

X-ray studies of bulk structure of bismuth show that it has a rhombohedral structure (space group  $D_{3D}^5-R\bar{3}M$ ) with  $a_0 = 4.736 \text{ \AA}$  and  $\alpha = 57^\circ 14' 13''$ . The corresponding hexagonal parameters are  $a_0 = 4.546 \text{ \AA}$  and  $c_0 = 11.86 \text{ \AA}$  (A.S.T.M. Card

No. 5-0519). Antimony has also a similar structure with lattice parameters as  $a_0 = 4.4976 \text{ \AA}$  and  $\alpha = 57^\circ 6' 27''$ . The corresponding hexagonal parameters are  $a_0 = 4.307 \text{ \AA}$  and  $c_0 = 11.273 \text{ \AA}$  (A.S.T.M. Card No. 5-0562).

The present study revealed that even in the thin film state, whether formed at low temperatures or high temperatures, there was no phase change for Bi or Sb films and the  $d_{hkl}$  observed for these films were the same as those for the bulk. The discrepancy observed in the intensity distribution of different rings was, however, due to preferred orientations, which were easily developed during the growth process. The results obtained on single crystal substrates at various substrate temperatures revealed that the epitaxial growth was favoured at higher substrate temperatures. At low temperatures, however, the deposits had a tendency to become polycrystalline with or without a preferred orientation. It was also noted that even at high temperatures deposits had a tendency to become polycrystalline provided the film thickness was high.

#### Orientations and epitaxy of bismuth and antimony films

For interpreting the results, orientations obtained both by reflection and by transmission were taken into consideration. Even though it is comparatively easy to treat the patterns from the pseudocubic point of view, as has been done by some previous workers, the treatment in

this work was given from the hexagonal (rhombohedral) point of view as this method gives more accurate information about the growth process, the orientation relationship etc. between the deposits and the substrates.

During the epitaxial growth both Bi and Sb developed one or more two-degree orientations depending on the nature of the substrate and also on the temperature. The planes of the deposit films, lying exactly parallel to the substrate surfaces were often high indexed ones and sometimes with fractional indices. These fractional indices were, however, simplified by taking the nearest whole numbers.

Detailed considerations of the reflection patterns of Bi on the cube face of rocksalt revealed that the deposits developed mainly 2-d  $\{10.2\}$  normal and anti orientations with a trace of a 2-d  $\{01.1\}$  orientation, but by transmission 2-d  $\{30.7\}$  normal and anti orientations were noted. Similar results were also obtained in the case of Sb. On the (110) face of rock salt Bi developed a 2-d  $\{110\}$  orientation of the pseudocubic form. When considered from the hexagonal point of view the orientation was 2-d  $\{30.\bar{1}4\}$  or nearly  $\{10.\bar{5}\}$ . At higher temperatures say at about  $150^{\circ}$  to  $200^{\circ}\text{C}$  additional orientations namely a 2-d  $\{\bar{1}1.0\}$  and 2-d  $\{11.\bar{7}\}$  (both normal and anti) also developed. In the case of Sb only a 2-d  $\{10.\bar{5}\}$  orientation was observed. On the octahedral face of rock salt both Bi and Sb developed 2-d  $\{00.1\}$  as well as 2-d  $\{\bar{1}\bar{1}.\bar{9}\}$  orientations, but for the later orientation the deposit crystals were rotated by  $60^{\circ}$ . On the

cleavage face of mica the Bi deposits developed in such a way that the basal plane of hexagonal was parallel to the substrate surface. In the case of Sb, however, in spite of several trials no 2-d orientation could be obtained but the deposits had a tendency to develop a 1-d  $\{01.1\}$  orientation.

When substrates were not of single crystal nature or when the deposits on single crystal substrates were thick, the top surface layers of deposits became polycrystalline often with a preferred orientation. Thus Bi and Sb developed respectively 1-d  $\{01.1\}$  and 1-d  $\{12.4\}$  orientations on glass substrates. The ultimate 1-d orientation may, however, change depending on various evaporation conditions especially the rate of deposition, inclination of the substrate with the evaporating filament i.e. the angle of incidence of vapour (Evans, 1950).

As already pointed out more than one orientations developed simultaneously on the same substrate face such as (100), (110) and (111) faces of rock salt. This appears to be related to the possibility of different planes having a similar disposition of atoms conforming to the surface structure of the substrate. It is now well known that accurate matching of atoms in the substrate and deposit contact layers need not always be an essential condition for the epitaxial growth. Even on considering the disposition of atoms in the contact region, the matching of atoms can be possible only at a long range. Hence epitaxy due to a



good fit of atoms does not seem to take place in this case. Effects of temperature and also of the nature of the deposited material on the epitaxial growth were clearly shown by an easy epitaxial growth of Bi films even at  $100^{\circ}\text{C}$  whilst for Sb, temperature was only in the neighbourhood of  $200^{\circ}\text{C}$ .

The apparent discrepancy in the nature of orientations on the same face by reflection and by transmission methods viz. 2-d {10.2} and 2-d {30.7} can easily be explained. It has already been seen in the reflection pattern that 10.2 reflection was not exactly in the plane of incidence but slightly away. This was more clearly visible while considering the higher orders of this reflection. This shows that the plane of orientation was lying very close to (10.2) plane. Considering the orientation from the transmission pattern the angle between (10.2) and (30.7) planes was found to be about  $3^{\circ}$ . This shows why an approximately (10.2) plane appears as the plane of incidence in the reflection patterns. In many of the patterns both normal and anti type of orientations of deposit crystals were observed. These were, no doubt, due to alternative ways in which these planes could grow on the substrate without affecting the matching arrangement.

Even though the interpretations were on the basis of hexagonal structure of Bi or Sb, it was observed that many of the patterns were very much akin to those having nearly a cubic structure (pseudocubic). In fact many of the previous workers have carried out the interpretation of 1-d oriented

patterns from Sb deposited on glass from the pseudocubic point of view. If that is done it was found that 01.1, 10.2 and 11.0 reflections of the hexagonal structure correspond to 111, 200 and 220 of the pseudocubic. Thus a 1-d {211} orientation of the pseudocubic structure as observed by Wilman (1952) corresponds to a 1-d {12.4} orientation of the hexagonal form, which was observed in this work. The reason why pseudocubic structure is often adopted for interpretation of Bi and Sb is that an ideal f.c.c. has a primary rhombohedral structure with  $\alpha = 60^\circ$ , whilst angles in the present case are nearly so i.e. about  $57^\circ 14'$  and  $57^\circ 6'$  respectively for Bi and Sb. Though the patterns from a pseudocubic structure will be approximately similar to those from a f.c.c., the angles between the three axes not being  $90^\circ$  any more, the reciprocal lattice rows therefore for two parallel but opposite beam directions may not coincide thus giving rise to normal and anti-orientations as observed in many cases.

#### Crystal growth process

From the above study of the growth of deposits on different substrates at various substrate temperatures, with varying film thickness it can easily be seen that the growth process of deposits observed especially on single crystal substrates consisted of three stages in sequence viz.

(i) epitaxial layer conforming substrate structure, (ii) polycrystalline deposits indicating change from the influence of

the substrate to the influence of evaporating conditions and temperature, and finally (iii) one degree oriented layer conforming only to the evaporating conditions. A change of conditions in (iii) may lead to a new one-degree orientation.

#### Effect of heating

A significant difference in the behaviour of Bi and Sb in the thin film state was observed when these were heated to about 200°C in vacuum for some time. Whilst bismuth films retained their one degree oriented characteristics even when heated, antimony films on the other hand had a tendency to become randomly disposed though these were initially one degree oriented. It is normally expected that the effect of heating inter alia would generally be to increase the grain size, thus yielding sharper diffraction patterns. The so called "disorientation effect" observed in the case of antimony films suggests that the heat energy was either (i) disturbing the deposit film in such a way so as to cause the above effect (ii) or removing the top deposit layers conforming to 1-d oriented growth leaving behind only the randomly disposed layers over which the one degree oriented layers were formed.

The later alternative appears to be more likely since it is well known that Sb metal sublimes easily whilst Bi does not. Further this sublimation process will be much more facilitated when the metal is in the thin film state. This

is also in accordance with the observations made during different experiments that Sb was difficult to deposit at higher substrate temperatures and even when the deposits were formed, these sublimed easily during the cooling period. Since during the growth process one-degree oriented layers are formed over the randomly disposed polycrystalline layers. Thus due to sublimation the top layers corresponding to 1-d oriented Sb were gradually removed, leaving behind the randomly disposed layers. The above suggestion is in agreement with the general understanding of the crystal growth process.

-----

## CHAPTER - IV

### STUDIES ON THE SUBOXIDE OF BISMUTH (BiO)

#### (A) INTRODUCTION

Bismuth forms two well known oxides namely  $\text{Bi}_2\text{O}_3$  and  $\text{Bi}_2\text{O}_5$ . The existence of the suboxide of bismuth has occasionally been reported but its structure has not yet been fully established. Tanatar (1901) obtained the suboxide by heating the basic oxalate of bismuth which decomposed into bismuth suboxide and carbon dioxide. This compound was previously reported by Schneider (1853 and 1898) but its existence was not confirmed by other workers. Brislee (1908) claimed the formation of BiO by the reduction of  $\text{Bi}_2\text{O}_3$  with carbon monoxide. Treubert and Venino (1914) assumed it to be a mixture of Bi and  $\text{Bi}_2\text{O}_3$ . Herz (1915), however, did not agree with this view. Bhatnagar (1930) observed that both powder and colloidal bismuth contained bismuth suboxide, which was weakly diamagnetic or even paramagnetic. Jenkins (1935) when studying the oxide films of bismuth by electron diffraction method, observed a new hexagonal structure with  $a_0 = 4.02 \text{ \AA}$  and  $c_0/a_0 = 1.57$ ). Bound and Richards (1939) studied by electron diffraction the films of bismuth heated at  $300^\circ\text{C}$  and obtained a face centred cubic structure with  $a_0 = 5.7 \text{ \AA}$ . Acharya (1943) also obtained a face centred cubic oxide of bismuth but having  $a_0 = 5.4 \text{ \AA}$ . Bridge and

Howell (1954) measured the absorption spectrum of bismuth vapour at  $1500^{\circ}\text{C}$  and they attributed the spectrum to  $\text{BiO}$ . Semiletov (1957) studied the oxidation of  $\text{Bi}_2\text{Se}_3$  and  $\text{Bi}_2\text{Te}_3$  films in air, and revealed the presence of a new phase with face centred cubic lattice ( $a_0 = 5.5$  to  $5.6 \text{ \AA}$ ), and this he attributed to the formation of  $\text{BiO}$ , with  $\text{NaCl}$  type structure. Aggarwal and Goswami (1958) studied the oxidation of bismuth films and obtained new forms of bismuth oxide with  $a_0 = 5.65 \text{ \AA}$  and  $7.02 \text{ \AA}$ , both of them being cubic in structure. Recently Zavyalova and Pinsker (1964) have studied the bismuth-oxygen system by electron diffraction and found a new tetragonal variety with  $a_0 = 3.85 \text{ \AA}$  and  $c_0 = 12.25 \text{ \AA}$ , with a composition  $\text{Bi}_2\text{O}_{2.7}$  to  $2.8$ . The same workers (1965) have claimed a hexagonal (rhombohedral) phase of the composition  $\text{BiO}$  with  $a_0 = 3.38 \text{ \AA}$  and  $c_0 = 9.71 \text{ \AA}$ .

The above studies by different workers suggest the formation of new phases of bismuth oxide but whether the oxides with cubic or hexagonal structure obtained by different workers were really bismuth suboxide or not has not yet been proved. In the following work, an attempt has been made to prepare the compound in a suitable way and examine the structure of the compound by electron diffraction methods.

## (B) EXPERIMENTAL

### (a) Preparation of Bismuth Suboxide

Bismuth nitrate was dissolved in water and any opalescence observed was cleared by adding a few drops of

concentrated nitric acid. To the above solution finely powdered oxalic acid was added, when bismuth oxalate was formed. The mixture was further boiled for a few minutes to ensure complete reaction. The precipitate was then washed thoroughly with distilled water to make it free from oxalic acid, then dried at about  $60^{\circ}\text{C}$  and finally preserved in a desiccator.

The above powder of bismuth oxalate was heated to about  $200^{\circ}\text{C}$  at about 0.2 mm of air pressure, when copious evolution of gases took place and the white powder of oxalate decomposed into the suboxide having a black colour. The above temperature and pressure was maintained for some time more to assure the completion of the reaction.

In order to test the BiO content in the above product, a known weight of the powder was taken in a crucible and very cautiously heated by means of a bunsen burner for a sufficiently long time, to convert it into  $\text{Bi}_2\text{O}_3$ . After cooling, the weight of  $\text{Bi}_2\text{O}_3$  formed was found out. From the above analysis it was observed that the BiO content of the specimen was more than 98%. This suggests that at least chemically, the ratio of Bi: $\text{O}_2$  was nearly the same as calculated with the formula BiO.

#### (b) Study of BiO by Electron Diffraction

- (1) The above black powder was then finely ground in an agate mortar and sprinkled over distilled water in a petri dish. The fine layer of sample was picked on a

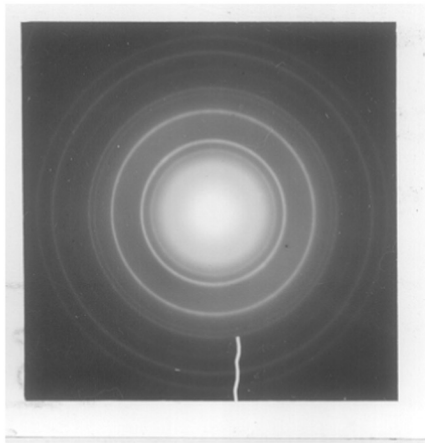


(Fig 43)  
BiO on Collodion by sprinkling  
a fine powder.

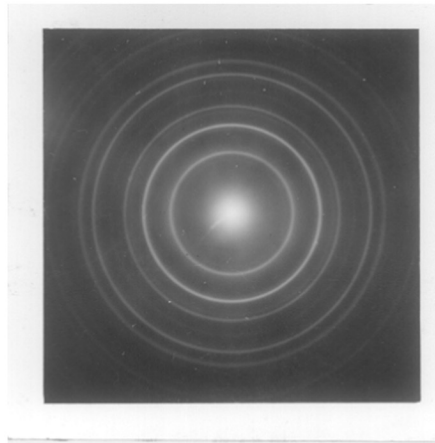


(Fig 44)  
Bismuth produced by decomposition  
of BiO by red hot filament.

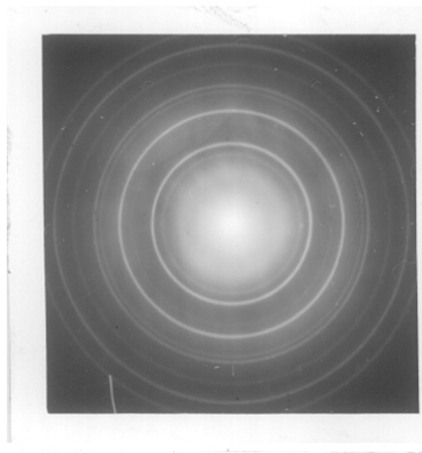


(Fig 45)  
BiO on collodion at room temperature  
Deposition from vapour phase.



BISMUTH SUBOXIDE (BiO)

TABLE - 3

(Ref. page 55)

Analysis of the pattern

Figure-43

$I/I_0$	d	hkl (cubic)	$a_0$ $\text{\AA}$
m	3.28	111	5.69
s	2.85	200	5.70
s	2.01	220	5.68
f	1.72	311	5.71
m	1.65	222	5.72
vvf	1.43	400	5.72
ms	1.27	420	5.70
m	1.16	422	5.68

average  $a_0 = 5.70 \text{\AA}$

s - strong                      f - faint  
ms - medium strong      vvf - very very faint  
m - medium

collodion and examined by transmission in the electron diffraction camera.

- (11) The sample was also evaporated from a kanthal filament (basket) on different substrates at different temperatures such as glass, collodion, different faces of rock salt as well as mica at different temperatures in the usual way and then studied by electron diffraction.

### (C) RESULTS

#### (a) On Collodion by Fine Powder Method

Specimens prepared by the method as described above (experimental - 'b(1)'), yielded patterns as in Figure 43. The pattern consisted of rings, which even on tilting of the specimen with respect to the beam, did not show any change in the intensities of rings or arcing of them, thus suggesting that the films were polycrystalline in nature without any preferred orientation. It is also noted that the diameters of the rings are in the ratio  $\sqrt{3} : \sqrt{4} : \sqrt{8} : \sqrt{11}$  etc. confirming only to all odd or all even indices, thus suggesting a cubic structure with  $a_0 = 5.70 \text{ \AA}$ . Table-3 shows the analysis of the pattern (Fig. 43). Intensity distribution of the different hkl rings, however, suggests NaCl type of structure.

#### (b) Deposition of Bismuth Suboxide from Vapour Phase

##### (1) On collodion

When BiO was deposited on this substrate either at

room temperature or at about  $50^{\circ}\text{C}$  from a Kanthal filament which was glowing red hot, the deposits obtained yielded patterns as in Figure 44. These patterns do not conform to the cubic pattern as seen in Figure 43. Figure 44, on the other hand, appears to be due to bismuth (cf. Fig. 1). Repeated experiments with red hot filament condition always yielded patterns due to bismuth instead of the suboxide. Evaporation of bismuth oxalate under similar conditions also led to the formation of bismuth.

Preliminary experiments showed that the formation of bismuth was linked with the red hot condition of the filament i.e. the temperature to which bismuth suboxide was subjected before evaporation. In order to avoid the excessive heat and hence the decomposition of  $\text{BiO}$  to metallic bismuth, evaporation was carried out at a comparatively lower temperature as for instance only at dull red hot condition of the filament or even below that. Figure 45 shows the patterns obtained at dull red hot condition or below. This pattern is exactly similar to the patterns yielded by the films of  $\text{BiO}$  (cf. Fig. 43). This clearly shows that  $\text{BiO}$  can be obtained even by evaporation if the temperature of the filament was less. Similar results viz. the formation of  $\text{BiO}$  was also observed by a direct evaporation of bismuth oxalate under the same condition. It may be mentioned here that in the above Figure 45, there is an additional ring ( $d = 2.23$ ) which appears to be due to 11.0 reflection of  $\text{Bi}$ .

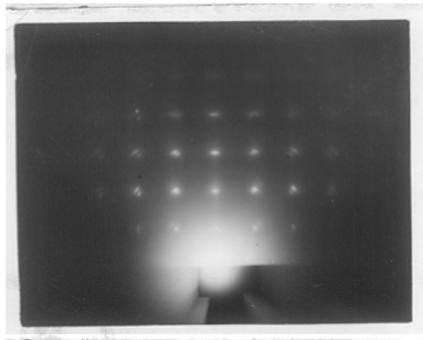


(Fig 46)

BiO on Rocksalt (100) at 200°C.  
Beam  $\langle 100 \rangle$ ; 2-d  $\{100\}$  parallel orn.

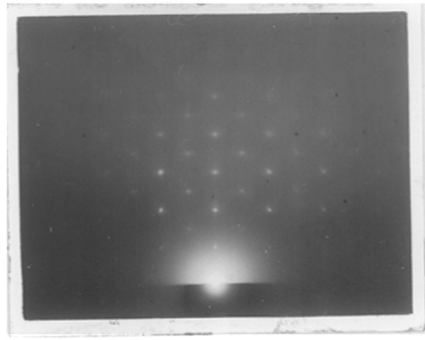


(Fig 47)

Specimen in Fig 46, Beam  $\langle 110 \rangle$   
2-d  $\{100\}$  parallel orn.

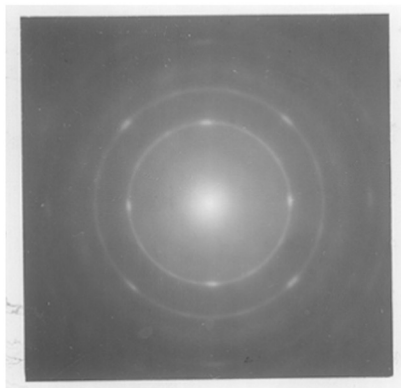


(Fig 48)

Transmission pattern from  
specimen in Fig 46.  
2-d  $\{100\}$  parallel orn.

It was also found that when bismuth oxalate was slightly heated in situ in the diffraction camera a similar pattern due to a cubic structure of BiO was observed.

(ii) On (100) face of rock salt

The deposits formed upto  $100^{\circ}\text{C}$  of substrate temperature were polycrystalline in nature (cf. Fig. 43). Above this temperature the deposits grew epitaxially on the substrate. Deposits formed at about  $200^{\circ}\text{C}$  yielded patterns (Figs. 46 and 47) by reflection when the beam was along  $\langle 100 \rangle$  and  $\langle 110 \rangle$  of the substrate respectively. The disposition of spots in Figure 46 was such that they form a square network with 200, 400 etc. reflections in the plane of incidence. With the beam along  $\langle 110 \rangle$  the pattern changed into centred  $\sqrt{2}$  type of rectangles, again with 200, 400 etc. reflections in the plane of incidence, as seen in Figure 47. These clearly show that the deposits developed a 2-d  $\{100\}$  parallel orientation with respect to the substrate. Transmission pattern (Fig. 48) of the same film also confirmed the above results.

(iii) On (110) face of rock salt

Deposits formed at room temperature and also at about  $50^{\circ}\text{C}$  yielded polycrystalline patterns similar to those in Figure 43. Patterns from deposits formed at  $100^{\circ}\text{C}$ ,

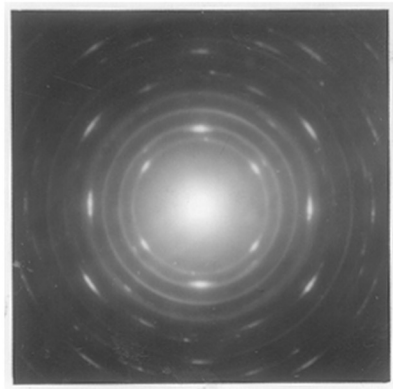


(Fig 49)  
BiO on (110) of Rock salt at 200°C  
2-d {110} orn. Few crystallites  
rotated by 45°.

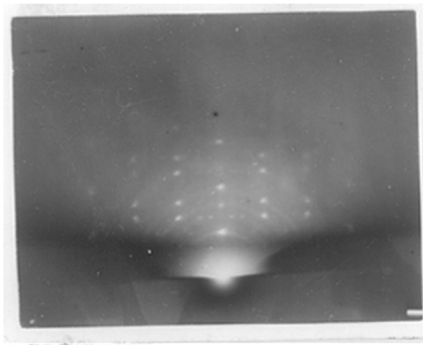


(Fig 50)  
BiO on mica at 200°C.  
2-d {111} orn. & super structure

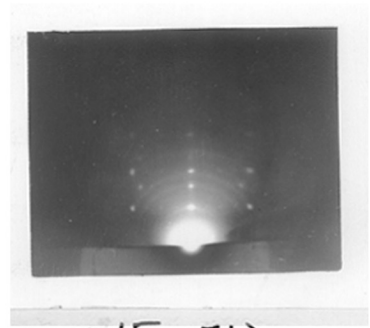


(Fig 51)  
Beam direction changed by  
30° wrt. to fig 50.

consisted of rings as well as spots showing epitaxial growth of BiO. These patterns were not so sharp.

Deposits formed at about  $200^{\circ}\text{C}$  of substrate temperature, yielded patterns (Fig. 49) consisting of spots as well as rings. Centred  $\sqrt{2}$  type rectangles formed by strong spots suggest the development of a 2-d  $\{110\}$  orientation of the deposit crystals. It was further noted that there were additional faint spots, which also formed centred  $\sqrt{2}$  type rectangles, but rotated by about  $45^{\circ}$  with respect to the strong spots. These suggest that the deposits developed a 2-d  $\{110\}$  orientation but some of the crystallites were rotated by about  $45^{\circ}$ . The ring patterns passing through the spots are, no doubt due to the polycrystalline nature of some of the deposit. There are additional rings which are due to bismuth formed during the vacuum decomposition of BiO, as observed previously.

(iv) On cleaved face of mica

Deposits formed at room temperature produced diffuse patterns. Deposits formed at about  $50^{\circ}\text{C}$  and  $100^{\circ}\text{C}$  were polycrystalline in nature as revealed by the ring patterns. The films formed at about  $200^{\circ}\text{C}$  when examined by reflection method yielded spot patterns (Fig. 50) forming  $\sqrt{3}:\sqrt{24}$  type rectangles with spots at  $1/3$  and  $2/3$  distance along the diagonals. The strong spots in the plane of incidence were due to  $111$  reflection and

its higher orders. The pattern changed considerably by changing the beam direction. When the specimen was rotated through  $30^\circ$ , the pattern (Fig. 51) thus obtained consisted of  $\sqrt{3}:\sqrt{3}$  type rectangles with 111 reflection and its higher orders still in the plane of incidence. This suggests that the deposit has developed a 2-d  $\{111\}$  orientation, both normal and anti. Additional faint reflections such as 220 were also noted in the plane of incidence suggesting a 2-d  $\{110\}$  orientation of the deposit. It will be seen that there are a number of additional spots, comparatively weaker present in the patterns. The main spot row along the horizontal direction ~~and~~ is divided into four equal parts by these faint spots, thus giving rise to a superstructure (Fig. 51). The lattice parameter of this superstructure was found to be  $22.84 \text{ \AA}$  i.e. about 4 times the lattice parameter of the cubic structure ( $a_0 = 5.7 \text{ \AA}$ ) of BiO as mentioned previously.

#### (D) DISCUSSION

Previous workers postulated the presence of a suboxide of bismuth (BiO) either from the physical and chemical properties (Schneider, 1853, 1898; Brislee, 1908; Bhatnagar, 1930; Bridge and Howell, 1954), or from the structure study of the oxidised bismuth films (Jenkins, 1935; Bound and Richards, 1939; Acharya, 1948; Semiletov, 1957; Goswami, 1958). None of these studies give any idea about the composition of the postulated suboxide, which according to



Zavvalova and Pinsker (1964), can have intermediate compositions like  $\text{Bi}_2\text{O}_{2.7-2.8}$ .

In the present work the suboxide was prepared by the method described in the experimental part. The method used was that of Tanatar (1901). The suboxide ( $\text{BiO}$ ) thus prepared was studied in the form of fine powder, which avoided the possibility of any decomposition or phase change which is likely to take place when the deposition is carried out from the vapour phase. The intensity distribution of the ring pattern shows that  $\text{BiO}$  thus obtained has a NaCl type structure, with  $a_0 = 5.70 \text{ \AA}$ . Similar patterns were also observed from films obtained by vapour phase deposition. This structure was further confirmed by the disposition of spots in the patterns obtained from epitaxially grown deposits on rock salt (100), (110) faces and also on cleaved face of mica. During the diffraction of electrons by  $\text{BiO}$ , the scattering of electrons will be more predominant by Bi atoms than by oxygen atoms because of the large difference in atomic numbers. Hence even for the 111 reflection intensity will be sufficiently strong, as observed in the pattern (Fig. 43).

As already mentioned before, at a high temperature of the filament and in a high vacuum  $\text{BiO}$  decomposed into Bi. This is similar to the observations made by Herz and Guttman (1907). Bound and Richards (1939) obtained an oxide by the oxidation of Bi films, which they presumed to be  $\text{BiO}$ . The reaction mechanism may be expressed as,



By the law of mass action, the reverse process i.e. the decomposition of BiO will be favoured at a low pressure of oxygen and bismuth will be formed. Under high vacuum conditions, pressure of oxygen becomes very low hence causing the conversion of BiO into Bi even at a comparatively low temperature.

-----

## CHAPTER - V

### STRUCTURE AND GROWTH OF OXIDE FILMS OF

#### BISMUTH AND ANTIMONY

#### PART-1 : OXIDATION OF BISMUTH FILMS

##### A. INTRODUCTION

Three different oxides of bismuth viz.  $\text{BiO}$ ,  $\text{Bi}_2\text{O}_3$ ,  $\text{Bi}_2\text{O}_5$  have been reported. The structure-study of the suboxide ( $\text{BiO}$ ) has occasionally been attempted. A detailed study of the suboxide has already been presented in the previous chapter. In this chapter a study of the oxidation of Bi films under various conditions is reported.

A survey of literature for the oxidation of bismuth films has already been given in the previous chapter. Various workers have proposed different structures for the oxidised films. Jenkins (1935) has given a hexagonal structure with  $a_0 = 4.02 \text{ \AA}$ ,  $c/a = 1.57$ , and Bound and Richards (1939) in the oxidation of Bi films at  $300^\circ\text{C}$  observed a cubic oxide ( $a_0 = 5.7 \text{ \AA}$ ). Sillen (1937), Schumb and Rittner (1943), Aurivilliams and Sillen (1945) reported the existence of polymorphism in  $\text{Bi}_2\text{O}_3$ .  $\alpha$ - $\text{Bi}_2\text{O}_3$  is monoclinic and stable below  $710^\circ\text{C}$  and has parameters  $a_0 = 5.83 \text{ \AA}$ ,  $b_0 = 8.14 \text{ \AA}$ ,  $c_0 = 7.48 \text{ \AA}$ ,  $\beta = 67^\circ 7'$ .  $\beta$ -form of  $\text{Bi}_2\text{O}_3$  is a high temperature modification and has tetragonal structure with  $a_0 = 10.93 \text{ \AA}$ ,  $c_0 = 5.63 \text{ \AA}$ . The  $\gamma$ - $\text{Bi}_2\text{O}_3$  has b.c.c. type structure ( $a_0 = 10.09 \text{ \AA}$ ) and probably contains  $\text{Bi}_{26}\text{O}_{39}$ . In addition

a fourth simple cubic modification with  $a_0 = 5.525 \text{ \AA}$  (Sillen, 1936-38) also exists. Acharya (1948) obtained a f.c.c. oxide of bismuth, with  $a_0 = 5.40 \text{ \AA}$ , during the oxidation of bismuth single crystals. Glemser and Filcek (1952) studied the formation of oxides under various conditions such as (i) heating stoichiometric mixture of Bi and  $\text{Bi}_2\text{O}_3$  at various temperatures, (ii) thermal decomposition of  $(\text{BiO})_2\text{CrO}_4$  or  $\text{Bi}_2\text{O}(\text{CrO}_4)_2$ , (iii) reduction of  $\text{Bi}(\text{OH})_3$  by sodium stannite, and in all cases obtained a mixture of Bi and  $\text{Bi}_2\text{O}_3$ . Aggarwal and Goswami (1958) have studied the thermal oxidation of bismuth films on glass and observed two new f.c.c. modifications with  $a_0 = 5.65 \text{ \AA}$  and  $a_0 = 7.02 \text{ \AA}$ . They have also suggested that the tetragonal variety of  $\text{Bi}_2\text{O}_3$  ( $a_0 = 10.93 \text{ \AA}$ ,  $c_0 = 5.63 \text{ \AA}$ ) could be taken as a superstructure of the oxide with  $a_0 = 5.65 \text{ \AA}$ . It seems from the above survey of the literature that there is a lack of a systematic study of the oxidation process of bismuth. No attempt has been made to study the formation of bismuth suboxide (BiO) by direct oxidation of bismuth films and also the mechanism of oxidation process. In the following work a detailed study has been made to elucidate the above points.

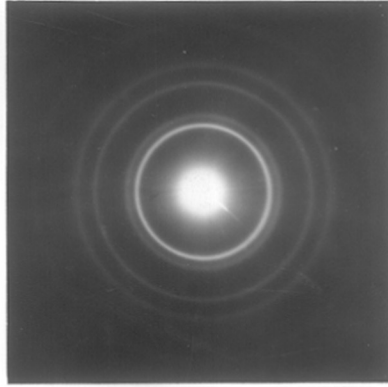
## B. EXPERIMENTAL

Bismuth films were initially deposited in vacuo, on different faces of rock salt at about  $150^\circ\text{C}$  and on collodion at room temperature, in the manner already described in

Chapter-III. These deposits were epitaxial i.e. two degree oriented as well as polycrystalline in nature. These films were then subjected to oxidation at about  $300^{\circ}$ - $350^{\circ}$ C under various conditions of air pressure, as mentioned below and then examined by electron diffraction, in the usual way as described in previous chapters.

### C. RESULTS

In order to set up the appropriate condition of temperature for oxidation at various pressures, preliminary experiments were carried out. It was found that bismuth films formed on collodion when heated in open air at  $100^{\circ}$ C for about an hour did not show any sign of oxidation as revealed by electron diffraction. On raising the temperature to  $200^{\circ}$ C and heating in open air it was observed that after heating for about 2 to 3 hours the films were partially oxidised. At a higher temperature say at about  $250^{\circ}$ C the results were inconsistent in the sense that only thinner films got oxidised even at pressures as low as 0.03 mm of Hg in about an hour's time, whereas thicker films did not, even at higher pressure of about 0.2 mm to 0.3 mm of Hg. When the temperature was in the range of  $300^{\circ}$ - $350^{\circ}$ C, it was found that most of the films were oxidised within a short duration of time, even at a low pressure of about 0.02 mm of Hg. Since oxidation could be easily controlled at this temperature, by varying the pressures, all the study was carried out in the range of  $300^{\circ}$ - $350^{\circ}$ C at various pressures.



Bi<sub>2</sub>O<sub>3</sub>

(Fig 52)  
Bismuth on collodion oxidised  
in open atmosphere. f.c.c. structure

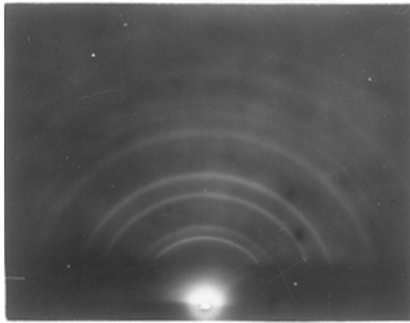


(Fig 53)  
Bismuth film on glass oxidised  
at atmospheric pressure.  
f.c.c. structure

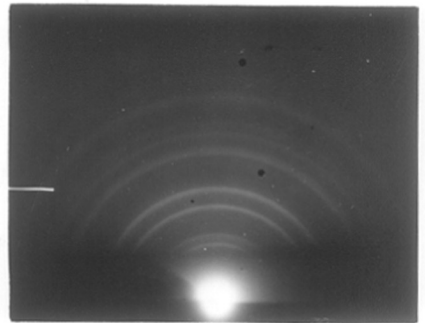


(Fig 54)  
BiO film on glass oxidised  
in open air.  
f.c.c. structure

BISMUTH SESQUI OXIDE (Bi<sub>2</sub>O<sub>3</sub>)

TABLE - 4

(Ref. page 65)

Analysis of the pattern

Figure-52

<u>I/I<sub>0</sub></u> <u>visual</u>	<u>d</u>	<u>hkl</u> <u>(b.c.c.)</u>	<u>hkl</u> <u>(f.c.c.)</u>
vs	3.22	310	111
m	2.72	400	200
m	1.92	440	220
mf	1.66	541	311
mf	1.61	622	222
f	1.25	822	331

b.c.c. a<sub>0</sub> = 10.88 Å      f.c.c. a<sub>0</sub> = 5.44 Å

vs - very strong  
m - medium  
mf - medium faint  
f - faint

(1) On Collodion

(a) Oxidation at atmospheric pressure

Deposits of bismuth formed on collodion at room temperature, were heated by increasing the temperature slowly to about  $300^{\circ}\text{C}$  and these were then maintained for various durations of time ranging between 15 minutes and 2 hours. During the oxidation it was found that the original shining colour of the metal film changed to yellow. These films when examined by electron diffraction yielded patterns (Fig. 52) the analysis of which is given in Table-4. It was found that even though the  $d_{hkl}$  calculated from the pattern corresponded to  $\text{Bi}_2\text{O}_3$  (ASTM Card No.6-0312), the disposition of the rings in the pattern and the visual comparison of the intensities, however, suggest a cubic structure of  $\text{Bi}_2\text{O}_3$  with  $a_0 \simeq 5.44 \text{ \AA}$ . Deposits of Bi and of BiO formed on glass were also oxidised simultaneously and yielded patterns as shown by Figures 53 and 54 respectively, suggesting a cubic structure with the same parameters as above.

(b) Oxidation under reduced pressure

When bismuth films formed on collodion were heated at about  $300^{\circ}\text{C}$ - $350^{\circ}\text{C}$  under a reduced pressure of 2.0 mm of Hg. the deposits of oxide formed yielded patterns similar to those yielded by films oxidised in open air (cf. Fig. 52), thus suggesting the cubic type structure of  $\text{Bi}_2\text{O}_3$ .



$\text{Bi}_2\text{O}_3$

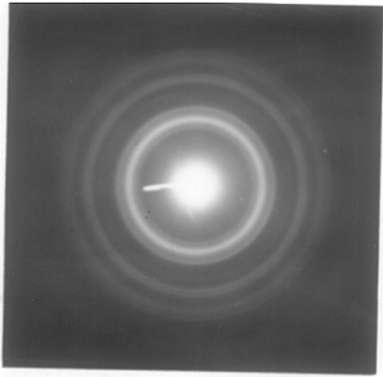


(Fig 55)  
Oxidation of bismuth film on  
collodion at 0.5 to 0.7 mm.

$\alpha\text{-Bi}_2\text{O}_3$

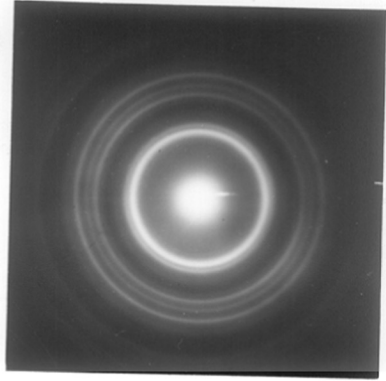


(Fig 56)  
Oxidation of Bismuth films on  
collodion at a press. of 0.2 mm.

$\alpha\text{-Bi}_2\text{O}_3$

Monoclinic  $\text{Bi}_2\text{O}_3$

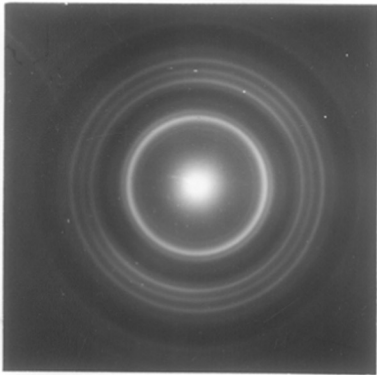


(Fig 57)  
Oxidation of bismuth film on  
collodion at 0.03 mm  $\gamma\text{-Bi}_2\text{O}_3$   
b.c.c.

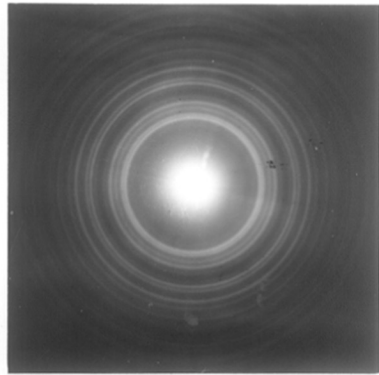


(Fig 58)  
Oxidation of bismuth films on  
collodion at 0.03 mm. Short duration  
 $\alpha\text{-Bi}_2\text{O}_3$  monoclinic

BISMUTH SESQUI OXIDE (Bi<sub>2</sub>O<sub>3</sub>)

TABLE - 5

(Ref. page 66)

Analysis of the pattern

Figure-57 (B203)

<u>I/I<sub>0</sub></u> <u>visual</u>	<u>d</u>	<u>hkl</u> <u>(b.c.c.)</u>
vvf	4.18	211
vf	3.74	220
vs	3.23	310
s	2.74	400
mf	2.38	420
m	1.95	440
mf	1.84	530
m	1.66	640
vvf	1.52	444
f	1.29	822

analysis of the pattern  
average  $a_0 = 10.72 \text{ \AA}$

vvf - very very faint      s - strong  
vf - very faint            mf - medium faint  
f - faint                    m - medium  
vs - very strong

It was found that even at low pressure of 1.2 and 1.0 mm of Hg, results similar to the above were obtained. When the pressure was reduced to about 0.5 to 0.7 mm of Hg, the oxide film obtained by heating bismuth deposit for about one hour yielded pattern (Fig. 55) consisting of some additional reflections which did not fit in the usual f.c.c. structure but conform to a b.c.c. structure with  $a_0 = 10.78 \text{ \AA}$ . The same film, on further heating, for 1 or 2 hours more under the same conditions of temperature and pressure, yielded patterns again showing the f.c.c. structure. The deposits of bismuth oxidised at still lower pressures when examined by electron diffraction (Fig. 56) were found to correspond to the b.c.c. structure, thus suggesting the formation of  $\gamma\text{-Bi}_2\text{O}_3$ . At a pressure of 0.03 mm and when the duration of heating was about half an hour or more, the oxide films yielded patterns (Fig. 57, Table-5) mainly due to  $\gamma\text{-Bi}_2\text{O}_3$ . When the duration of heating was shortened to about only 15 minutes keeping other conditions unchanged a sudden change was observed in the patterns (Fig. 58). They consisted of a very large number of rings, which on analysis were found to be due to a mixture of  $\gamma\text{-Bi}_2\text{O}_3$  (b.c.c.) +  $\alpha\text{-Bi}_2\text{O}_3$  (monoclinic). With the time of oxidation of about 15 minutes and a temperature about  $300^\circ\text{C}$  -  $350^\circ\text{C}$  but with the pressure as low as 0.015 to 0.02 mm., it was found that a number of reflections in these patterns were reduced but the reflections could still be

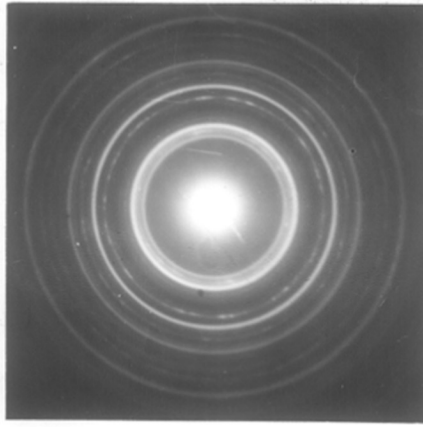


(Fig 59)  
Oxidation of bismuth films on  
collodion at 0.01 mm. Mix of  
 $\text{Bi}_2\text{O}_3$  &  $\text{BiO}$ .

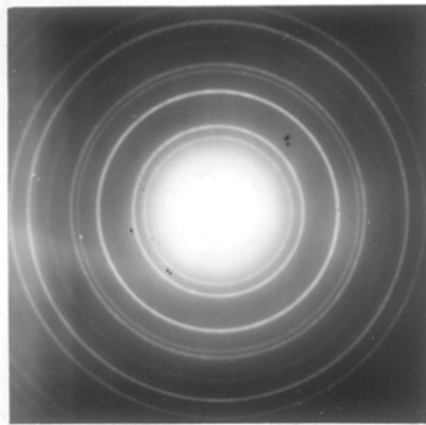


(Fig 60)  
Oxidation of bismuth films on  
collodion at about  $10^{-5}$  mm.  
Formation of  $\text{BiO}$ .

accounted for a mixture of  $\alpha$ - $\text{Bi}_2\text{O}_3$  +  $\gamma$ - $\text{Bi}_2\text{O}_3$ . Further reduction in pressure to 0.010 and 0.005 mm Hg produced oxide films yielding patterns (Fig. 59) which were entirely different from the previous ones. It was found that the reflections due to  $\alpha$  or  $\gamma$ - $\text{Bi}_2\text{O}_3$  practically disappeared, whilst some new strong reflections appeared. It was found that the strong reflections correspond to 111, 200, 220 etc. of the suboxide of bismuth ( $\text{BiO}$ ). This showed that bismuth could be oxidised to the intermediate stage of  $\text{BiO}$  by appropriate adjustment of the conditions of temperature and low pressures. The results of the oxidations carried out under reduced pressure are summarised in the Table-6.

(c) Oxidation at very low pressures (about  $10^{-5}$  mm.)

Bismuth films deposited on collodion support were then heated at about  $350^\circ\text{C}$  in a vacuum of about  $4 \times 10^{-5}$  mm. for about 20 minutes. It was found that the metallic lustre of the films was completely lost and the colour turned grey. The specimens when cooled in vacuo and then examined by electron diffraction, yielded pattern (Fig. 60) consisting of rings. The disposition of the reflections was found to be different from that of  $\text{Bi}_2\text{O}_3$  (cf. Fig. 56). On analysis it was found that the pattern was entirely due to bismuth suboxide ( $\text{BiO}$ ), the structure of which has already been established in Chapter-IV. These experiments conclusively proved that the suboxide was formed

TABLE - 6

(Ref. pages 65,66,67)

Oxidation of bismuth films at different pressures  
at about 300°C

(On collodion support)

	Pressure	Duration of heating	Results
1.	Atmospheric pressure	15 minutes	b.c.c. ( $\gamma$ -Bi <sub>2</sub> O <sub>3</sub> , $a_0 = 10.88 \text{ \AA}$ ) or f.c.c. $a_0 = 5.44 \text{ \AA}$ (Figure 52).
2.	Atmospheric pressure	1 to 2 hrs.	-----"
3.	2.0 mm of Hg	-----"	-----"
4.	1.5 mm of Hg	-----"	-----"
5.	1.0 mm of Hg	-----"	-----"
6.	0.5 to 0.7 mm of Hg	1 hour	Mixture of b.c.c. and f.c.c. (Fig. 55).
7.	0.5 to 0.7 mm of Hg	3 hours	b.c.c. or f.c.c. structure (cf. Fig. 52).
8.	0.2 mm of Hg	1 hour	b.c.c. (Fig. 56). $\gamma$ -Bi <sub>2</sub> O <sub>3</sub> .
9.	0.1 mm of Hg	1 hour	-----"
10.	0.03 mm of Hg	30 minutes	$\gamma$ -Bi <sub>2</sub> O <sub>3</sub> Sharp patterns (Fig. 57).
11.	0.03 mm of Hg	15 minutes	$\gamma$ -Bi <sub>2</sub> O <sub>3</sub> i.e. b.c.c. + $\alpha$ -Bi <sub>2</sub> O <sub>3</sub> i.e. monoclinic (Fig. 58).
12.	0.015 to 0.02 mm Hg	15 minutes	-----"
13.	0.005 to 0.01 mm Hg	15 minutes	Mixture of $\alpha$ -Bi <sub>2</sub> O <sub>3</sub> + presumably BiO (Fig. 59).
14.	About 10 <sup>-5</sup> mm of Hg and about 350°C	About 20 minutes	BiO with f.c.c. structure (Fig. 60)

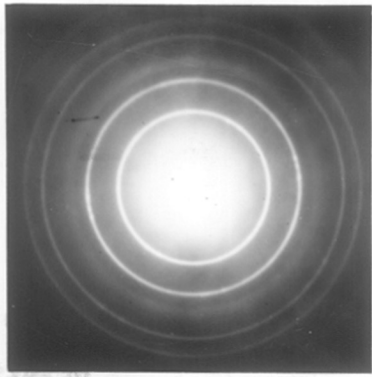


(Fig 61)  
Bismuth films on Rocksalt (100)  
oxidised in open air  
Probably a new cubic phase.

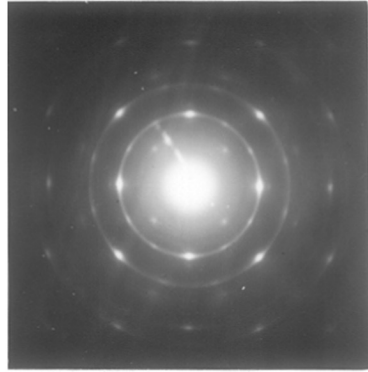


(Fig 62)  
Oxidation of bismuth films  
on Rocksalt (100) at 0.2 nm  
2-d {100} form of b.c.c.  $\text{Bi}_2\text{O}_3$   
rotated by  $30^\circ$ .

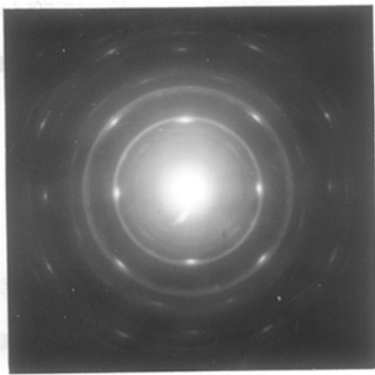


(Fig 63)  
Specimen in Fig 62 heated  
for longer time. 2-d {100}  
b.c.c. Changes to f.c.c.

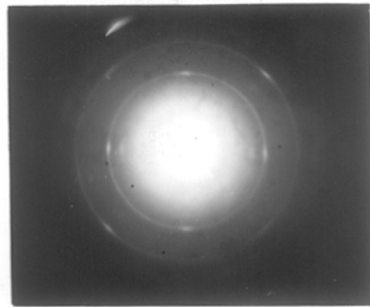


(Fig 64)  
Oxidation of bismuth films on  
Rocksalt (100) at  $10^{-5}$  nm.  
2-d {100} form of  $\text{BiO}$ .

at low pressure, provided that the temperature was favourable for oxidation.

(11) On (100) Face of Rock Salt

(a) Oxidation at atmospheric pressure

Epitaxially grown bismuth films on (100) faces of rock salt, were heated in air for different durations of time varying from 15 minutes to 2 hours. The oxide films formed were invariably yellow in colour. When examined by electron diffraction all these yielded continuous ring pattern (Fig. 61) because of the polycrystalline nature of the oxide films. The disposition of rings and their intensities did not correspond to b.c.c. type of structure. From the visual comparison of intensities and disposition <sup>of</sup> prominent reflections it can be suggested that  $\text{Bi}_2\text{O}_3$  may have formed a new f.c.c. NaCl type structure with  $a_0 \approx 5.84 \text{ \AA}$ .

(b) Oxidation at reduced pressure

Bismuth films grown epitaxially on (100) face of rock salt were heated at about  $300^\circ\text{-}350^\circ\text{C}$  at a pressure of about 0.2 mm for about an hour. The transmission pattern (Fig. 62) obtained from the oxide film consisted of few rings and a centred square type of network of spots suggesting a b.c.c. type structure of the oxide film ( $\gamma\text{-Bi}_2\text{O}_3$ ) which had developed a 2-d  $\{100\}$



orientation. Eight additional spots on 400 and 440 reflections suggest that this orientation was rotated by  $30^{\circ}$ . When the oxidation was carried out at about 0.5 mm pressure for about an hour the films yielded pattern similar to Figure 62. But when these films were further oxidised for one or two hours more it was found that the nature of oxide film was changed and they yielded pattern as in Figure 63. It can be noted that those spots of the centred square networks, which were situated at the corners have become more prominent whilst those at the centres have practically disappeared, suggesting a phase change from b.c.c. to f.c.c.

(c) Oxidation at very low pressure (about  $10^{-5}$  mm.)

Bismuth films deposited on (100) face of rock salt were heated to about  $350^{\circ}\text{C}$  in a vacuum of about  $10^{-5}$  mm. for about 20 minutes. The film lost the metallic lustre and turned grey and yielded pattern (Fig. 64) which on analysis was found to be due to the formation of bismuth suboxide ( $\text{BiO}$ ). From the pattern it is clear that  $\text{BiO}$  films grew epitaxially on rock salt producing a 2-d  $\{100\}$  orientation.

(iii) On (110) Face of Rock Salt

Bismuth films epitaxially grown on (110) face of rock salt were oxidised at  $300^{\circ}\text{C}$ - $350^{\circ}\text{C}$  for about 2 hours at a pressure of about 0.5 mm Hg. The pattern (Fig. 65)

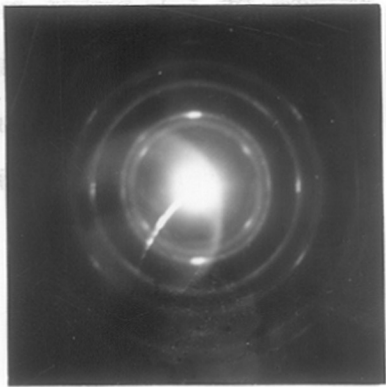


(Fig 65)  
Bismuth films on (110) face of  
rock salt oxidised.  
2-d  $\frac{1}{2}$  form. of  $\text{Bi}_2\text{O}_3$ .

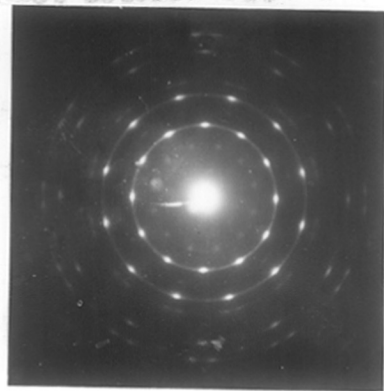


(Fig 66)  
Bismuth films on (111) face of  
rock salt oxidised. 2-d  $\frac{1}{2}$  form  
of b.c.c.  $\text{Bi}_2\text{O}_3$ , rotated by  $30^\circ$ .

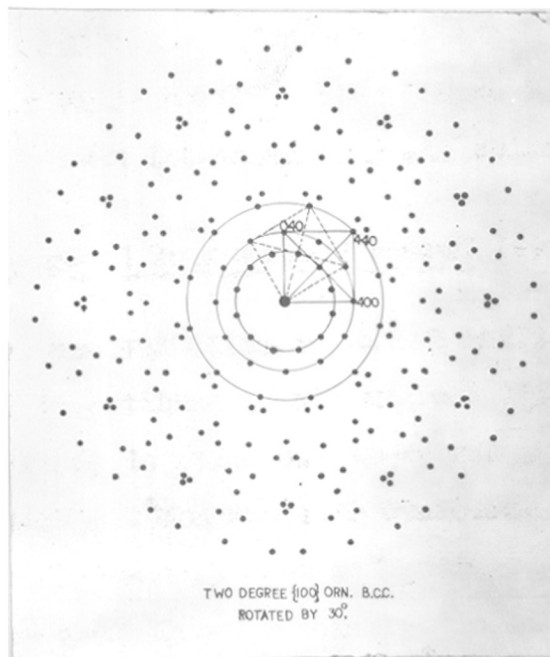


(Fig 67)

obtained from the oxide film consisted of spots and rings. The  $\sqrt{2}$  type centred rectangles formed by the spots suggest a 2-d  $\{110\}$  orientation of the oxide ( $\gamma$ - $\text{Bi}_2\text{O}_3$ ) films. The ring pattern, however, corresponds to the f.c.c. structure ~~as~~ as the spots are lying on the rings due to 111, 200, 220 and 222 reflections.

(iv) On (111) Face of Rock Salt

Bismuth films epitaxially grown on (111) face of rock salt were oxidised at about 0.2 mm. pressure between  $300^\circ$ - $350^\circ\text{C}$  for two hours. The patterns (Fig. 66) apparently complicated, arose from a 2-d  $\{100\}$  orientation of  $\gamma$ - $\text{Bi}_2\text{O}_3$  (b.c.c.), the crystallites being rotated by  $30^\circ$ . This is further confirmed by the construction of the reciprocal lattice, rotated by  $30^\circ$  (Fig. 67) and it is seen that almost all the reflections are thus accounted for.

(v) Vacuum Treatment of  $\text{Bi}_2\text{O}_3$  Films

Bismuth films formed on collodion and on cleavage faces of rock salt were initially oxidised to  $\text{Bi}_2\text{O}_3$ , by heating the films for about two hours at about 0.2 mm. pressure and at a temperature of about  $350^\circ\text{C}$ . Films on both these substrates were yellow in colour and when examined by transmission, yielded patterns corresponding to  $\text{Bi}_2\text{O}_3$  (cf. Figs. 56 and 62).

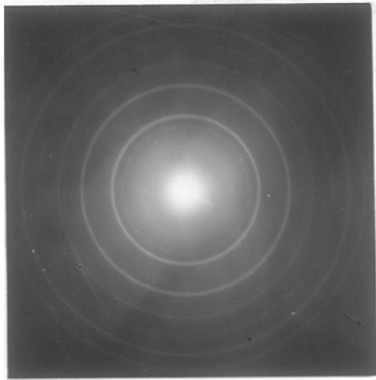


(Fig 68)  
High vacuum treatment of  $\text{Bi}_2\text{O}_3$   
films on collodion. Formation of  
 $\text{BiO}$ .

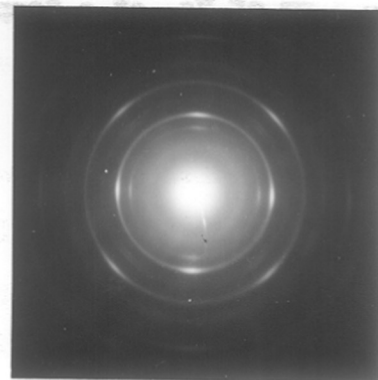


(Fig 69)  
High vacuum treatment of  $\text{Bi}_2\text{O}_3$   
films on rock salt (100)  
2-d {100} of  $\text{BiO}$ .

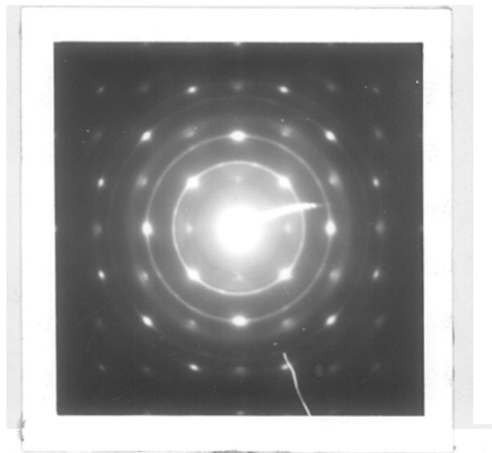


(Fig 70)  
Oxidation of bismuth during  
deposition in low vacuum on  
(100) of rock salt 2-d {100} b.c.c.  
 $\text{Bi}_2\text{O}_3$  rotated by  $30^\circ$ .

These films were then subjected to a vacuum of about  $10^{-5}$  mm of Hg, at a temperature of  $350^{\circ}\text{C}$ , it was found that the colour of original oxide films changed from yellow to grey, in a short time. The heating was, however, continued for 20 minutes or little more. The specimens when cooled in vacuo and examined by electron diffraction yielded patterns of bismuth suboxide (Figs. 68 and 69). The pattern in Figure 68 was obtained by the reduction of  $\text{Bi}_2\text{O}_3$  on collodion in vacuo, whilst Figure 69 comes from a 2-d  $\{100\}$  orientation of  $\text{BiO}$  under similar conditions, by the reduction of epitaxially grown  $\text{Bi}_2\text{O}_3$  on rock salt.

(vi) Oxidation of Bismuth During Deposition

It was observed that if bismuth was deposited in poor vacuum, the deposits instead of having a metallic lustre, developed yellowish colour presumably due to oxidation during evaporation. To test these, the metal was evaporated at about 0.3 mm. of Hg on rock salt at about  $200^{\circ}\text{C}$  for a few minutes. Figure 70 shows the pattern consisting of spots and rings, obtained from such film. It was found that the pattern was due to b.c.c. i.e.  $\gamma\text{-Bi}_2\text{O}_3$  which developed a 2-d  $\{100\}$  orientation on the cube face of rock salt. The presence of four strong and eight faint spots on 400 and 440 rings suggests that a few crystallites have been rotated by  $30^{\circ}$ . It can be further noted that there are also a few very faint reflections, which appear to be due to unoxidised bismuth film.

PART-2 : OXIDATION OF ANTIMONY FILMS

A. INTRODUCTION

Antimony forms three well known oxides namely  $Sb_2O_3$ ,  $Sb_2O_4$ ,  $Sb_2O_5$ . The existence of the suboxide  $SbO$  has recently been reported by Shimaushi (1960) and he has claimed that absorption and emission spectra of  $SbO$  were photographed for the first time. The pentoxide is not formed by the direct oxidation of antimony metal. The tetroxide is formed when  $Sb_2O_3$  is heated in air or oxygen to red heat. Dehlinger (1927) and Natta (1933) found that  $Sb_2O_4$  has a cubic structure. Dihlstrom (1937, 1938), however, proved that this cubic phase was due to  $Sb_3O_6OH$  and not due to  $Sb_2O_4$ , and also showed that  $Sb_2O_4$  has orthorhombic structure ( $a_0 = 4.804 \text{ \AA}$ ,  $b_0 = 5.424 \text{ \AA}$ ,  $c_0 = 11.76 \text{ \AA}$ ). According to Wyckoff (1931) the oxides of antimony present a striking case of several compounds of very different compositions but almost of identical X-ray diffraction patterns. The X-ray patterns from four oxides namely  $Sb_2O_3$ ,  $Sb_2O_4$ ,  $Sb_6O_{13}$ ,  $Sb_2O_5$ , have been obtained. Except  $Sb_6O_{13}$  all are cubic and these yield similar X-ray patterns with similar positions of reflections. The oxide  $Sb_6O_{13}$  gives in addition some faint lines which are not due to the cubic structure.

The trioxide ( $Sb_2O_3$ ) also known as sesquioxide is of common occurrence and exists in two different forms. This dimorphism was demonstrated experimentally by Tutton (1926).

One form known as Valentinite, is stable above  $570^{\circ}\text{C}$  and has an orthorhombic structure with  $a_0 = 4.92 \text{ \AA}$ ,  $b_0 = 12.46 \text{ \AA}$ ,  $c_0 = 5.42 \text{ \AA}$ , as determined by Buerger (1936, 1937-38) from examination of single crystals. The other form known as Senarmonite, is stable below  $570^{\circ}\text{C}$  and has a cubic structure as found by Bozorth (1923) by X-ray examination. This was further confirmed by Almin and Westgren (1941-42) and found  $a_0 = 11.13 \text{ \AA}$ . Bound and Richards (1939) oxidised the antimony films formed on collodion in vacuo and found that no detectable oxidation took place upto  $250^{\circ}\text{C}$  and above this the patterns were due to a cubic structure with  $a_0 = 11.1 \text{ \AA}$ , which was quite well in agreement with  $\text{Sb}_2\text{O}_3$  seen above. Acharya (1948) has studied the oxidation of cleavage face (111) of antimony single crystals by heating in open air and found to yield only a cubic form of  $\text{Sb}_2\text{O}_3$  with  $a_0 = 11.12 \text{ \AA}$ . The structure of valentinite was studied again by Bystrom (1951) and he supported the observations of Buerger (1938) and observed the same lattice parameters for the orthorhombic  $\text{Sb}_2\text{O}_3$ . In the circular published by the National Bureau of Standards, Swanson et al. (1955) have given  $\text{Sb}_2\text{O}_3$  as cubic with  $a_0 = 11.152 \text{ \AA}$  at  $25^{\circ}$ - $27^{\circ}\text{C}$ . Sawaki (1958) has shown that thin films of  $\text{Sb}_2\text{O}_3$  formed by vacuum deposition are useful as achromatic anti-reflection coatings. Akishin et al (1962) have given an account of the molecular structure of  $\text{Sb}_2\text{O}_3$  in gaseous state using electron and neutron diffraction methods.

This survey of the literature shows that nobody has gone into much details of the oxidation process of antimony

films or of the study of epitaxy of antimony oxide. Similarly no attempts have been made to check the existence of the newly reported suboxide ( $SbO$ ) during the oxidation process or its preparation by other methods. Taking these points into consideration the present work has been carried out to study the oxidation process of antimony films and to study the epitaxy of antimony oxide and to test the possibility of the existence of the suboxide ( $SbO$ ).

#### B. EXPERIMENTAL

Antimony films were initially prepared on collodion at room temperature and on rock salt at about  $200^{\circ}C$  in the usual way. These films were then subjected to oxidation at about  $350^{\circ}C$  under different conditions of pressures, varying from atmospheric pressure to 0.2 mm. pressure, as mentioned below, and then examined by electron diffraction in the usual way as discussed in previous chapters.

#### C. RESULTS

Preliminary experiments showed that antimony films formed on collodion when heated in open air for about an hour at  $100^{\circ}C$ , did not show any sign of oxidation, as revealed by electron diffraction. On heating the specimen to the higher temperatures it was found that the films were completely oxidised in open air at about  $300^{\circ}C$  in about half an hour. On heating at lower pressures, say at about 0.5 mm., even at  $300^{\circ}C$  the films were only partially oxidised. On



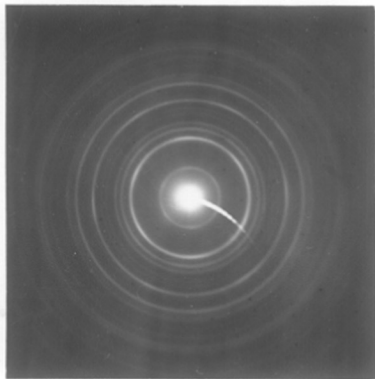


(Fig 71)  
 $Sb_2O_3$  formed by oxidation of  
 antimony films on collodion,  
 in open air.

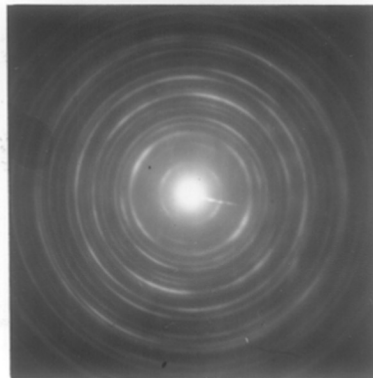


(Fig 72)  
 Highly oriented antimony films  
 produced highly oriented  $Sb_2O_3$ .

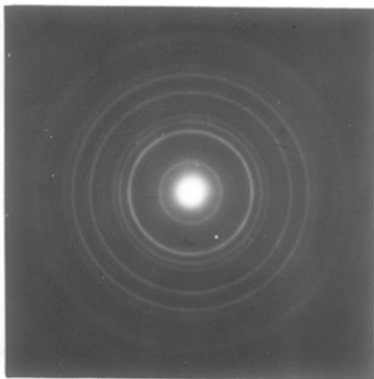


(Fig 73)  
 Oxidation of antimony films  
 on collodion at 2'0 mm.  
 Producing  $Sb_2O_3$ .

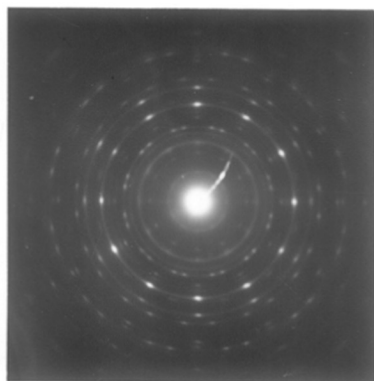


(Fig 74)  
 Antimony films on rocksalt  
 oxidation in  
 (100) face by open air.  
 $2-d\{100\} + 2-d\{111\}$  rotated by  $30^\circ$ .

ANTIMONY TRIOXIDE(Sb<sub>2</sub>O<sub>3</sub>)

TABLE - 7

(Ref. page 75)

Analysis of the pattern

Figure-71

$I/I_0$ visual	d	hkl (f.c.c.)
m	6.45	111
vvf	3.92	220
vs	3.22	222
m	2.78	400
m	2.54	331
vf	2.28	422
vf	2.14	511
ms	1.97	440
ms	1.63	622
f	1.55	711

average  $a_0 = 11.13 \text{ \AA}$

m - medium  
vvf - very very faint  
vs - very strong

vf - very faint  
ms - medium strong  
f - faint

increasing the temperature to about  $350^{\circ}\text{C}$  it was found that oxidation was possible in most of the cases even at pressures of 0.5 mm. in a short duration of about 15 minutes. Oxidation of antimony films was hence further carried out at about  $350^{\circ}\text{C}$  under varying conditions of air pressure.

(i) On Collodion

(a) Oxidation at atmospheric pressure

Antimony films when heated in open air at about  $350^{\circ}\text{C}$  for about 15 minutes, lost their metallic lustre and changed to grey colour. These when examined by electron diffraction yielded ring patterns (Fig. 71), the analysis (Table-7) of which clearly indicated the formation of  $\text{Sb}_2\text{O}_3$  having a cubic structure. Even when the films were heated in open air at  $350^{\circ}\text{C}$  for longer periods, the patterns were similar in nature. It was observed that not only thicker films of antimony were highly oriented but also the corresponding oxide films obtained from them were preferably oriented (Fig. 72). This resembles epitaxial growth on a substrate having a preferred orientation.

(b) Oxidation of antimony at low pressures between 2 mm. to 0.2 mm.

Oxidation of antimony at varying pressures from 2 mm. to lower ranges was also studied. The oxide films formed between 2 mm. to 0.5 mm. of air pressure when examined

by electron diffraction, consistently yielded patterns as in Figure 73, thereby suggesting the formation of  $Sb_2O_3$  with cubic structure. At about 0.2 mm. of air pressure, the film did not show any sign of oxidation even after heating for 2 hours, but after about 3 hours of heating only two strong reflections namely 400 and 440 of  $Sb_2O_3$  appeared in the pattern. Heating at still lower pressures did not show any sign of oxidation even after heating for a longer period. The following Table-8 summarizes the different conditions of oxidation and the results obtained.

(ii) On (100) face of Rock Salt

(a) Oxidation at atmospheric pressure

Antimony films grown epitaxially on rock salt were heated in open air at about  $350^{\circ}C$ . The specimens when examined by reflection did not yield clear patterns. It was observed that spots corresponding to 222 and 400 reflections were in the plane of incidence, thus suggesting the development of 2-d  $\{111\}$  and 2-d  $\{100\}$  orientations. When examined by transmission the specimen yielded patterns (Fig. 74) consisting of a large number of spots. On analysis it was found that the patterns were due to two types of networks of spots viz. (i) consisting of centred rectangles with 000, 220, 044, 224 reflections at the corners suggesting a 2-d  $\{111\}$  orientation, and (ii) rectangles formed by 000, 111, 311,

TABLE - 8

(Ref. pages 75,76)

Oxidation of antimony films at different pressures  
at about 350°C

(On collodion support)

Pressure	Duration of heating	Results
1. Atmospheric pressure	15 minutes	Patterns correspond to f.c.c. structure of $Sb_2O_3$ (Fig. 71).
2. Atmospheric pressure	3 hours	----"---- (Fig. 71)
3. 2.0 mm of Hg	1 hour	----"---- (Fig. 73)
4. 1.0 mm of Hg	3 hours	----"---- (Fig. 73)
5. 1.0 mm of Hg	2 hours	----"---- ----"----
6. 1.0 mm of Hg	1 hour	----"---- ----"----
7. 0.5 mm of Hg	1 hour	----"---- ----"----
8. 0.2 mm of Hg	1 hour	No oxidation
9. 0.2 mm of Hg	2 hours	----"----
10. 0.2 mm of Hg	3 hours	Only 400, 440 of $Sb_2O_3$ developed.
11. 0.1 mm of Hg	4 hours	No oxidation

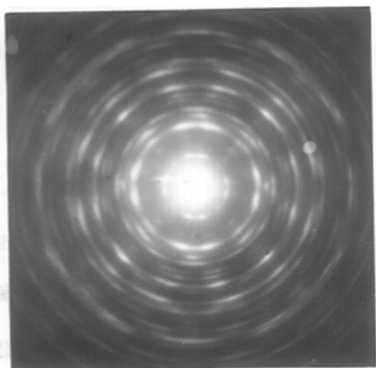


(Fig 75)  
Antimony film on (100) of rock salt  
detached from rock salt and heated.  
 $2-d\{111\} + \{211\}$  rotated by  $30^\circ + \{100\}$   
of  $Sb_2O_3$

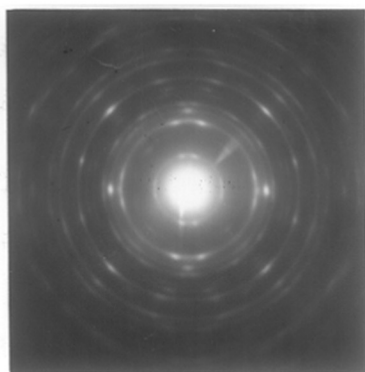


(Fig 76)  
Antimony film on (100) of rock salt  
Oxidised at 1mm.  
 $2-d\{211\}$  rotated by  $30^\circ + 2-d\{100\}$  of  $Sb_2O_3$

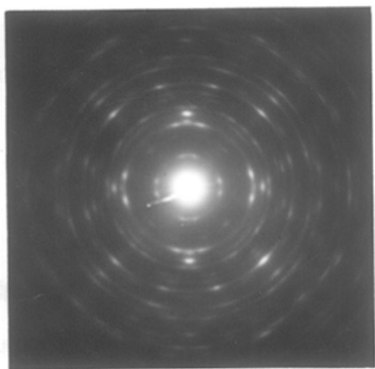


(Fig 77)  
Antimony film Fig 76 heated  
for longer duration developed  
additional  $2-d\{111\}$  form of  $Sb_2O_3$ .

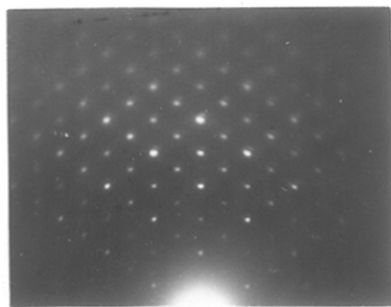


(Fig 78)  
 $Sb_2O_3$  formed during deposition  
of Sb in low vacuum on (100) of  
Rock salt  $2-d\{100\}$  on. Beam  $\langle 110 \rangle$

$Sb_2O_3$

220 reflections due to a 2-d {211} orientation. It was further noted that there were many additional spots which could be explained on the basis of the rotation of the above crystallites by  $30^\circ$ .

When the film of antimony deposited epitaxially on rock salt as in Chapter-III (cf. Fig. 38) was removed from rock salt and then heated in open air at  $350^\circ\text{C}$  for about an hour yielded patterns (Fig. 75). The disposition of spots showed that the oxide deposits developed 2-d {111} + 2-d {211} orientations, both being rotated by  $30^\circ$ , along with an additional 2-d {100} orientation of  $\text{Sb}_2\text{O}_3$  (cubic). This clearly showed that the nature of the epitaxial oxide layer formed on antimony film was influenced more pronouncedly by the orientation of the metal film than by the original substrate of rock salt, on which metal film was grown. This observation was similar to that in the case of oxidation of epitaxial bismuth films.

(b) Oxidation at reduced pressures

The deposits of antimony on (100) face of rock salt were heated at about  $350^\circ\text{C}$  at a pressure of 1 mm. for about an hour. When examined by transmission the specimen yielded patterns (Fig. 76), consisting of a network of spots which on analysis were found to be due to 2-d {100} orientation and a 2-d {211} orientation (crystallites rotated by  $30^\circ$ ) of the cubic  $\text{Sb}_2\text{O}_3$ . When

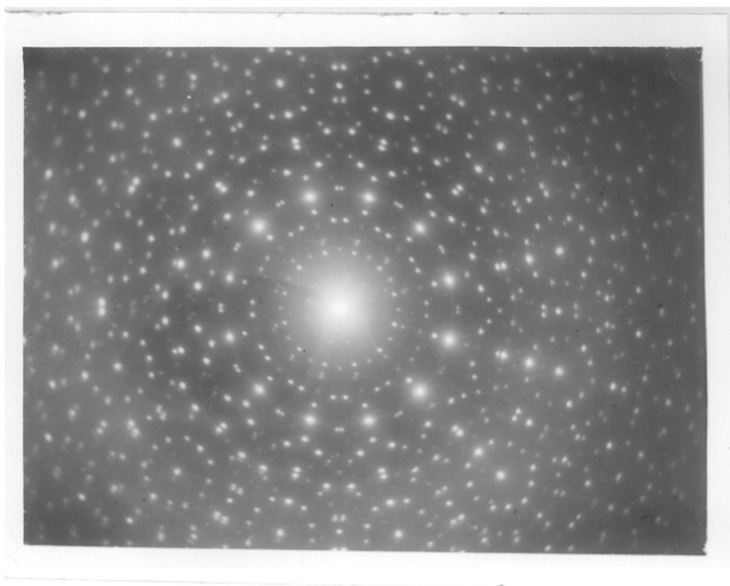


(Fig 79)

Transmission pattern of specimen in Fig 78.  
 $Sb_2O_3$  2-d  $\{100\}$  + 2-d  $\{111\}$  both rotated by  $30^\circ$

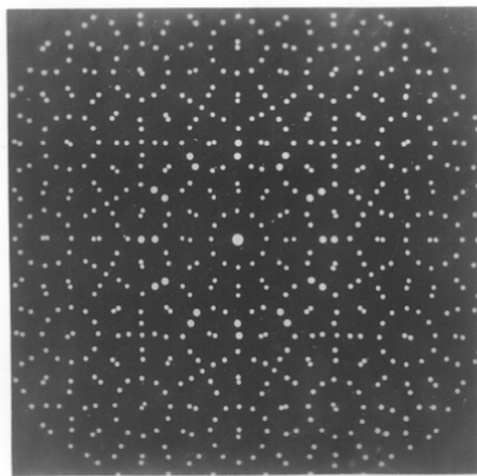


(Fig 81)

Theoretical pattern for 2-d  $\{100\}$   
and 2-d  $\{111\}$  both rotated by  $30^\circ$   
as in fig 79.



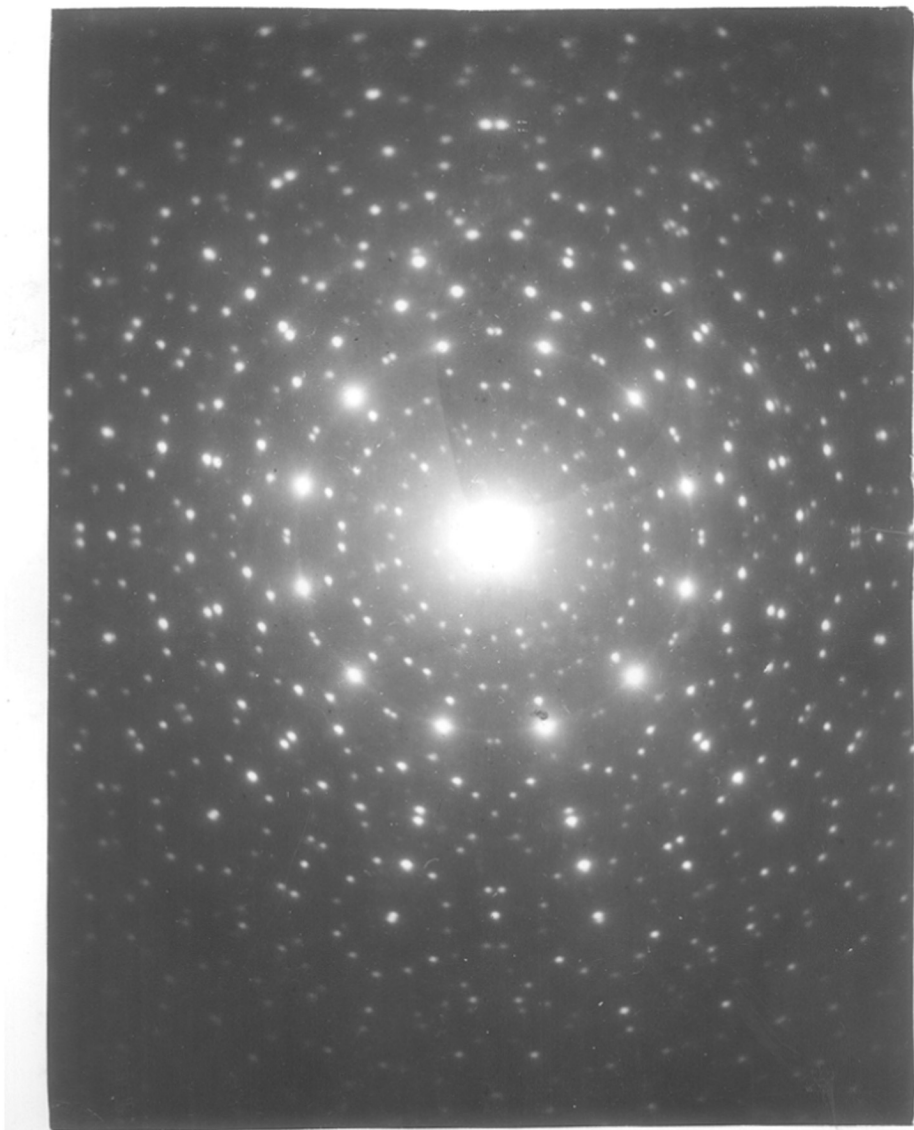


(Fig 80)  
Enlarged Photograph of Fig 79.

the same specimen was heated for about one hour or more yielded pattern (Fig. 77) consisting of additional reflections due to a 2-d  $\{111\}$  orientation, the crystallites being rotated by  $30^\circ$ . The specimen when heated further for an hour the pattern did not change.

On lowering of pressure of oxidation upto 0.5 mm. it was found that patterns as above with similar orientations were produced. When the air pressure as low as 0.2 mm. was employed for oxidation, the film remained unoxidised even after heating for about two hours, as seen previously in the case of oxidation of antimony deposits on collodion. At a lower pressure no oxidation was observed.

### (iii) Oxidation of Antimony During Deposition

Deposition of antimony was attempted rather at a low vacuum of about 0.3 mm. on various faces of rock salt at a substrate temperature of about  $250^\circ\text{C}$ , and it was found that very complicated patterns due to various orientations of the deposits of  $\text{Sb}_2\text{O}_3$  resulted.

#### (a) On (100) face of rock salt

The deposits formed on this face, on examination by reflection yielded pattern (Fig. 78) when beam was along  $\langle 110 \rangle$  of rock salt. The disposition of spots was such that a network of  $\sqrt{2}$  type centred rectangles was formed with higher orders of 100 reflection in the plane of

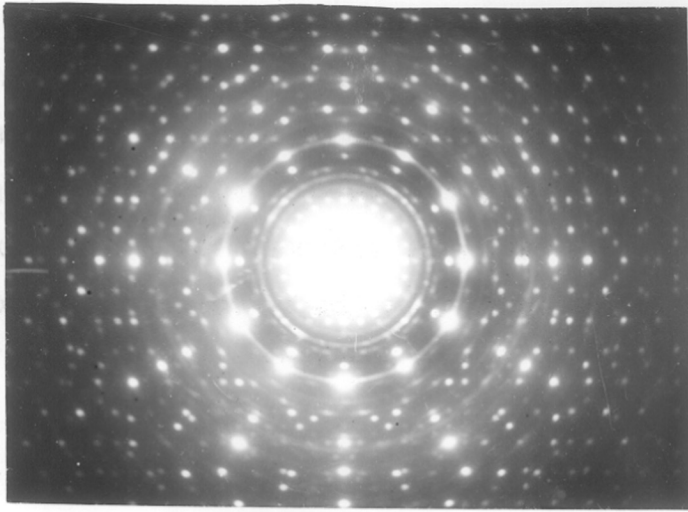


(Fig 82)

$Sb_2O_3$  formed during deposition of Sb in low vacuum on (110) face of rock salt.  $2-d\{111\} + 2-d\{100\}$  orn. both rotated by  $30^\circ$ .

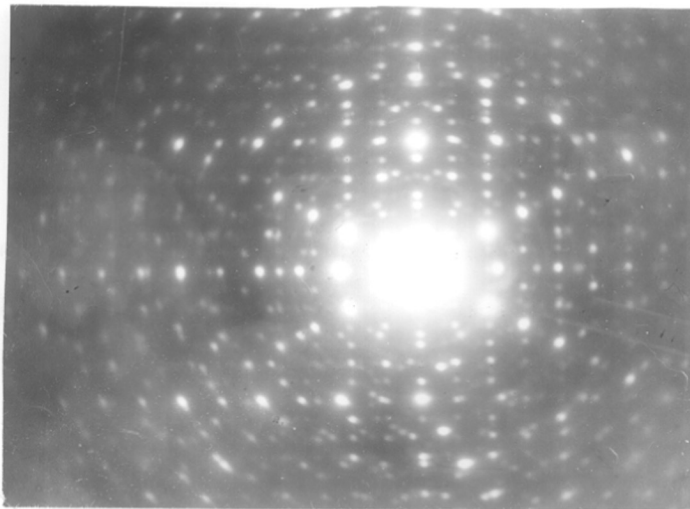


(Fig 83)

$Sb_2O_3$  formed during deposition of Sb in low vacuum on (111) face of rock salt.  $2-d\{100\} + 2-d\{211\}$  orn. both rotated by  $30^\circ$ .

incidence suggesting a 2-d  $\{100\}$  orientation of  $Sb_2O_3$  film. When the same specimen was examined by transmission yielded apparently highly complicated patterns (Fig. 79), which consisted of networks of spots forming picturesque designs. Figure 80 shows an enlarged photograph of the same pattern. On a very careful study it was found that the patterns consisted of networks of spots due to a mixture of a 2-d  $\{100\}$  and a 2-d  $\{111\}$  orientations of  $Sb_2O_3$  crystallites, which were rotated through  $30^\circ$ . A reciprocal lattice network (Fig. 81) constructed for these mixed orientations when compared with the patterns accounted for almost all the reflections as seen in the diffraction patterns. The apparent complexity of the patterns observed in the present case, is due to the appearance of a number of higher order reflections of  $Sb_2O_3$  because of the high lattice parameter of  $Sb_2O_3$  ( $a_0 = 11.15 \text{ \AA}$ ).

(b) On (110) face of rock salt

Deposits formed on this face under the above mentioned conditions when examined by transmission yielded pattern (Fig. 82) which consisted of a network of spots formed due to 2-d  $\{100\}$  and 2-d  $\{111\}$  oriented crystallites rotated by  $30^\circ$ . Though these orientations were similar to those on a (100) face the patterns however appeared to be different from those yielded by the deposits on (100) face. A closer examination revealed that the reflections due to a 2-d  $\{111\}$  orientation in this

pattern were very strong whilst those due to a 2-d {100} orientation were weaker, thus making the pattern apparently look different.

(c) On (111) face of rock salt

Deposits formed on this face yielded spot patterns (Fig. 83) by transmission which appeared to be complicated. On a closer examination it was possible to explain the pattern to be due to two different orientations of  $\text{Sb}_2\text{O}_3$  crystallites. There was a network of very faint spots due to 2-d {100} orientation, whilst the network formed by very strong spots produced by a 2-d {211} orientation of crystallites. Both these oriented crystallites were rotated by  $30^\circ$ .

(iv) Existence of Suboxide of Antimony

From the work described above it was found that oxidation of antimony at and above 0.5 mm. led to the formation of  $\text{Sb}_2\text{O}_3$  (f.c.c.  $a_0 = 11.15 \text{ \AA}$ ). There was no evidence, either for the existence of any other phase of  $\text{Sb}_2\text{O}_3$  or for the suboxide of antimony just as for the suboxide of bismuth. At low pressures say at about 0.2 mm. no oxidation of antimony was noted even after 2 hours of heating at about  $350^\circ\text{C}$ . An attempt was made to prepare suboxide of antimony, in the same way as of bismuth. Antimony oxalate was prepared which was white in colour. This when heated at about  $200^\circ\text{C}$  in a vacuum of 0.2 mm. decomposed into a grey

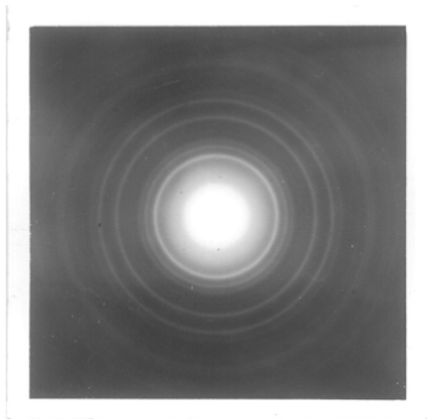


(Fig 84)  
 $Sb_2O_3$  formed by heating  
antimony oxalate in vacuum.

black powder. This was finely ground and when examined by electron diffraction yielded pattern (Fig. 34). On analysis, the pattern was found to be due to the formation of  $Sb_2O_3$ . The decomposition of oxalate was tried a few times by changing the conditions of temperature and pressure, however, it was found that the oxide in every case to be  $Sb_2O_3$  and not any other type of oxide of antimony.

### DISCUSSION

Bismuth sesquioxide ( $Bi_2O_3$ ) exists in different forms viz. monoclinic or  $\alpha$ - $Bi_2O_3$  ( $a_0 = 5.83 \text{ \AA}$ ,  $b_0 = 8.14 \text{ \AA}$ ,  $c_0 = 7.48 \text{ \AA}$ ,  $\beta = 67.7^\circ$ , S.G.  $C_{2H}^5-P2_1/C$  A.S.T.M. Card No.6-C294); cubic b.c. ( $a_0 = 10.09 \text{ \AA}$  A.S.T.M. Card No.6-C312) as revealed by X-ray studies. In addition, other structures such as tetragonal ( $a_0 = 10.93 \text{ \AA}$ ,  $c_0 = 5.63 \text{ \AA}$ ), cubic with different parameters ( $a_0 = 5.65 \text{ \AA}$ , Goswami, 1953;  $a_0 = 5.4 \text{ \AA}$ , Acharya, 1948 etc.) have also been reported to be formed under special conditions.

Epitaxial Bi or Sb films formed on different faces when oxidised under different conditions were also epitaxial in nature depending on the thickness of the film. Even when the metal films were detached from rock salt and oxidised, the oxide layers were two degree oriented as were revealed by the spot patterns.

Oxidation of Bi or Sb was not noted at about  $200^\circ C$  even at a pressure of 0.5 mm. But when these elements were

deposited at about a temperature of  $200^{\circ}\text{C}$  of the rock salt substrate in a low vacuum of about 0.3 mm., the films thus obtained consisted of oxides of Bi and Sb. The patterns produced by these deposits were extremely sharp and picturesque. The apparent ease of oxidation during deposition at low vacuum is due to the fact that at the red hot condition of the filament under the poor vacuum the metals themselves were oxidised during their vapourisation before condensing on the substrates. The oxides thus formed grew epitaxially if the substrate temperature was suitable. Thus the deposits had a better chance of growing epitaxially than in the usual oxidation method, where the oxide had to grow on the substrate metal films which were not usually perfectly 2-d oriented.

#### Orientations of oxide-films of Bi and Sb

Bismuth films epitaxially grown on a cubic face of rock salt when heated in open air invariably produced polycrystalline oxide deposits. Antimony oxide, on the other hand, developed 2-d  $\{211\}$ , 2-d  $\{111\}$  and 2-d  $\{100\}$  orientations, under more or less the same conditions of experiment.

Deposits of Bi on a (100) face of rock salt on oxidation at low pressures produced 2-d  $\{100\}$  orientations of the b.c.c. structure whilst on prolonged heating there was a tendency of this orientation to change into a 2-d  $\{100\}$  of the f.c.c. type. In the case of Sb the oxide film formed



at low pressures consisted of crystallites with 2-d {211} (rotated by  $30^\circ$ ) + 2-d {100} while prolonged heating produced an additional 2-d {111} orientation (rotated by  $30^\circ$ ).

Deposits of Bi on a (110) face on oxidation produced 2-d {110} orientation of  $\text{Bi}_2\text{O}_3$  while on a (111) face produced 2-d {100} (rotated by  $30^\circ$ ) with a b.c.c. structure.

When the deposition of Bi was carried out in a low vacuum, at about  $200^\circ\text{C}$  the pattern was of a 2-d {100} oriented  $\text{Bi}_2\text{O}_3$  with a b.c.c. type of structure, a few crystallites being rotated by  $30^\circ$ . In the case of Sb on a (100) face of rock salt the orientations were 2-d {111} + 2-d {100} for the cubic  $\text{Sb}_2\text{O}_3$  (both rotated by  $30^\circ$ ). On a (110) face the same two orientations were produced and were also rotated by  $30^\circ$ . The deposits thus formed on the octahedral face consisted of 2-d {211} + 2-d {100} oriented crystallites, both being rotated by  $30^\circ$ .

#### Phase changes in the oxidation process

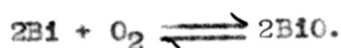
From the study of the oxidation of Bi films carried out in this work it appears that the products of oxidation as well as their structures depend on the conditions of oxidation. The oxidation of Bi films formed on collodion revealed that at very low pressures of about  $10^{-5}$  mm. the films were oxidised to  $\text{BiO}$  (suboxide) with a f.c.c. structure having  $a_0$  about  $5.7 \text{ \AA}$ . The patterns from deposits

of oxide formed at about 0.005 mm. consisted of a mixture of BiO and probably a monoclinic  $\text{Bi}_2\text{O}_3$ . At a little higher pressure say at about 0.015 mm.  $\alpha$ - $\text{Bi}_2\text{O}_3$  i.e. the monoclinic oxide was produced. The d-values of some of the reflections of  $\gamma$ - $\text{Bi}_2\text{O}_3$  (b.c.c.) and  $\alpha$ - $\text{Bi}_2\text{O}_3$  (monoclinic) being very near it was difficult to decide unequivocally the definite structure. Anyhow the overall disposition of the reflections suggested mainly a monoclinic structure. This phase was also observed upto a pressure of 0.03 mm. depending upon the oxidation time. As the pressure was in the range of 0.03 to 1.2 mm. the patterns were due to the formation of a b.c.c. type structure. At still higher pressures the patterns again showed a change from b.c.c. to f.c.c. as previously observed. This observation was also supported by results obtained on rock salt as substrate. Bi films on collodion when heated in open air produced patterns due to a f.c.c. structure with  $a_0 = 5.42 \text{ \AA}$ , whilst the oxide films formed on a rock salt cube face revealed an entirely different f.c.c. type of  $\text{Bi}_2\text{O}_3$  with  $a_0 = 5.84 \text{ \AA}$ . Semiletov (1957) reported a NaCl type structure for the oxide of bismuth with  $a_0 = 5.6 \text{ \AA}$ . This may be due to the presence of BiO for which an f.c.c. NaCl type structure with  $a_0 = 5.7 \text{ \AA}$  has been established in this work. The above study revealed that depending on the air pressure, not only different oxides of bismuth such as ( $\text{Bi}_2\text{O}_3$  and BiO) were formed, but

also different phases of the same oxide ( $\text{Bi}_2\text{O}_3$ ) developed. In the case of antimony, however, only one cubic type of oxide ( $\text{Sb}_2\text{O}_3$  f.c.c.  $a_c = 11.12 \text{ \AA}$ ) without any phase change was noted.

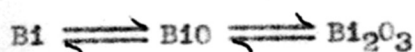
#### Mechanism of oxidation of bismuth

In Chapter-IV it has been shown that  $\text{BiO}$  when heated strongly in vacuum during deposition decomposed to  $\text{Bi}$  by the heat of the filament. Oxidation of bismuth films at a very low pressure shows the formation of  $\text{BiO}$ . Thus the oxidation reaction can be represented as,



When deposits of  $\text{BiO}$  on glass were heated in air,  $\text{Bi}_2\text{O}_3$  was formed. A high vacuum treatment (about  $10^{-5}$  mm Hg) of  $\text{Bi}_2\text{O}_3$  films at about  $350^\circ\text{C}$  transformed them into  $\text{BiO}$ .  $\text{Bi}$  films under the similar conditions were oxidised to  $\text{BiO}$ . Thus a temperature of  $350^\circ\text{C}$  and pressure of about  $4 \times 10^{-5}$  mm. seem to be reasonable conditions for the formation of the suboxide  $\text{BiO}$ .

$\text{Bi}$  film can be oxidised in stages to  $\text{BiO}$  and  $\text{Bi}_2\text{O}_3$ . In high vacuum and at suitable temperature, on the other hand, the reverse process i.e. successive decomposition of  $\text{Bi}_2\text{O}_3$  into  $\text{BiO}$  and  $\text{Bi}$  is favoured (according to the law of mass action). The overall process can be represented by an equilibrium reaction.



Further the structure of  $\text{Bi}_2\text{O}_3$  formed depends on the conditions of reaction.

The above vacuum treatment was not successful in the case of  $\text{Sb}_2\text{O}_3$  in producing any other lower oxide or suboxide presumably because of non-existence of them.

-----

## CHAPTER - VI

### BISMUTH-ANTIMONY-SYSTEM (Bi-Sb)

#### A. INTRODUCTION

Bismuth and antimony both belonging to 5th group of periodic table, form a continuous solid solution. This system was first studied by Bowen and Morris-Jones (1932) who calculated the lattice spacings in terms of f.c. rhombohedral unit cell. Ehret and Abramson (1934) prepared alloys of bismuth and antimony with varying proportions ranging between 0 to 100 %. They found the lattice parameters on the basis of rhombohedral unit cell, which vary from  $a_0 = 4.492 \text{ \AA}$  and  $\alpha = 57^{\circ}5'$  for 100 % Sb to  $a_0 = 4.749 \text{ \AA}$  and  $\alpha = 57^{\circ}16'$  for 100 % Bi, the results being fairly in agreement with those of Bowen and Morris-Jones. The variation of the (110) interplaner spacing of Bi-Sb system with concentration was studied by Hofe and Hanemann (1940). Thermoelectric properties of Bi-Sb were studied by Wright (1958). Electrical resistivity and Hall effect of single crystals of Bi-Sb were measured between  $4.2^{\circ}\text{K}$  and  $300^{\circ}\text{K}$  by Jain (1959). He has also measured by X-ray methods, the lattice parameters in terms of hexagonal (rhombohedral) structure for the entire range of solid solution. Tanuma (1959) also studied the same properties but for 4% to 50% of Sb. Because of the growing interest in semiconducting materials, the semiconducting and electrical properties of

Bi-Sb have been studied in details by Ramazanov (1961), Smith and Wolfe (1962), using various compositions of the alloys, and found that these behave as the small energy gap semiconductors. As regards the structural studies of the Bi-Sb alloys, recently Cucka and Barrett (1962) measured the lattice constants and also the atomic positional parameters for bismuth rich binary solid solutions. They found that lattice constants of Bi-Sb alloys vary linearly in the composition range  $x = 0$  to 30 % Bi and suggested the equations  $a_0 = 4.546 - 23.84 \times 10^{-4} \cdot X$  and  $c_0 = 11.863 - 51.66 \times 10^{-4} \cdot X$  at  $298 \pm 3^\circ\text{K}$ . An electron microscopic study of the structure of the Bi-Sb alloys has been done by Sella et al. (1964). Recently Short and Schott (1965) have reported the construction of a special instrument for the preparation of highly homogeneous single crystals of Bi-Sb alloys.

It is evident from the survey of the literature that very little attention has been paid to the structural study of Bi-Sb alloys in the thin film states, their crystal growth process, epitaxy and orientation relationship. In the following work some of the above properties have been studied.

## B. EXPERIMENTAL

### (i) Preparation of the Alloy

Analytical grade bismuth and antimony were taken in stoichiometric proportion (1:1) in a silica tube, which

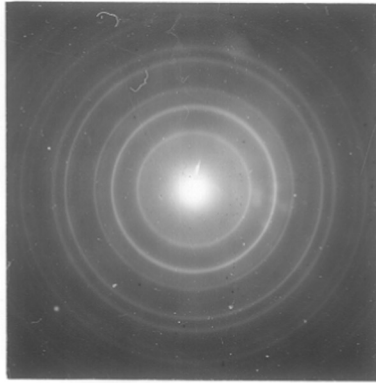


(Fig 85)  
Bi-Sb on collodion at  
room temperature.

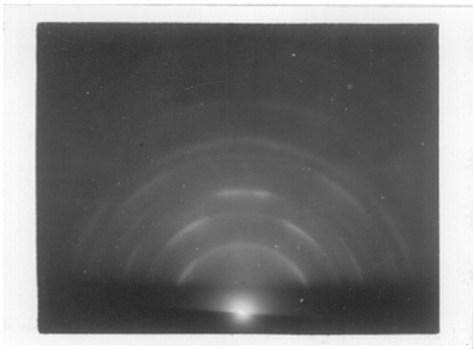


(Fig 86)  
Bi-Sb on glass at room temp.  
1-d {01.1} orientation.

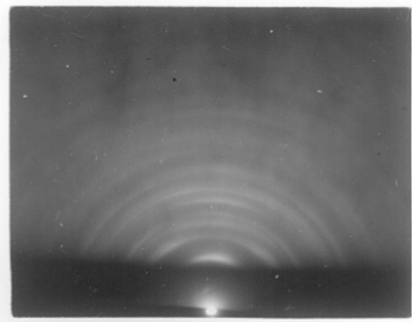


(Fig 87)  
Bi-Sb on glass between 100°  
to 200° C. 1-d {10.2} orientation.

BISMUTH ANTIMONY SYSTEM (Bi-Sb)

TABLE - 9

(Ref. page 90)

Analysis of the pattern

Figure-85

$I/I_0$	d	hkl (hexagonal)
vvf	3.64	01.1
m	3.18	10.2
vvf	2.29	01.4
s	2.20	11.0
vvf	1.87	20.1
m	1.81	02.2
vvf	1.58	20.4
vvf	1.43	11.6
m	1.39	21.2
vf	1.31	12.4
f	1.28	00.9
f	1.26	30.0

$a_0 = 4.38 \text{ \AA}$

$c_0 = 11.52 \text{ \AA}$

s - strong  
m - medium  
f - faint

vf - very faint  
vvf - very very faint



was then evacuated and sealed. It was then slowly heated in a furnace to about 800°C and maintained at this temperature for about twenty four hours. The tube was then quenched by dropping in water and the alloy thus formed was used for deposition.

#### (11) Deposition of the Alloy Films

Bismuth-antimony alloy (Bi-Sb) thus obtained was then vacuum deposited at about  $10^{-4}$  mm of Hg on different substrates such as collodion, polycrystalline sodium chloride, glass, various faces of rock salt, as well as on cleavage faces of mica at various temperatures. The deposits were then examined in the usual manner. During the preliminary experiments it was, however, noticed that when the deposition was carried in the usual way, the patterns consisted mostly of antimony. On the other hand if flash evaporation method was adopted, the patterns were due to Bi-Sb films. Hence in all the subsequent experiments this technique was followed.

### C. RESULTS

#### (1) On Collodion and Polycrystalline

##### Sodium Chloride

Deposits formed on the above substrates between the range of room temperature to 200°C, yielded patterns (Fig.85) consisting of continuous rings, which did not break even on tilting the specimen, thus suggesting that the polycrystalline deposits did not develop any preferred orientation.

The d-values of the rings were calculated using graphite ( $11\bar{2}0$  reflection,  $d = 1.23 \text{ \AA}$ ) as standard (Table-9). From the earlier studies of Bi-Sb system by X-ray, it is known to have a rhombohedral unit cell or modified hexagonal structure. The d-values as obtained from the above electron diffraction patterns were therefore compared with a chart for hexagonal structure and it was found to correspond very well for a c/a ratio about 2.65. All the observed reflections were then given provisional indices, satisfying the rhombohedral conditions (expression (V), page-29). Lattice parameters were however determined from single crystal patterns as explained later on.

#### (ii) On Glass

Deposit of Bi-Sb on glass at room temperature produced polycrystalline films with or without a preferred orientation, depending on the thickness of the films. Figure-86 shows a pattern from thicker deposits having a preferred orientation. The presence of 02.2 reflection in the plane of incidence suggests the formation of a 1-d  $\{01.1\}$  orientation of the hexagonal (rhombohedral) structure. The films formed at  $100^{\circ}\text{C}$  and  $200^{\circ}\text{C}$  of the substrate temperature, however, developed a 1-d  $\{10.2\}$  orientation (Fig. 87).

#### (iii) On (100) Face of Rock Salt

Deposits formed at room temperature and also at  $100^{\circ}\text{C}$  on this face were polycrystalline in nature, as revealed by

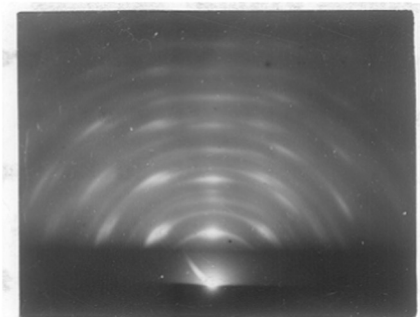


(Fig 88)  
Bi-Sb on Rock salt (100) at 200°C.  
Beam  $\langle 100 \rangle$  of Rock salt  
 $2-d\{10.2\} + \{01.1\}$  orientation

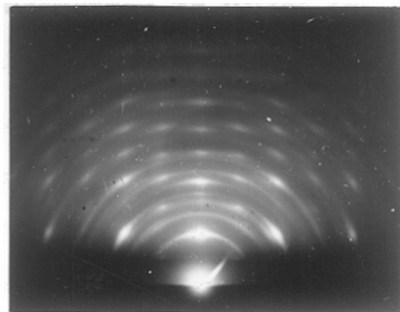


(Fig 89)  
Specimen in 88, Beam  $\langle 110 \rangle$  of  
Rock salt  
 $2-d\{10.2\} + \{01.1\}$  orientation

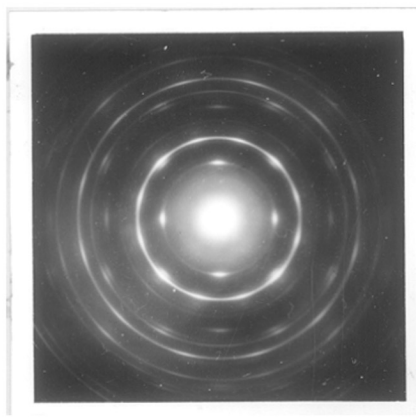


(Fig 90)  
Transmission pattern from  
specimen in Fig 88.  $2-d\{00.1\}$   
+  $2-d\{30.7\}$  orientation.

the diffraction patterns. Bi-Sb films deposited at 200°C and 300°C of substrate temperatures yielded patterns (Figs. 88, 89) by reflection when beam directions were respectively along  $\langle 100 \rangle$  and  $\langle 110 \rangle$  of rock salt. Assuming that the provisional h,k,l indices assigned to the different d-values were correct, it was observed that strong 10.2 and faint 01.1 reflections were in the plane of incidence thus suggesting a 2-d  $\{10.2\}$  + 2-d  $\{01.1\}$  orientations of the deposit crystals. These observations were similar to those observed for bismuth or antimony films formed over rock salt.

These specimens when examined by transmission yielded patterns as shown in Figure-90. The d-values for different spots and rings were found out by using graphite as standard. It was seen that the pattern consisted of reflections of various types such as hk.0, 0k.1, h0.1. The values of lattice parameters for the hexagonal structure were found from the different observed reflections (hk.l) using the relations,

$$r^{*2} = 1/d^2 = (h^2+hk+k^2) a^{*2} + l^2 c^{*2} \quad \dots \text{ (IX)}$$

$$a^* = \frac{2}{a\sqrt{3}} \quad \dots \text{ (X)}$$

$$c^* = 1/c \quad \dots \text{ (XI)}$$

With the help of expressions (IX) and (X),  $a^*$  and  $a_0$  were calculated from hk.0 type reflections. Using the value of

$a^*$  in expression (IX),  $c^*$  was found out with the help of  $0k.l$ ,  $h0.l$ ,  $00.l$  or  $hk.l$  type reflections, and hence  $c_0$  was calculated by expression (XI). It was thus found that the hexagonal parameters were  $a_0 = 4.38 \text{ \AA}$  and  $c_0 = 11.52 \text{ \AA}$ . Using the above values of  $a$  and  $c$  the  $d_{hkl}$  values for various reflections were calculated using the formula given below,

$$d_{hkl} = \frac{1}{\sqrt{\frac{4}{3} \cdot \frac{h^2 + hk + k^2}{a^2} + \frac{l^2}{c^2}}} \quad \dots \text{ (XII)}$$

and were found to be in good agreement with observed values.

From the hexagonal parameters  $a_0$  and  $c_0$  the rhombohedral parameters were also evaluated using the expression,

$$a_R^2 = \frac{a_0^2}{3} + \frac{c_0^2}{9} \quad \dots \text{ (XIII)}$$

$$\sin \frac{\alpha}{2} = \frac{3}{2\sqrt{3 + \frac{c_0^2}{a_0^2}}} \quad \dots \text{ (XIV)}$$

and found to be  $a_R = 4.63 \text{ \AA}$  and  $\alpha = 56^\circ 50'$ . These parameters were also confirmed with the help of patterns yielded by deposits from (110) and (111) faces.

When the indices were confirmed in this way, it was found that nearly a square network was formed by reflections such as  $000$ ,  $11.\bar{2}$ ,  $1\bar{2}.0$ ,  $0\bar{1}.2$ . On detailed consideration of the positions of the reflection spots as was done in case of bismuth, it was concluded that Bi-Sb<sub>deposits</sub> had their (30.7) plane

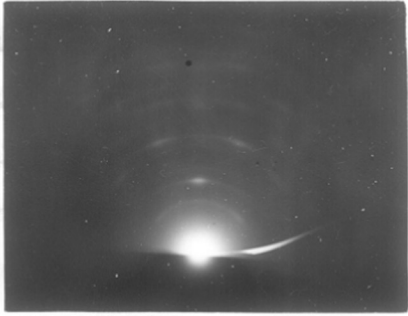


(Fig 91)  
Bi-Sb on Rock salt (110) at 200°C.  
Beam  $\langle 100 \rangle$  of Rock salt  
2-d  $\{11.0\}$  orientation

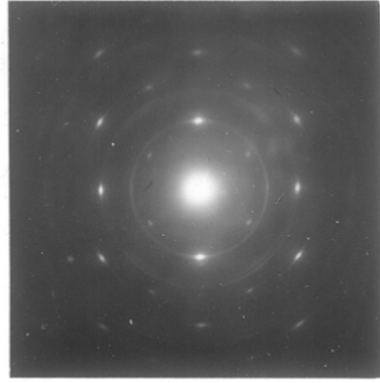


(Fig 92)  
Transmission Pattern from  
specimen in figure 91.  
2-d  $\{30.14\}$  orientation.

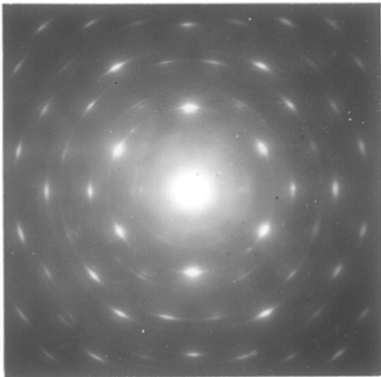


(Fig 93)  
Bi-Sb on (111) of Rock salt at  
200°C. 2-d  $\{00.1\} + \{1\bar{1}.3\}$  orientation

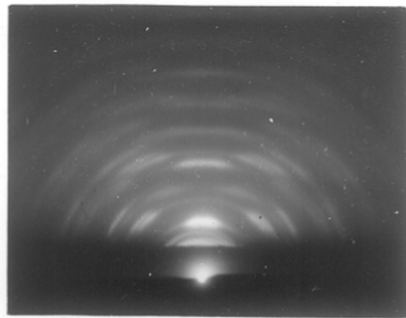


(Fig 94)  
Bi-Sb on mica at 200°C.  
1-d  $\{10.2\}$  orientation.

parallel to (100) face. Hence a 2-d  $\{30.7\}$  or approximately a 2-d  $\{10.2\}$  orientation was developed. Similarly the presence of 01.4 reflections which were just inside the 11.0 reflections was due to both the normal and anti orientations. These orientations alone cannot explain the eight extra spots lying on 11.0 ring. A closer examination revealed that faint spots (arcs) due to 30.0 reflections were also present. The hexagonal network of spots formed by different reflections such as 11.0 and 30.0 were no doubt, due to a 2-d  $\{00.1\}$  orientation, but the presence of 12 spots on 11.0 and 30.0 rings can be explained by a rotation of the  $\{00.1\}$  oriented crystallites through  $30^\circ$ . The deposits formed at  $300^\circ\text{C}$  of the substrate temperature yielded transmission patterns, which on analysis were found to be only due to a 2-d  $\{30.7\}$  or approximately a 2-d  $\{10.2\}$  orientation.

(iv) On (110) Face of Rock Salt

Deposits formed upto  $100^\circ\text{C}$  of substrate temperature, yielded patterns due to randomly disposed crystallites of Bi-Sb. Deposits formed between the temperature range of  $200^\circ\text{C}$  and  $300^\circ\text{C}$ , yielded faint spot patterns (Fig. 91) by reflection, with the 11.0 reflection of the hexagonal structure, in the plane of incidence when the beam was along  $\langle 100 \rangle$  of rock salt substrate. This suggested a 2-d  $\{11.0\}$  orientation of the hexagonal (rhombohedral) structure.

The above specimens when studied by transmission yielded patterns (Fig. 92) consisting of rings and spots. The disposition of the spots was such that they produced nearly  $\sqrt{2}$  type centred rectangles with 000, 10.2, 02.2,  $\bar{1}2.0$  reflection spots were at the corners while 01.1 reflection was at the centre. This disposition of spots, as was in the case of bismuth and antimony, suggests that the beam direction was  $\langle 21.\bar{1} \rangle$  and the plane perpendicular to this direction was  $(30.\bar{1}4)$ . These observations show that Bi-Sb films developed a 2-d  $\{30.\bar{1}4\}$  or approximately a 2-d  $\{10.\bar{5}\}$  orientation of the hexagonal (rhombohedral) structure. Thus the deposits developed both  $\{11.0\}$  and  $\{10.\bar{5}\}$  orientations.

(v) On (111) Face of Rock Salt

Deposits formed upto  $100^{\circ}\text{C}$  of substrate temperature were polycrystalline in nature as revealed by the diffraction patterns. Deposits formed at about  $200^{\circ}\text{C}$  and  $300^{\circ}\text{C}$  yielded patterns (Fig. 93) which were very similar to those of bismuth and antimony. The patterns showed two distinct networks of spots viz. (i) a hexagonal network formed by 000, 11.0, 30.0 reflections suggesting a 2-d  $\{00.1\}$  orientation, (ii) a rectangular network rotated by  $60^{\circ}$  formed by spots due to reflections such as 000, 11.0, 20.1, 01.1 as a result of a 2-d  $\{1\bar{1}.\bar{9}\}$  orientation. In the patterns from deposits formed at  $200^{\circ}\text{C}$ , reflections due to both these orientations were prominent, but in the case of deposits formed at  $300^{\circ}\text{C}$ , reflections due to  $\{1\bar{1}.\bar{9}\}$  orientation were comparatively weaker.



(v1) On Cleaved Faces of Mica

Patterns yielded by the deposits of Bi-Sb formed upto  $100^{\circ}\text{C}$  on mica, were mainly polycrystalline in nature with a little preferred orientation of the (10.2) type planes. Deposits formed at  $200^{\circ}\text{C}$ , yielded patterns (Fig.94), consisting of rather elongated spots, with 10.2 and its higher order reflections in the plane of incidence. The pattern, however, did not change on changing the beam direction, suggesting that Bi-Sb films developed a 1-d {10.2} orientation on mica.

D. DISCUSSION

Both Bi and Sb belong to the  $v^{\text{th}}$  group of the periodic table and are mutually soluble for all compositions. It appears that these do not form any distinct intermetallic compound. X-ray studies of the bulk structure of Bi-Sb system have shown that these alloys have also rhombohedral structures, but the lattice parameters varied with the composition of the alloy. Thus the parameters  $a_R$  and angle  $\alpha$  vary gradually from  $4.492 \text{ \AA}$  and  $57^{\circ}6'$  for 100% Sb to  $4.749 \text{ \AA}$  and  $57^{\circ}16'$  respectively for 100% Bi. These variations were studied by Ehret (1934) in terms of rhombohedral parameters while by Jain (1959) in terms of the corresponding hexagonal structure and has shown graphically the variation of lattice parameters with percentage composition of Bi-Sb. From these observations an alloy with 50% composition (1:1 atomic proportion of Bi and Sb) would have

lattice parameters  $a_0 = 4.42 \text{ \AA}$  and  $c_0 = 11.57 \text{ \AA}$  in terms of the hexagonal structure.

Even though the alloy taken was of nominal 50% composition, it was observed as mentioned before that the deposit film might consist of either one of the components or of the alloy depending on the method of deposition. Slow rate of deposition yielded films consisting mostly of Sb. This appears to be due to the high volatility of Sb in preference to Bi. The flash evaporation technique i.e. evaporating all the material suddenly at high filament temperature, however, favoured the retention of the composition similar to that of the bulk evaporated.

The lattice parameters for Bi-Sb films by electron diffraction method were found to be  $a_0 = 4.38 \text{ \AA}$  and  $c_0 = 11.52 \text{ \AA}$  corresponding to a film having about 56% of Sb and 44% of Bi. Lattice parameters obtained for different films of Bi-Sb in different experiments were nearly of the above value, though occasionally there was a little deviation.

The Bi-Sb alloy invariably produced polycrystalline patterns without a preferred orientation on collodion as substrate. On glass the deposits were 1-d  $\{01.1\}$  or  $\{10.2\}$  oriented depending on the conditions of evaporation.

On a single crystal substrate of mica, the alloy formed a 1-d  $\{10.2\}$  oriented deposits at about  $200^\circ\text{C}$ . On all the faces of rock salt, the alloy grew epitaxially,

provided the substrate temperature was suitably high i.e. about 200°C. At lower temperatures even on these faces the deposits were polycrystalline in nature with or without any preferred orientation. During the epitaxial growth on a (100) face the surface layers of the deposits developed 2-d {10.2} and 2-d {01.1} orientations, whereas the bulk film as seen by transmission consisted of 2-d {30.7} and 2-d {00.1} oriented crystallites, the latter being rotated by 30°. At higher temperatures only 2-d {10.2} by reflection and 2-d {30.7} by transmission were observed. On a (110) face the deposits developed 2-d {30.14} or roughly 2-d {10.5} orientation. On the octahedral face of rock salt the deposits developed 2-d {00.1} and 2-d {11.9} orientations for the bulk of the film. Thus the orientations of the Bi-Sb films on rock salt faces were practically similar to those of Bi and Sb on these faces.

-----

## C H A P T E R - V I I

### STRUCTURE AND CRYSTAL GROWTH OF ANTIMONY

#### TELLURIDE AND ANTIMONY SELENIDE

##### A. INTRODUCTION

The Sb-Te system contains an intermediate phase  $\text{Sb}_2\text{Te}_3$  having m.p.  $\approx 620^\circ\text{C}$ . Dönges (1951) was the first to report the structure-analysis of this phase by X-ray. He showed that  $\text{Sb}_2\text{Te}_3$  had an ordered hexagonal unit cell ( $a_0 = 4.25 \text{ \AA}$ ,  $c_0 = 5 \times 6 \text{ \AA}$ ,  $c_0/a_0 = 5 \times 1.43$ ), there being 3 atoms in the pseudo hexagonal cell and 15 in the super lattice. Harman et al. (1956) prepared  $\text{Sb}_2\text{Te}_3$  by the sintering and annealing technique and studied the electrical properties like Hall coefficient, resistivity, thermoelectric power etc. Semiletov (1956) also reported a hexagonal cell ( $a_0 = 4.24 \text{ \AA}$ ,  $c_0 = 29.9 \text{ \AA}$ ), by electron diffraction studies and suggested that there would be three molecules in the unit cell and it would be isotypic with  $\text{Bi}_2\text{Se}_3$  and  $\text{Bi}_2\text{Te}_3$ . He indexed the diffuse ring photographs, however, with a hexagonal cell having  $a_0 = 4.25 \text{ \AA}$  and  $c_0 = 5.99 \text{ \AA}$ . Thermoelectric properties of  $\text{Sb}_2\text{Te}_3$  and solid solutions of  $\text{Sb}_2\text{Te}_3$  and  $\text{Bi}_2\text{Te}_3$  were studied by Benel (1958) and Kokosh et al. (1960). Electron microscopic study of the dislocations of  $\text{Sb}_2\text{Te}_3$  and  $\text{Bi}_2\text{Te}_3$  was done by Amelinckx et al. (1960, 1961) and they have shown that  $\text{Sb}_2\text{Te}_3$  contains

large hexagonal loops. Various workers have studied the electrical properties, thermoelectric properties, Hall coefficients, resistivity etc. of  $Sb_2Te_3$  and  $Bi_2Te_3$ , either alone or of their solid solutions, in the form of thin films as well as in the form of single crystals, since these were important semiconductors (Rodot, 1960; Borodovyi, 1961; Ghosh, 1963; Garachuk, 1965). The structures of the amorphous films of the selenides and tellurides of Ga, In and Sb were studied by Andrievskii et al. (1963) using electron diffraction methods and they have shown that these compounds do not have a constant structure over the whole range of existence of the amorphous state but the structure depends on the temperature.

Antimony selenide ( $Sb_2Se_3$ ) has an orthorhombic structure with  $a_0 = 11.68 \text{ \AA}$ ,  $b_0 = 3.98 \text{ \AA}$ ,  $c_0 = 11.58 \text{ \AA}$  having 4 molecules in the unit cell and a space group Pnma as reported by Dönges (1953), but Tideswell et al. (1957) observed the unit cell dimensions to be as  $a_0 = 11.77 \text{ \AA}$ ,  $b_0 = 3.962 \text{ \AA}$ ,  $c_0 = 11.62 \text{ \AA}$ . Kolomiets (1955) studied solid solutions of  $Tl_2Se$  and  $Sb_2Se_3$  for their electrical and thermoelectric properties and found that these were p-type semiconductors. Pinsker et al. (1956) prepared the same compound and examined its structure by X-ray and electron diffraction and found it to be orthorhombic. Kolomiets et al. (1959A, 1959B) has also carried out work on photoconductivity and photosensitivity of thin  $Sb_2Se_3$  films formed in vacuo. The work of Tatarinova (1960) by electron

diffraction has proved that amorphous layers and crystalline layers of  $Sb_2Se_3$  have the same configuration. Skubenko (1960) has suggested special methods for the preparation of single crystals of  $Sb_2S_3$  and  $Sb_2Se_3$ . Makedonskii (1963) has carried out researches on the secondary electron emission of antimony chalcogenides. The study of amorphous films of  $Sb_2Se_3$  and  $Sb_2Te_3$  by Andrievskii (1963) has already been referred above. Recently Coultz and Levin (1967) have shown by electron diffraction and electron microscopy that on heating amorphous films of  $Sb_2Se_3$  and of mixtures of  $As_2Se_3$  with  $Sb_2Se_3$ , produce small single crystals which developed a 2-d  $\{010\}$  or 2-d  $\{100\}$  orientation.

From the above survey of literature it is clearly seen that the work done on  $Sb_2Te_3$  and  $Sb_2Se_3$  is mainly regarding their electrical properties, whilst very little work has been carried out on the epitaxy, crystal growth etc. of the thin films of  $Sb_2Te_3$  and  $Sb_2Se_3$ . In the present work a detailed study has been made on the epitaxial growth, phase transition, orientations etc. of the deposit films of  $Sb_2Se_3$  and  $Sb_2Te_3$ , on different single crystal substrates at various temperatures.

## B. EXPERIMENTAL

### (1) Preparation of Antimony Telluride ( $Sb_2Te_3$ ) and Antimony Selenide ( $Sb_2Se_3$ )

Antimony telluride ( $Sb_2Te_3$ ) was prepared by mixing antimony and tellurium in stoichiometric proportions

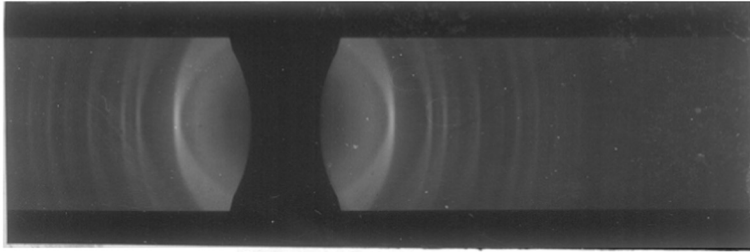


(Fig 95)  
X-ray pattern of  $Sb_2Te_3$  (powder pattern)

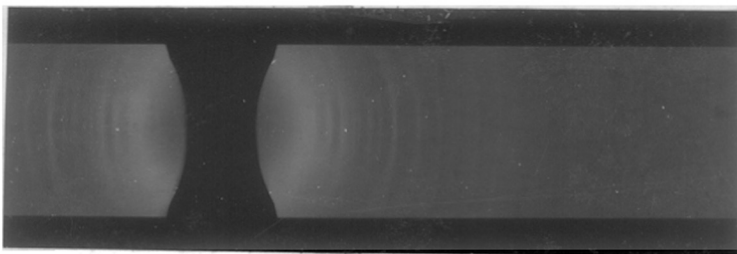


(Fig 96)  
X-ray pattern of  $Sb_2Se_3$  (powder pattern)

(2:3 atomic proportion) in a silica tube which was then sealed under vacuum ( $\approx 10^{-5}$  mm of Hg). The silica tube with the contents was then heated in an electrical furnace. The temperature of the furnace was increased slowly to  $500^{\circ}\text{C}$ , maintained at this temperature for about an hour and then further raised to about  $750^{\circ}\text{C}$ . The sample was heated for about eight hours at this temperature (the melting point of the compound is about  $670^{\circ}\text{C}$ ). The tube was then taken out of the furnace and quenched by immersing in cold water. The alloy was then removed from the tube and used for deposition. Antimony selenide ( $\text{Sb}_2\text{Se}_3$ ) was also prepared under similar experimental conditions by mixing antimony and selenium in stoichiometric proportions (2:3 atomic proportion).

(ii) Deposition of  $\text{Sb}_2\text{Te}_3$  and  $\text{Sb}_2\text{Se}_3$  films

The compounds prepared above were examined by X-ray powder method to know their bulk structures. Figures 95 and 96 represent the patterns for  $\text{Sb}_2\text{Te}_3$  and  $\text{Sb}_2\text{Se}_3$  respectively. The disposition of various reflections and their d-values agreed with a hexagonal (rhombohedral) structure for  $\text{Sb}_2\text{Te}_3$  and an orthorhombic structure for  $\text{Sb}_2\text{Se}_3$ . Antimony telluride ( $\text{Sb}_2\text{Te}_3$ ) and antimony selenide ( $\text{Sb}_2\text{Se}_3$ ) thus obtained were vacuum deposited ( $\approx 10^{-4}$  mm Hg) on different substrates such as collodion, glass, (100), (110) and (111) faces of rocksalt as well as on cleavage faces of mica at various substrate temperatures. The



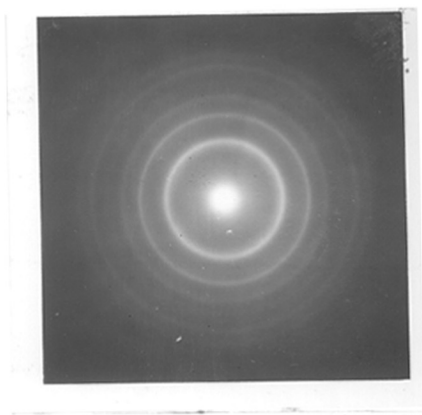


(Fig 97)  
 $Sb_2Te_3$  on collodion at room temperature

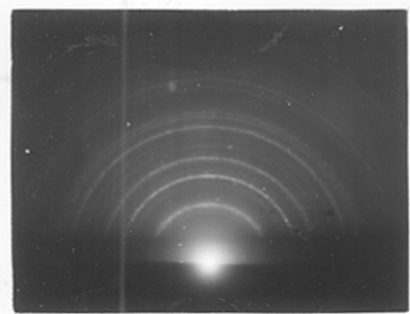


(Fig 98)  
 $Sb_2Te_3$  on glass at  $200^\circ C$ .

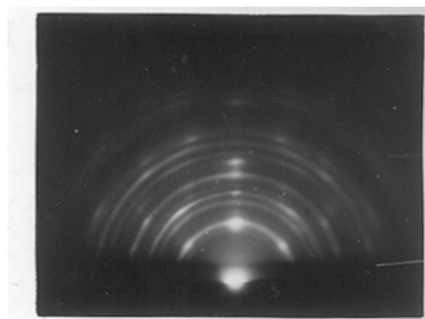


(Fig 99)  
 $Sb_2Te_3$  on glass at  $250^\circ C$   
 $1-d \{01.1\} + \{11.0\} + \{20.1\}$  etc.

ANTIMONY TELLURIDE (Sb<sub>2</sub>Te<sub>3</sub>)

TABLE - 10

(Ref. page 102)

Analysis of the pattern

Figure-97

<u>I/I<sub>0</sub></u>	<u>d</u>	<u>hkl</u> <u>(hexagonal)</u>
s	3.14	01.1
vvf	2.31	10.2
m	2.12	11.0
f	1.76	20.1
vvf	1.57	02.2
f	1.37	21.2
vf	1.24	30.0

s - strong  
vvf - very very faint  
m - medium  
f - faint  
vf - very faint

deposits were then examined both by reflection and transmission methods as previously described in Chapter-II.

### C. RESULTS

#### PART-1 : ANTIMONY TELLURIDE ( $Sb_2Te_3$ )

##### (1) On Collodion

Specimens prepared by the deposition of  $Sb_2Te_3$  on collodion support at room temperature or at higher temperatures upto  $150^{\circ}C$  yielded patterns (Fig. 97) consisting of continuous rings which did not break even on tilting of the specimen, thus suggesting the polycrystalline nature of the deposits. Table-10 gives the analysis of the pattern (Fig. 97). The d-values of different reflections fit in well for a hexagonal (rhombohedral) cell with  $a_0 = 4.25 \text{ \AA}$ ,  $c_0 = 6.0 \text{ \AA}$ , as was suggested by Semiletov (1956).

##### (ii) On Glass

Deposits formed on glass upto  $100^{\circ}C$  did not yield clear patterns, while those formed at  $200^{\circ}C$  yielded patterns (Fig. 98) consisting of continuous rings which did not change with a change in beam direction thus suggesting the polycrystalline nature of the deposits. Deposits formed at  $250^{\circ}C$  and  $300^{\circ}C$  of substrate temperature yielded patterns (Fig. 99) consisting of well defined spots and rings thus apparently suggesting a 2-d orientation of the deposit. It was further found that the patterns did not change at

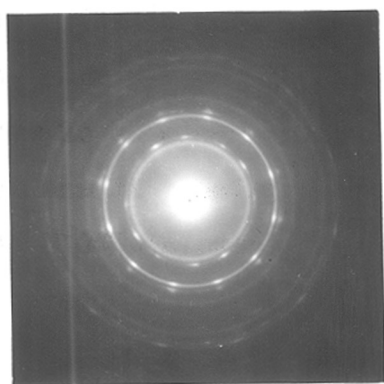


(Fig 100)  
 $Sb_2Te_3$  on (100) of rock salt at  
 $100^\circ C$ . 2-d  $\{00.1\}$  rotated by  $30^\circ$   
 + 2-d  $\{30.4\}$  orientations

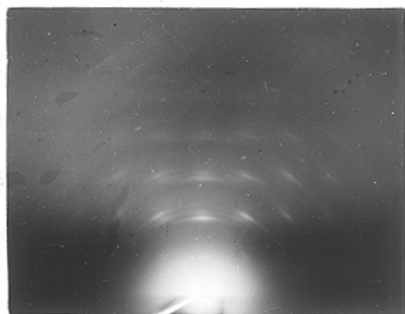


(Fig 101)  
 $Sb_2Te_3$  on rock salt (100) at  
 $200^\circ C$ . Beam  $\langle 100 \rangle$  of rock salt  
 2-d  $\{01.1\}$  orientation.

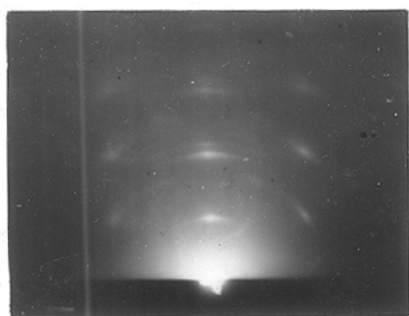


(Fig 102)  
 Specimen in  $\{101$  but beam  
 $\langle 110 \rangle$  of rock salt. 2-d  $\{01.1\}$   
 orientation.

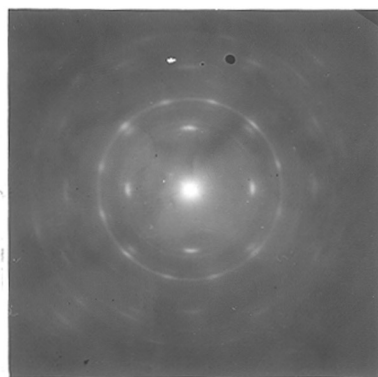


(Fig 103)  
 Specimen in  $\{101$  seen by  
 Transmission.  
 2-d  $\{00.1\}$  rotated by  $30^\circ + \{30.4\}$   
 orientation.

all even by the change of beam direction. Hence the deposits developed a 1-d orientation. Appearance of strong reflections such as 01.1 and 11.0 and somewhat weak ones as 20.1 in the plane of incidence indicated the presence of various one degree orientations of the deposit films. It was noted that peculiarly enough patterns from deposits at 250°C were sharper than those formed at 300°C and the deposits formed at 350°C were again polycrystalline in nature.

(iii) On (100) face of rock salt

Deposits formed at room temperature were polycrystalline in nature. Deposits formed at 100°C, when examined by transmission, yielded patterns (Fig. 100) which consisted of mainly rings and a few spots. The presence of 12 spots both on 11.0 and on 30.0 type reflections forming a hexagonal network of spots in each case suggests a 2-d  $\{00.1\}$  orientation of the deposits, which were mutually rotated by 30°. Further there is an additional square type (approximately) network of spots due to 000, 01.1, 11.0,  $1\bar{1}.1$  reflections with extra spots just inside the 11.0 reflections. This disposition of spots is similar to that observed in the patterns yielded by bismuth deposits (cf. Fig. 7). From the considerations of the reciprocal lattice it was found that the beam direction was along  $\langle 21.\bar{1} \rangle$  and the deposits had their  $(30.\bar{4})$  plane parallel to the substrate and has developed a 2-d  $\{30.\bar{4}\}$  orientation. The presence of 10.2 reflection was no doubt due to normal and anti orientations

of the deposit crystals. Further the presence of 12 spots on each of 01.1, 10.2 and 11.0 rings thus appears to be due to the rotation of the crystallites by  $30^\circ$ .

When reciprocal lattices were constructed for both these orientations of the deposits, it was found that the reciprocal lattice rows containing 01.1 and  $\bar{1}1.\bar{1}$  reflections and passing through the undeflected spot are apparently at right angles. When calculations were carried out using expression (I) in Chapter-III, it was found the angle was not  $90^\circ$  but  $84^\circ 48'$ . On constructing the reciprocal lattice, considering both the normal and anti type of orientation development and rotating them through  $30^\circ$ , it was found that the patterns fitted well with the hexagonal (rhombohedral) cell. These observations suggest that on rock salt (100) face the deposits developed a 2-d  $\{30.\bar{4}\}$  orientation. The above patterns were also considered for the possibility of the formation of a superstructure of  $Sb_2Te_3$ . It was found that the above patterns can be fully explained only by the normal cell and one need not assume any superstructure.

The deposits formed at  $200^\circ\text{C}$  and  $300^\circ\text{C}$  of substrate temperature yielded patterns (Figs. 101 and 102) by reflection when the beam was along  $\langle 100 \rangle$  and  $\langle 110 \rangle$  respectively of rock salt. The presence of strong 01.1, 02.2 etc. reflections in the plane of incidence suggests a 2-d  $\{01.1\}$  orientation. Additional faint spot due to

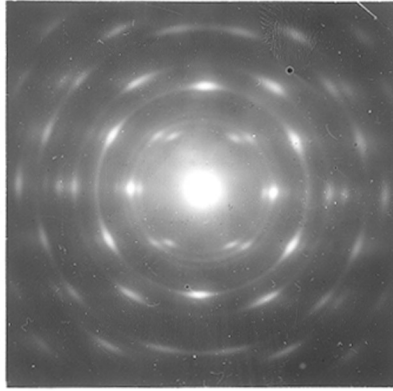


(Fig 104)  
 $Sb_2Te_3$  on (110) of rocksalt at  $200^\circ C$   
2-d  $\{00.1\}$  orientation.

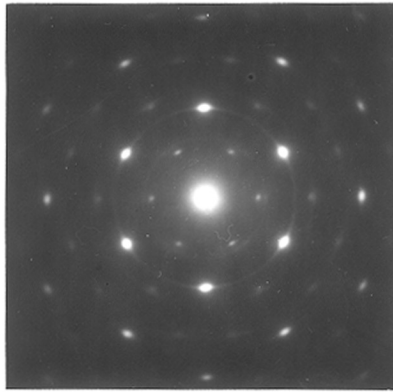


(Fig 105)  
 $Sb_2Te_3$  on (111) of rocksalt  
at  $200^\circ C$ , 2-d  $\{00.1\}$  orientation.

00.2 was also noted in the plane of incidence corresponds to a 2-d  $\{00.1\}$  orientation.

Transmission pattern (Fig. 103) of the same specimen showed that the deposits developed a 2-d  $\{00.1\}$  orientation of the crystallites mutually rotated by  $30^\circ$  along with a very prominent 2-d  $\{30.\bar{4}\}$  orientation. Deposits formed at  $350^\circ\text{C}$  were polycrystalline in nature, with or without any preferred orientation. It is worth noting that the deposits at higher temperature in this case, however, showed a tendency to disorientation, the reason for which is not yet clear.

(iv) On (110) Face of Rock Salt

Deposits formed upto  $150^\circ\text{C}$  of substrate temperature were polycrystalline in nature. Deposits formed between  $200^\circ\text{C}$  to  $300^\circ\text{C}$  yielded patterns (Fig. 104) consisting of mainly spots and a few rings but those formed at  $200^\circ\text{C}$  had less number of spots. It is rather interesting to note that the hexagonal network of spots suggests a 2-d  $\{00.1\}$  orientation formed on a (110) face. Moreover the presence of layer lines has also indicated an additional 1-d orientation of the deposits.

(v) On (111) Face of Rock Salt

Deposits formed upto  $150^\circ\text{C}$  of substrate temperature were polycrystalline in nature. Deposits formed between the temperature range of  $200^\circ\text{C}$  and  $350^\circ\text{C}$  yielded patterns



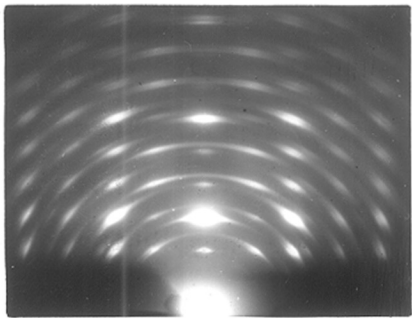


(Fig 106)  
 $Sb_2Te_3$  on mica at  $200^\circ C$ .  
 $2-d\{00.1\}$  rotated by  $30^\circ$ .

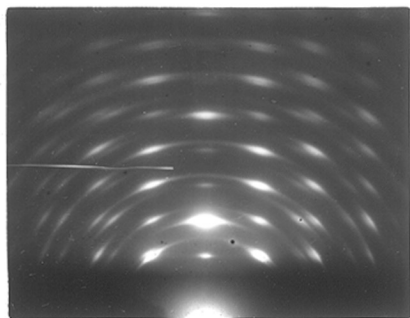


(Fig 107)  
Specimen in fig 106 rotated  
by  $30^\circ$  azimuth.

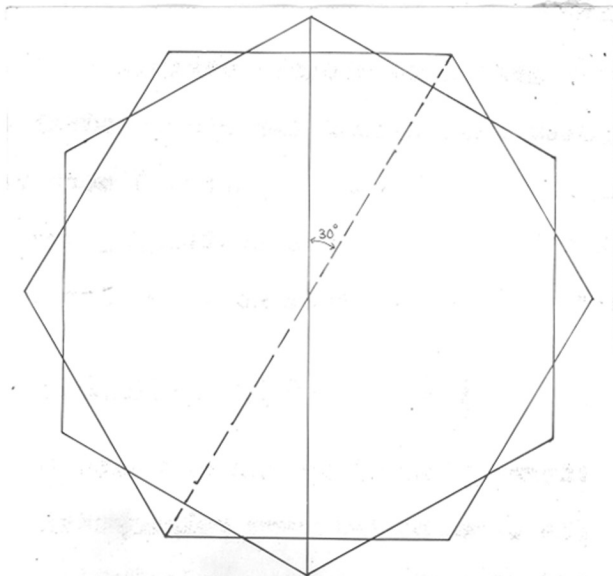


(Fig 108)

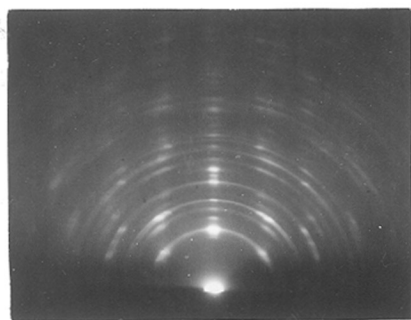


(Fig 109)  
 $Sb_2Te_3$  on mica at  $300^\circ C$  various 1-d orientations.

(Fig. 105) showing the hexagonal disposition of spots. The networks of strong spots were due to 11.0 and 30.0 reflections whilst the weak spots were due to 10.0, 20.0, 40.0 reflections such that 10.0 reflections were nearest to the central undeflected beam. The beam direction for all these networks was found to be  $\langle 00.1 \rangle$  thus suggesting that the deposits developed a 2-d  $\{00.1\}$  orientation.

It may be mentioned here that though reflections such as 10.0 and 20.0 are forbidden by the structure factor considerations for the rhombohedral cell of  $\text{Sb}_2\text{Te}_3$ , these reflections are quite clearly visible in these patterns. This suggests that either the rhombohedral conditions given by the expression (V) in Chapter-III were relaxed in the epitaxial films or a double scattering was taking part so that the forbidden reflections were also observed.

(vi) On Cleaved Face of Mica

Patterns yielded by the deposits formed upto  $150^\circ\text{C}$  of substrate temperature were polycrystalline in nature with or without any preferred orientation. Deposits formed at  $200^\circ\text{C}$  yielded patterns (Fig. 106) such that  $00.l$  type reflections were in the plane of incidence. It was further found that out of the  $00.l$  type reflections in the plane of incidence, reflections for which  $l = 3n$ , where  $n = 1, 2$  etc. were very strong, whereas the others were comparatively weaker. It can be also seen that the spot pattern arose out of two types of rectangular networks of spots (1) formed

with 000, 00.1, 01.1, 01.0 and (11) with 000, 00.1, 11.1 and 11.0 reflections, the corresponding beam directions being along  $\langle 01.0 \rangle$  and  $\langle \bar{1}1.0 \rangle$  respectively of the deposit. Thus the deposits developed a 2-d  $\{00.1\}$  orientation of the hexagonal (rhombohedral) structure. The 01.1 and 10.0 reflections in the pattern are very strong while 11.0 and 11.1 are comparatively weaker. When the above specimen was rotated through  $30^\circ$ , similar patterns (Fig.107) were obtained. Similarity of the patterns at the two azimuths of  $30^\circ$ , apparently suggests that the deposits might have developed a preferred orientation, however, the detailed consideration of the disposition of spots, by rotation of the specimen through angles other than  $30^\circ$ , clearly showed that the deposits grew epitaxially with a 2-d orientation. The nature of the pattern thus suggests that the crystallites were rotated by  $30^\circ$  as shown in Figure 108 so that for both these azimuths the patterns will be similar. There is also a little doubling of spots, which is probably due to the presence of both Te and  $\text{Sb}_2\text{Te}_3$  deposits and a very small difference in the  $c_0$  and  $c_0/a_0$  values of Te and  $\text{Sb}_2\text{Te}_3$  can account for the proximity of the spots. It was thus found that  $\text{Sb}_2\text{Te}_3$  developed a 2-d  $\{00.1\}$  orientation and the crystallites were rotated by  $30^\circ$  on mica. The patterns (Fig. 109) yielded by deposits formed between  $250^\circ$  and  $300^\circ\text{C}$  consisted of a number of spots and rings and were highly complicated in nature. A number of reflections such

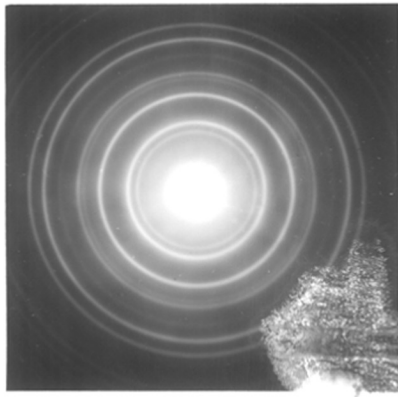


(Fig 110)

$Sb_2Se_3$  on polycrystalline  
sodium chloride at  $200^\circ C$ .



(Fig 111)

$Sb_2Se_3$  on glass at  $200^\circ C$ .  
1-d{110} orientation.

ANTIMONY SELENIDE (Sb<sub>2</sub>Se<sub>3</sub>)

TABLE - 11

(Ref. page 108)

Analysis of the pattern

Figure-110

<u>I/I<sub>0</sub></u> <u>visual</u>	<u>d</u>	<u>hkl</u> <u>(orthorhombic)</u>
vf	4.14	220
m	3.58	111
vs	3.13	211
vvf	2.89	400
s	2.09	440
vf	1.99	002
f	1.87	202
m	1.78	222
vf	1.56	422
ms	1.34	480
m	1.29	840

$a_0 = 11.60 \text{ \AA}$ ,     $b_0 = 11.75 \text{ \AA}$ ,     $c_0 = 3.98 \text{ \AA}$

vf - very faint  
m - medium  
vs - very strong  
s - strong

vvf - very very faint  
ms - medium strong  
f - faint

as 10.0, 01.1, 10.2 and 11.0 etc. in the plane of incidence suggested a number of possible orientations. However, the pattern did not change on changing the beam azimuth with respect to the deposit film because of a perfect 1-d orientation of the deposit films.

PART-2 : ANTIMONY SELENIDE ( $Sb_2Se_3$ )

(i) On Collodion and Polycrystalline  
Sodium Chloride

Deposits formed either at room temperature or at  $100^{\circ}C$  on these substrates yielded diffuse patterns. The deposition when carried out at  $200^{\circ}C$  produced polycrystalline films as revealed by the pattern (Fig. 110). The analysis of this pattern (Table-11) shows that the d-values agree with those of the orthorhombic structure.

(ii) On Glass

Deposits formed on glass upto  $150^{\circ}C$  yielded diffuse patterns. Deposits formed at and above  $200^{\circ}C$ , yielded ring patterns with or without any preferred orientation depending on the thickness of the film. The  $d_{hkl}$  of the rings were in accordance with those of the orthorhombic structure. Figure-111 shows a typical pattern yielded by thicker deposits formed at  $200^{\circ}C$ . The presence of 110 reflection in the plane of incidence and also the arcing of some of the rings suggest a 1-d  $\{110\}$  orientation of the deposits.

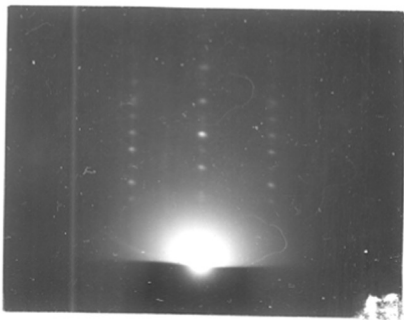


(Fig 112)  
 $Sb_2Se_3$  on rocksalt (100) at  $200^\circ C$ .  
 Beam  $\langle 100 \rangle$  of rocksalt  
 2-d  $\{100\} + \{110\} + \{120\}$  orientations

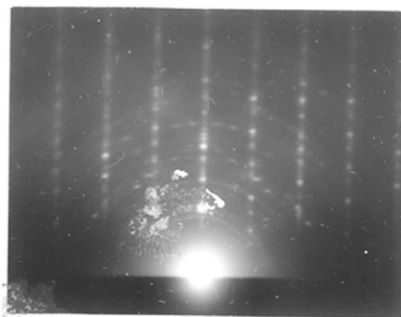


(Fig 113)  
 Specimen in 112 but  
 beam  $\langle 110 \rangle$  of rocksalt.

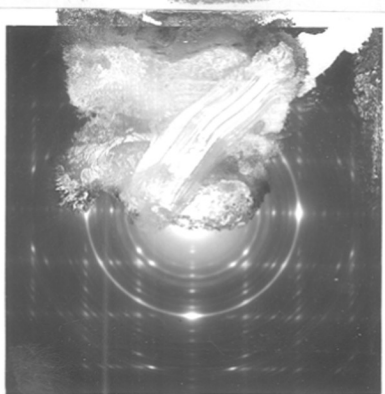


(Fig 114)  
 $Sb_2Se_3$  on rock salt (100) at  $250^\circ C$ .  
 2-d  $\{100\} + \{110\} + \{120\} + \{230\}$   
 orientations all rotated by  
 $90^\circ$ .

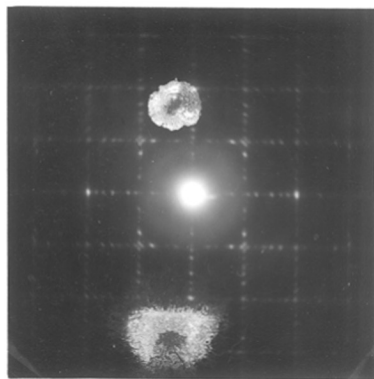


(Fig 115)  
 $Sb_2Se_3$  on rock salt (100) at  $350^\circ C$ .  
 2-d  $\{100\} + \{110\} + \{120\} + \{230\}$   
 all rotated by  $90^\circ$ .

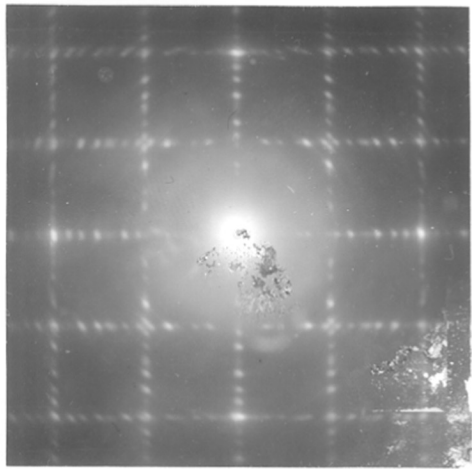


(Fig 116)  
Enlarged photograph of fig 115.

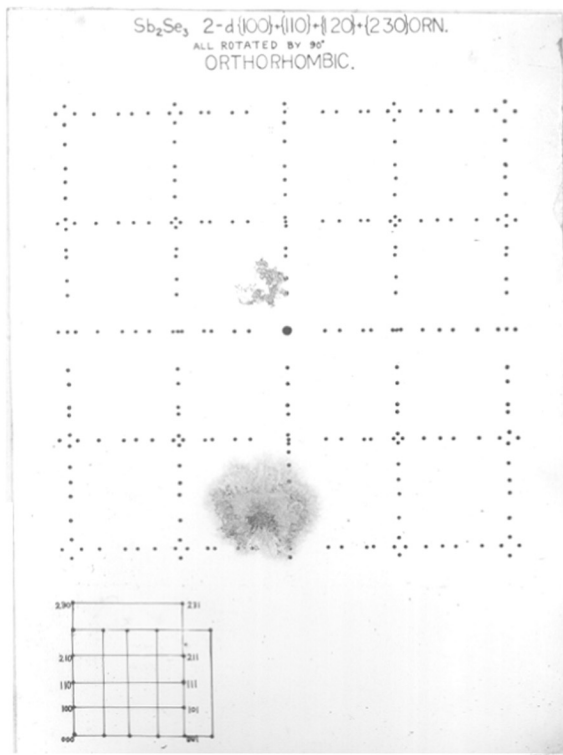


(Fig 117)  
Theoretical pattern for fig 116.

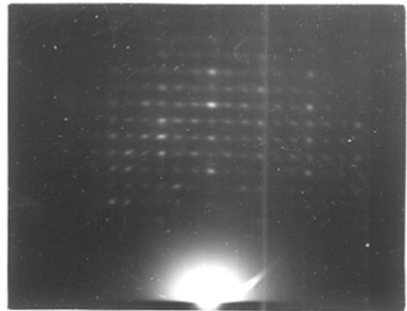


(Fig 118)  
 $Sb_2Se_3$  on rock salt (100) at  $400^\circ C$   
Beam  $\langle 110 \rangle$  of rock salt.  
2-d {100} or {010} orientation  
of orthorhombic structure

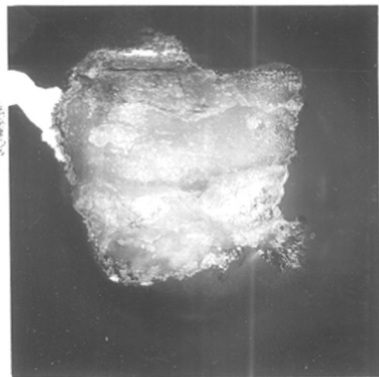


(Fig 119)  
Transmission pattern from  
specimen in fig. 118.  
2-d {100} orientation of cubic structure



(111) On (100) Face of Rock Salt

Deposits formed on this face upto  $150^{\circ}\text{C}$  yielded diffuse patterns, due to either amorphous nature or very fine grain structure of the films. Deposits formed between  $200^{\circ}\text{C}$  and  $250^{\circ}\text{C}$  yielded both ring and spot patterns, whilst those between  $300^{\circ}\text{C}$  and  $350^{\circ}\text{C}$  purely spot patterns. The deposits formed at about  $300^{\circ}\text{C}$  when examined by reflection yielded patterns (Figs. 112 and 113) when the beam was respectively along  $\langle 100 \rangle$  and  $\langle 110 \rangle$  directions of rock salt. Though the nature of the patterns changed considerably on changing the beam direction, strong reflections such as 100 and its higher orders and also some weak reflections i.e. 110, 120 were always in the plane of incidence thus suggesting the development of 2-d  $\{100\}$ , 2-d  $\{110\}$  and 2-d  $\{120\}$  orientations of the deposit crystallites. The specimen when examined by transmission yielded very interesting patterns. Figure-114 represents patterns from the deposits formed at  $250^{\circ}\text{C}$  and Figures 115 and 116 represent actual and enlarged patterns from the deposits formed at  $350^{\circ}\text{C}$ . The patterns consist of two sets of parallel rows of spots at right angles to each other, thus giving an effect of a square network of spots. It is also noted that the second order rows of each set intersect each other approximately at a point, whereas the region of intersection of the first order rows of these consisted of four strong spots. Further the distances between two successive spots in any row were unequal. It should be mentioned here that the

distance between the two sets of parallel rows was found to be equal to  $c_0$  ( $\approx 3.96 \text{ \AA}$ ) of the orthorhombic structure of  $\text{Sb}_2\text{Se}_3$  crystals. The above features of the pattern, especially the unequal distances between successive spots in a row suggest that this peculiar disposition of spots must have arisen out of the development of several orientations. From the reflection patterns it was concluded that the deposits developed 2-d  $\{100\} + \{120\} + \{110\}$  orientations. Considering the reciprocal lattice diagram for these orientations of deposit crystallites for the transmission patterns, it was found that quite a number of spots remain unexplained. Further consideration of the spot patterns led to conclude that the oriented crystallites were rotated by  $90^\circ$  in each case and the corresponding reciprocal lattice diagram (Fig. 117) agreed well with the pattern observed, thus confirming that the deposits of  $\text{Sb}_2\text{Se}_3$  developed 2-d  $\{100\} + 2\text{-d } \{110\} + 2\text{-d } \{120\} + 2\text{-d } \{230\}$  orientations.

The deposits formed at about  $400^\circ\text{C}$  yielded very interesting spot patterns (Fig. 118) when the beam was along  $\langle 110 \rangle$  of the substrate. It was also found that the pattern changed with the beam azimuth thus suggesting that the deposits grew epitaxially on this substrate. It is peculiar to note that alternate spots in the plane of incidence are stronger. It was also seen that every third spot in the horizontal rows corresponding to the spacing  $c_0$  is considerably stronger compared to the others in the same row. Further the spacing between the two spots in the plane of incidence

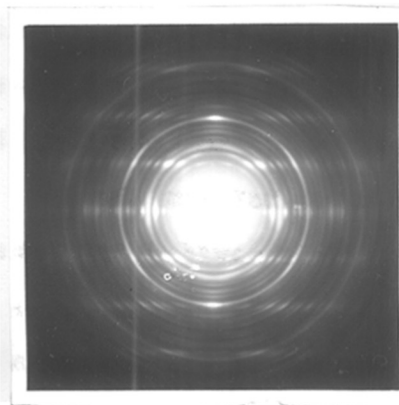


(Fig 120)  
 $\text{Sb}_2\text{Se}_3$  on rocksalt (110) at  $250^\circ\text{C}$   
 $2\text{-d}\{100\} + \{110\} + \{120\} + \{230\}$   
 orientations.

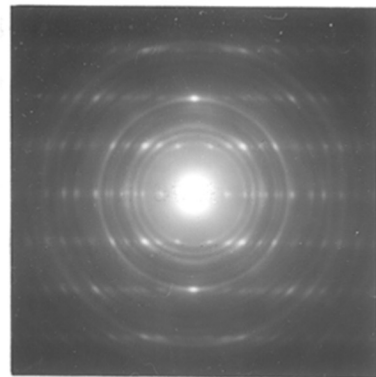


(Fig 121)  
 $\text{Sb}_2\text{Se}_3$  on (110) of rocksalt at  $350^\circ\text{C}$ .  
 $2\text{-d}\{100\} + \{110\} + \{120\} + \{230\}$   
 orientations.

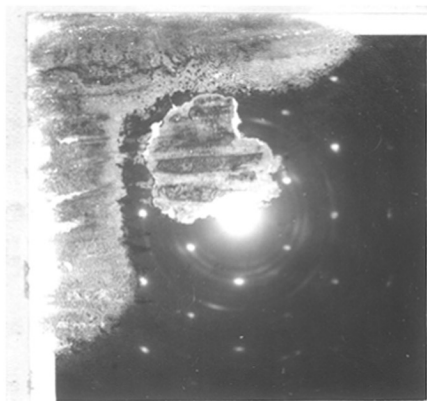


(Fig 122)  
 $\text{Sb}_2\text{Se}_3$  on (110) of rocksalt at  $400^\circ\text{C}$ .  
 $2\text{-d}\{110\}$  orientation of cubic structure.

corresponds to either  $a_0$  or  $b_0$  which are nearly equal. Thus the deposits developed either a 2-d  $\{100\}$  or 2-d  $\{010\}$  orientation in such a way that the cube face diagonal of the substrate was parallel to either 'b' or 'a' axis respectively of the deposits. It is also interesting to note that the spacing of  $3.96 \text{ \AA}$  corresponding to  $c_0$  between the two strong spots in the horizontal rows is divided into three equal parts by additional spots, thus giving rise to a superstructure with a new  $c_0$  of  $11.88 \text{ \AA}$ , which is equal to three times the original  $c_0$ . This means that as if the deposit assumed a cubic structure with  $a_0 \simeq 11.88 \text{ \AA}$ . Transmission patterns from the same deposits on the other hand give rise to a simpler spot pattern (Fig. 119) showing a square type of network suggesting a cubic structure with  $a_0$  about  $5.84 \text{ \AA}$  which is very nearly equal to  $\frac{a_0}{2}$  or  $\frac{b_0}{2}$  or  $\frac{3c_0}{2}$  of the orthorhombic form.

#### (iv) On (110) Face of Rock Salt

Deposits formed below  $200^\circ\text{C}$  yielded diffuse ring patterns, while those formed between  $200^\circ\text{C}$  to  $350^\circ\text{C}$  when examined by transmission yielded patterns (Figs. 120, 121) consisting of rings and also of spots lying in rows and the distance between the spot rows was found to be equal to  $c_0$  ( $= 3.96 \text{ \AA}$ ). Deposits formed between  $300^\circ\text{C}$  and  $350^\circ\text{C}$  yielded sharper spot patterns. The disposition of the spots in all these patterns was such that they conformed to the 2-d  $\{100\}$ , 2-d  $\{110\}$ , 2-d  $\{120\}$  and 2-d  $\{230\}$  orientations as was observed previously on a cube face. In the

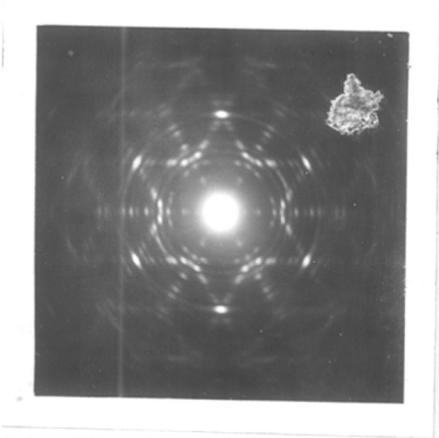


(Fig 123)  
 $Sb_2Se_3$  on rock salt (111) at  $250^\circ C$ .  
 2-d  $\{100\} + \{110\} + \{120\} + \{30\}$   
 orientations all rotated by  $60^\circ$ .

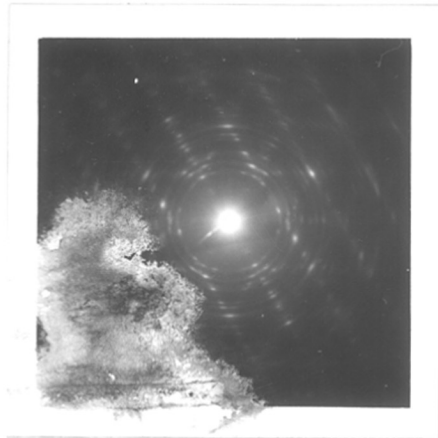


(Fig 124)  
 $Sb_2Se_3$  on rock salt (111) at  $350^\circ C$ .  
 orientations same as at  $250^\circ C$ .

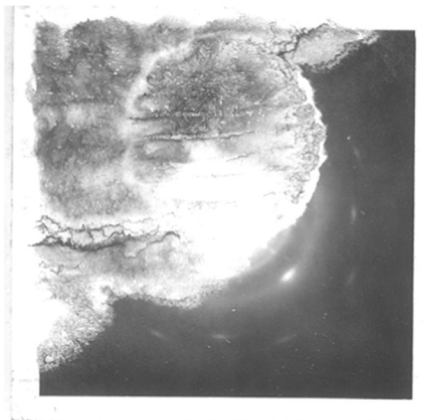


(Fig 125)  
 $Sb_2Se_3$  on (111) face of rock salt at  $400^\circ C$ .  
 2-d  $\{100\}$  orientation of cubic structure.

present case, however, the crystallites were not rotated and hence the pattern had an appearance of parallel rows of spots.

At about  $400^{\circ}\text{C}$  of the substrate temperature the deposits yielded interesting patterns (Fig. 122) consisting of strong spots as well as a few faint rings. The disposition of the strong spot patterns together with the  $d$ -values measured with graphite as standard suggest that these spots arose from crystals having a cubic structure ( $a_0 = 5.84 \text{ \AA}$ ). It may further be noted that some of the faint rings due to the orthorhombic structure are passing through the spots. It thus appears that at about  $400^{\circ}\text{C}$ ,  $\text{Sb}_2\text{Se}_3$  formed a new cubic phase which developed a 2-d  $\{110\}$  parallel orientation on this substrate.

(v) On (111) Face of Rock Salt

Deposits formed on this face below  $200^{\circ}\text{C}$  yielded only diffuse patterns. Deposits formed between  $200^{\circ}\text{C}$  and  $350^{\circ}\text{C}$ , when examined by transmission, yielded apparently complicated patterns (Figs. 123, 124) consisting of spot rows which were apart from each other by a distance equal to the  $c_0$  ( $3.96 \text{ \AA}$ ) of the orthorhombic structure. It is also observed that there are six equidistant strong spots on the rings corresponding to 002 reflection of the orthorhombic structure. Moreover the disposition of the spots along the rows was similar to those seen previously in patterns obtained from the deposits on (110) face of

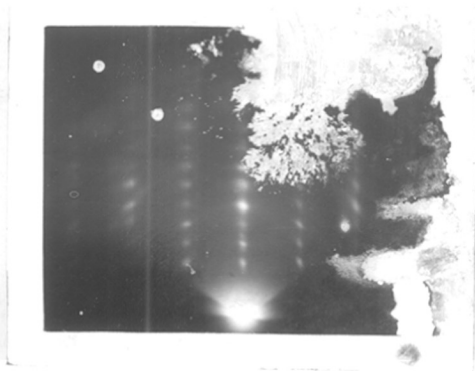


(Fig 126)  
 $Sb_2Se_3$  on mica at  $400^\circ C$ .

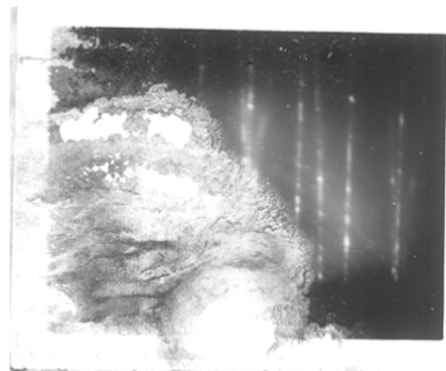


(Fig 127)  
 $Sb_2Se_3$  on mica at  $300^\circ C$ .



(Fig 128)  
 $Sb_2Se_3$  on mica at  $250^\circ C$ .

rock salt. These suggest that  $\text{Sb}_2\text{Se}_3$  developed a mixture of 2-d  $\{100\}$ , 2-d  $\{110\}$ , 2-d  $\{120\}$  and 2-d  $\{230\}$  orientations. It can be seen that merely these dispositions of the crystallites will not give rise to the observed patterns, but if all these crystallites are rotated by  $60^\circ$  a pattern consisting of a network of spots forming rhombohedrons, would be produced as observed.

Deposits formed at  $400^\circ\text{C}$  yielded pattern (Fig. 125) corresponding to the cubic pattern as observed in the case of deposits formed on (100) face, thus suggesting a 2-d  $\{100\}$  orientation of the cubic phase ( $a_0 = 5.84 \text{ \AA}$ ).

(vi) On Cleavage Face of Mica

Deposits formed on this face upto about  $150^\circ\text{C}$  did not yield any clear patterns, but at higher substrate temperature say about  $300^\circ\text{C}$  and above most of these deposits grew epitaxially on the substrate. It was, however, found that patterns obtained from deposits formed at different substrate temperatures between  $200^\circ\text{C}$  and  $400^\circ\text{C}$ , varied considerably in details and the deposits at higher temperature were simpler in nature. Figure 126 shows a pattern yielded by deposits formed at a substrate temperature of  $400^\circ\text{C}$ . The disposition of the spots suggests that  $\text{Sb}_2\text{Se}_3$  developed a 2-d  $\{100\}$  or a 2-d  $\{010\}$  orientation, which is also confirmed by patterns taken in other beam azimuths. Patterns formed at  $300^\circ\text{C}$  (Fig. 127) or even at lower temperature such as  $250^\circ\text{C}$  (Fig. 128) showed many additional



interesting features namely (i) streaks passing through normal spot positions (cf. Figure at  $400^{\circ}\text{C}$ ), (ii) additional spots in the plane of incidence as well as in other directions, and (iii) additional streaks passing through spot positions which were absent for deposits at  $400^{\circ}\text{C}$ . It can also be seen that some of the streaks (as mentioned in (iii) above) show a sort of curvature with respect to the main spot rows lying in the direction normal to the shadow edge. The horizontal distances between these streaks in the above two figures (at  $250^{\circ}\text{C}$  and  $300^{\circ}\text{C}$ ) are not equal. It can also be noted that some of the streaks with similar curvatures are also passing through the spot rows lying in a direction normal to the shadow edge. It is not, however, easy to interpret these patterns unequivocally, but it can be said that the additional spots lying in the plane of incidence are due to the development of other orientations of the deposits. The presence of streaks suggest that the deposits were very smooth in atomic scale and the curvature of some of the streaks appears to be linked with the lamellar nature of the deposits and these lamellae being not exactly parallel to the beam. Wycoff (1964) also suggested the bulk structure of  $\text{Sb}_2\text{Se}_3$  to consist of sheets of  $\text{Sb}_2\text{Se}_3$  indefinitely prolonged in the plane parallel to  $c_0$  axis and roughly diagonal to  $a_0$  and  $b_0$  axes.

#### D. DISCUSSION

The above results revealed that both  $\text{Sb}_2\text{Te}_3$  and  $\text{Sb}_2\text{Se}_3$  grow epitaxially on all the single crystal substrates, even though the structures of these films are quite different namely rhombohedral in the case of  $\text{Sb}_2\text{Te}_3$  and orthorhombic for  $\text{Sb}_2\text{Se}_3$ . The bulk structure of  $\text{Sb}_2\text{Te}_3$  has been found (Donge, 1951) to be rhombohedral ( $a_0 = 4.25 \text{ \AA}$ ,  $c_0 = 6.0 \text{ \AA}$ , for the corresponding hexagonal structure). A super lattice with 5 times  $c_0$  has also been reported (Semiletov, 1956). The bulk structure of  $\text{Sb}_2\text{Se}_3$  has been found to be orthorhombic ( $a_0 = 11.62 \text{ \AA}$ ,  $b_0 = 11.77 \text{ \AA}$ ,  $c_0 = 3.962 \text{ \AA}$ , Pinsker, 1956). It is interesting to point out that even though Se and Te belong to the same group of the periodic table, the compounds formed by them with Sb have different structures.

#### Antimony Telluride

The present work clearly shows that most of the reflections observed from deposits either on polycrystalline or single crystal substrate consisted of hkl values conforming to simpler smaller lattice cell. Thus different orientations observed were (a) 2-d  $\{30.\bar{4}\}$  normal and anti together with 2-d  $\{00.1\}$  on cube face of rock salt, (b) 2-d  $\{00.1\}$  orientation on (110) face and (c) 2-d  $\{00.1\}$  orientation on octahedral face of rock salt as well as on cleaved face of mica. It is worth mentioning here that even though the atomic arrangement of different faces was completely different, the same orientation namely 2-d  $\{00.1\}$  was observed in all the cases. This is rather unusual and it is not, however,

easy to see through the cause of such orientations. It may also be mentioned that the transmission patterns yielded by deposits, formed on (111) face of rock salt consisted of reasonably strong  $h0.0$  type reflections such as 10.0, 20.0, 40.0, 50.0 etc. where  $h$  is not a multiple of 3. Such reflections are forbidden by the structure factor considerations of a primary rhombohedral cell. The appearance of these reflections seems to be due to (i) relaxation of the rhombohedral conditions in the thin film state giving rise to unrestricted hexagonal reflections or (ii) dynamical condition of the scattering of electrons when passing through the deposit film. It is however difficult to determine uniquely which of these two conditions prevailed in the above observations.

Even though the patterns from polycrystalline deposits formed on collodion can fit in both the normal and super-structure from the consideration of  $d$ -values, still the disposition of reflections in the single crystal patterns is completely in agreement with the simple cell and there is no positive evidence for the super-structure of  $Sb_2Te_3$ .

#### Antimony Selenide

These films also grew epitaxially on all the single crystal substrates provided that the temperature was favourable. On amorphous substrates the deposit films were randomly disposed with or without preferred orientation. In contrast with  $Sb_2Te_3$  films,  $Sb_2Se_3$  was found to develop a new cubic phase ( $a_0 = 5.84 \overset{\circ}{\text{A}}$ ) when substrate temperature was

about  $400^{\circ}\text{C}$ . The transition was irreversible, similar to that of  $\text{SnS}$  and  $\text{Bi}_2\text{Se}_3$  films observed by Goswami and his coworkers (1964, 1965).

On the cube face of rock salt the orthorhombic form grew epitaxially in such a way that the deposit crystals had their (100), (110), (120) and (230) planes parallel to the substrate face upto a temperature of about  $350^{\circ}\text{C}$ . It was also observed that some of the above oriented crystals were simultaneously rotated by  $90^{\circ}$  with respect to each other. It is interesting to mention here that on the other faces namely (110) and (111) also the deposits developed similar orientations. Deposit crystallites were found to be rotated when grew on (111) face, the rotation angle was  $60^{\circ}$  instead of  $90^{\circ}$  as on the cube face. Deposit crystals on (110) face showed no such rotation. It is not yet clearly understood that what might be the reason for the same orientations even when the substrate surfaces were different. When the substrate temperature was more than  $350^{\circ}\text{C}$  the deposits were of the cubic phase and grew epitaxially on all the faces of rocksalt. The orientations developed were 2-d  $\{100\}$  on the cube face as well as on the octahedral face, while a 2-d  $\{110\}$  orientation developed on a (110) face.

The formation of cubic phase from the orthorhombic one can be easily visualised since the  $a_0$  of cubic phase is nearly equal to half of  $a_0$  or  $b_0$ , or  $3/2$  of  $c_0$  of the

orthorhombic form. It is very likely that during the epitaxial growth, at higher substrate temperatures, the atoms in the deposit layer slightly adjust themselves in such a way as to form a new cubic phase. This slight adjustment is not unusual in vapour phase deposits and in fact this has been found to take place in the case of  $\text{SnS}$  and  $\text{Bi}_2\text{Se}_3$  (Goswami and coworker, 1964) as well as in the case of  $\text{Ag}_2\text{Se}$  and  $\text{Ag}_2\text{Te}_3$  (Goswami and coworker, 1965).

It may be mentioned here that the  $\text{Sb}_2\text{Se}_3$  deposits formed above  $350^\circ\text{C}$  on a (100) face of rock salt were found to consist of a cubic phase when examined by transmission methods but of orthorhombic form when studied by reflection technique. This explains why on mica, even at a higher temperature of  $400^\circ\text{C}$ , the deposits were found to be of orthorhombic nature.

-----

SUMMARY AND CONCLUSIONS

The present work concerns with the electron diffraction studies of the structures of the vapour phase deposits of Bi, Sb, Bi-Sb system, the chalcogenides of Sb such as  $Sb_2Se_3$  and  $Sb_2Te_3$ , the suboxide of bismuth ( $BiO$ ) and also the oxidation process of Bi and Sb films under varying conditions of air pressures, on amorphous substrates such as glass and collodion and on single crystal substrates like rock salt faces as well as on cleaved faces of mica. The present study has also thrown some new light on the crystal growth process and the development of orientations of the rhombohedral structures. Moreover some chemical aspects of the oxidation process of Bi and Sb have been clarified by this work.

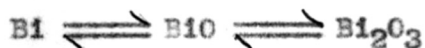
The results obtained from the studies of the deposits of Sb, Bi, Bi-Sb,  $Sb_2Te_3$  and  $Sb_2Se_3$ , have clearly shown that inspite of the differences between the structures of the deposits and substrates with widely different lattice fits, the crystal growth process was very similar in all the cases. On single crystal substrates the initial deposits were epitaxially grown provided that the substrate temperature was favourable. Even at room temperature initial few layers grown on the substrate are also likely to be epitaxial. With the rise of substrate temperature the thickness of epitaxial layers would also increase. With the increasing film

thickness the substrate influence on the growth gradually decreases and ultimately a stage is reached when the substrate no longer influences the growth process and ultimately the effect of deposition conditions prevails. This generally leads to one degree orientations of the deposits. In the intermediate stage, however, the deposits become completely random.

Bismuth grew epitaxially in the temperature range of  $100^{\circ}\text{C}$  to  $200^{\circ}\text{C}$  whilst in the case of Sb and Bi-Sb, the epitaxial growth was obtained at about  $200^{\circ}\text{C}$  and above. All these deposits were found to have hexagonal (rhombohedral) structures and no phase change was observed. These films developed 2-d  $\{10.2\}$  and 2-d  $\{30.7\}$  orientations on a cube face of rock salt. On a (110) face, 2-d  $\{30.\bar{1}4\}$  i.e. approximately  $\{10.\bar{5}\}$  orientation was observed for all the above films. In the case of Bi additional orientations viz. 2-d  $\{\bar{1}1.0\}$  and 2-d  $\{11.\bar{7}\}$  were also observed. On the octahedral face these developed 2-d  $\{00.1\}$  and 2-d  $\{1\bar{1}.\bar{9}\}$  orientations, the crystallites for the later orientation were rotated by  $60^{\circ}$ . On the cleavage face of mica Bi developed a 2-d  $\{00.1\}$  orientation whereas epitaxy was not observed in the case of Sb and Bi-Sb. Thicker deposits of Bi and Bi-Sb on glass developed 1-d  $\{01.1\}$  and 1-d  $\{10.2\}$  orientations whilst Sb deposits developed a 1-d  $\{12.4\}$  orientation. Moreover Bi-Sb and Sb developed 1-d  $\{10.2\}$  and 1-d  $\{01.1\}$  orientations respectively on mica.

Bismuth suboxide (BiO) was prepared by chemical methods, analysed for its BiO contents and then studied by electron diffraction. The structure of this was found to be of cubic, NaCl type, with  $a_0 \simeq 5.7 \text{ \AA}$ . The epitaxial growth of BiO showed the development of 2-d {100} and 2-d {110} orientations respectively on the cube face and the (110) face of rock salt. On mica a 2-d {111} orientation and a super-structure with  $a_0$  equal to four times of the usual structure was noted. It was also noted that under high vacuum and at a suitable temperature the suboxide usually decomposed into metallic bismuth.

Oxidation of Bi showed various phases depending on the vacuum conditions. Thus at about  $10^{-5}$  mm BiO was formed. With the gradual decrease of vacuum  $\alpha$ -Bi<sub>2</sub>O<sub>3</sub> (monoclinic) then a mixture of  $\alpha$  and  $\gamma$ -Bi<sub>2</sub>O<sub>3</sub> (b.c.c.) followed by purely  $\gamma$ -Bi<sub>2</sub>O<sub>3</sub> and finally the b.c.c. changed to f.c.c. On a (100) face of rock salt, the deposits of Bi<sub>2</sub>O<sub>3</sub> formed were of b.c.c. type under high vacuum, whilst at low vacuum the patterns conformed more to the f.c.c. type. On (110) and (111) faces of rock salt the deposits developed respectively 2-d {110} and 2-d {100} orientations of the b.c.c. structure, the later being rotated by 30°. The oxidation of Bi under varying conditions and the vacuum treatment of Bi<sub>2</sub>O<sub>3</sub> showed that the oxidation process of Bi could be expressed in the following way:





Sb when oxidised under different conditions showed only the formation of  $Sb_2O_3$  and no other phase. The  $Sb_2O_3$  films formed on the cube face of rock salt developed simultaneously various orientations such as 2-d  $\{111\}$ , 2-d  $\{100\}$ , 2-d  $\{211\}$ .

It is worth mentioning here that the growth of the oxide films of Bi and Sb was more or less determined by the nature of the metal film rather than by the substrate. Thus highly 1-d oriented metal films produced highly 1-d oriented oxide films and 2-d oriented metal films when oxidised even after being detached from substrate, yielded 2-d oriented oxide layers.

The structure of  $Sb_2Te_3$  was found to be hexagonal (rhombohedral) type. No evidence could be obtained for a super structure as suggested by some workers. The deposits of  $Sb_2Te_3$  developed 2-d  $\{01.1\}$  + 2-d  $\{00.1\}$  + 2-d  $\{30.\bar{4}\}$  orientations on the cube face of rock salt, while on (110) and (111) faces of rock salt as well as on (0001) faces of mica a 2-d  $\{00.1\}$  orientation was observed. Thick deposits on glass and on mica produced simultaneously a number of 1-d orientations. Whilst  $Sb_2Te_3$  was rhombohedral,  $Sb_2Se_3$  was found to be orthorhombic upto a temperature of about  $350^\circ C$ . Above this temperature, orthorhombic phase changed into a cubic phase with  $a_0 = 5.84 \text{ \AA}$ . The orthorhombic phase developed mostly 2-d  $\{100\}$  + 2-d  $\{110\}$  + 2-d  $\{120\}$  + 2-d  $\{230\}$  on all the faces of rock salt. It was found that

crystallites for all these orientations were rotated by  $90^\circ$  on a cube face of rock salt and by  $60^\circ$  on an octahedral face but no such rotation was observed on the (110) face. The cubic phase developed a 2-d  $\{100\}$  orientation on the cube face as well as on the octahedral face of rock salt, whilst on a (110) face a 2-d  $\{110\}$  orientation was found. On mica the deposits had a lamellar nature.

From the above study though many a results have been obtained about epitaxy and orientations of rhombohedral systems formed on rock salt crystals and mica, it has not yet been possible to determine unequivocally all the factors which lead to the formation of the epitaxial growth. It is well known that high temperature, a close substrate deposit lattice fit, however favour epitaxy. Importance of highly clean surface of the single crystal substrate has also been recognized. But many of our results suggested that neither a scrupulously clean nature of the single crystal substrate nor a very close lattice fit is a necessary condition for the epitaxial growth.

-----

R E F E R E N C E S

- Acharya, H.K., (1948) Ph.D. Thesis, London University.
- Aggarwal, P.S. and Goswami, A., (1958) Z. Naturforsch., 13A, No.10, 835.
- Aggarwal, P.S. and Goswami, A., (1963) Indian J. Pure and Appl. Phys., 1, 366.
- Akishin, P.A., Vilkov, L.V. and Zazorin, E.Z., (1962) J. Phys. Soc. Japan, 17, Suppl.BII, 18.
- Almin, K.E. and Westgren, A., (1941-42) Arkiv. Kemi. Min. Geol., 15B, No.22.
- Amelinckx, S. and Delavignette, P. (1960) Phil. Mag., 5, 729; (1961) Phil. Mag., (G.B.), 6, 601.
- Andrievskii, A.I., Nabitovich, I.D. and Voloschuk, Ya.V. (1963) Soviet Physics Crystallography, 7, No.6, 704.
- Aurivilliams, B. and Sillen, L.G. (1945) Nature, 155, 305.
- Bacon, D.J., Heckscher, F. and Crocker, A.G. (1964) Acta Cryst. (Internat.), 17, Pt.6, 760.
- Bauer, E. (1964) "Single Crystal Films" Ed. Francombe, M.H. and Sato, H. Pergamon Press.
- Baux, M. and Couderc, J.J. (1963) C.R. Acad. Sci. (France), 256, No.10, 2141.
- Becker, R. and Doring, W. (1935) Ann. Phys., 24, 719; (1949) Disc. Faraday Soc., 5 (Crystal Growth), 55.
- Beeching, R. (1936) "Electron Diffraction" Methuen & Co. London.
- Benel, H. (1958) C.R. Acad. (Paris), 247, No.5, 584.
- Bhatnagar, S.S. (1930) J. Indian Chem. Soc., 7, 957.
- Bohotov, I.E. and Fishelova, S.B. (1965) Fiz. Metallov. Metallovedenie (U.S.S.R.), 20, No.3, 462.
- Bonfiglioli, G. and Malvano, R. (1959) Phys. Rev., 115, No.2, 330.

- Borodovyi, V.A. and Layashenko, V.I. (1961) *Ukrayin Fiz. Zh. (U.S.S.R.)*, 6, No.5, 664.
- Bound, M. and Richards, D.A. (1939) *Proc. Phys. Soc.*, 51, 256.
- Bowen, E.G. and Morris-Jones, W. (1932) *Phil. Mag.*, 13, 1029.
- Bozorth, R.M. (1923) *J. Amer. Chem. Soc.*, 45, 1621.
- Bridge, N.K. and Howell, H.G. (1954) *Proc. Phys. Soc.*, 67A, 44.
- Brislee, F.J. (1908) *J. Chem. Soc.*, 93, 154.
- Bryant, P.J., Rhodas, H.U. and Weber, H.A. (1954) *J. Appl. Phys.*, 25, No.10, 1343.
- Bublik, A.I. (1952) *Dokl. Acad. Nauk. S.S.S.R.*, 87, 215.
- Bublik, A.I. and Buntar, A.G. (1957) *Fiz. Metallov i Metallovedenie*, 5, No.1, 53.
- Buerger, M.J. (1936) *Amer. Min.*, 21, 206.
- Buerger, M.J. and Hendricks, S.B. (1937-38) *Z. Krist.*, A98, 1.
- Bunsen, W., Gross, F. and Hermann, K. (1930) *Z. Physik*, 64, 537.
- Burton, W.K. and Cabrera, N. (1949) *Disc. Faraday Soc.*, No.5 (Crystal Growth)
- Burton, W.K., Cabrera, N. and Frank, E.C. (1951) *Trans. Roy. Soc. (London)*, A243, 299.
- Byström, A. (1951) *Nature, London*, 167, 780.
- Capella, L. (1962) *C.R. Acad. Sci. France*, 254, No.7, 1309.
- Colombani, A., Vantier, C. and Huet, P. (1958) *C.R. Acad. Sci. (Paris)*, 247, No.21, 1338.
- Coults, M.D. and Levin, E.R. (1967) *J. Appl. Phys. (U.S.A.)*, 38, No.10, 4039.
- Cowley, J.M. (1953) *Acta. Cryst.*, 6, 516;  
(1956) *Acta. Cryst.*, 9, 397.
- Cowley, J.M. and Rees, A.L.G. (1958) *Reports on Progress in Phys.*, 21, 166.

- Cucka, P. and Barrett, C.S. (1962) Acta Cryst. (International), 15, Pt.9, 865.
- Curie, P. (1885) Bull. Soc. Franc. Miner., 8, 145.
- Davissou, C.J. and Germer, L.H. (1927) Phys. Rev., 30, 705-7.
- Dehlinger, U. (1927) Z. Krist., 66, 108.
- Dihlstrom, K. (1938) Z. anorg. Chem., 239, 57.
- Dihlstrom, K. and Westgren, A. (1937) Z. anorg. Chem., 235, 153.
- Dixit, K.R. (1933) Phil. Mag., 16, 1049.
- Dönges, E. (1951) Z. anorg. Chem., 265, 56;  
(1953) Z. anorg. Chem., 263, 280.
- Ehret, W.F. and Abragson, M.B. (1934) J. Amer. Chem. Soc., 56, 335.
- Evans, D.M. (1950) Ph.D. Thesis, London University.
- Finch, G.I. and Wilman, H. (1937) Erg. Exakt. Naturav., 16, 353.
- Finch, G.I., Wilman, H. and Yang, L. (1947) Disc. Faraday Soc., 1, 144.
- Finch, G.I., Sinha, K.P. and Goswami, A. (1955) J. Appl. Phys., 26, 250.
- Frank, F.C. and van der Merwe, J.H. (1949) Proc. Roy Soc. A193, 205.
- Frenkel, J. (1945) J. Phys. Moscow, 9, 392.  
(1946) "Kinetic Theory of Liquids" Clarendon Press, Oxford.
- Friedrich, W., Knipping, P. and Laue, M. (1912) S.B. Bayer Akad. Wiss, 303.
- Garachuk, V.K. and Nayer, V.A. (1965) IVUZ. Priborostroyenie, 8, 176.
- Ghosh, S.K. and Rajagopalan, N.S. (1963) Physica (Netherlands), 29, No.3, 234.

- Gibbs, J.W. (1878) Collected Works, 1928, Page 325.  
Longmans Green & Co., London.
- Glemser, O. and Filcek, M. (1952) Z. Anorg. u. allgem.  
Chem., 269, 99.
- Goetz, A. and Dodd, L.E. (1935) Phys. Rev., 48, 165.
- Goswami, A. (1954) J. Sci. Indust. Res., 13B, 677.
- Goswami and coworkers
- (a) Goswami, A. and Badachhane, S.B. (1964)  
Indian J. Pure and Appl. Phys., 2, No. 3, 250.
  - (b) (1965) Ph.D. Thesis, University of Poona,  
by N.G. Dhere under the guidance of Dr. A. Goswami.
- Goswami, A. and Trehan, Y.N. (1956) Trans. Faraday Soc.,  
52, 353.
- Gross, F. (1930) Z. Physik, 64, 520.
- Harman, T.C., Paris, B. and Goering, H.L. (1956)  
Electrochem. Soc. Meeting, Cleveland, Ohio.
- Herz, W. (1915) Z. Anal. Chem., 54, 103.
- Herz, W. and Guttman, A. (1907) Zeit. Anorg. Chem.,  
53, 63.
- Hirth, J.P., Hruska, S.J. and Pound, G.M. (1964)  
"Single Crystal Films" Ed. Francombe, M.H. and Sato, H.  
Pergamon Press.
- Hofe, H.V. and Hanemann, H. (1940) Z. Metallk., 32, 112.
- Hume-Rothery, W. (1945) "The Structure of Metals and Alloys"  
London.
- Jaggi, R. (1964) Helv. Physica. Acta (Switzerland),  
37, No. 7-8, 618.
- Jain, A.L. (1959) Phys. Rev., 114, No. 6, 1518.
- Jenkins, R.O. (1935) Proc. Phys. Soc., 47, 109.
- Jette, E.R. and Foote, F. (1935) J. Chem. Phys., 3, 605.
- Kahler, H. (1921) Phys. Rev., 18, 210.
- Kirchner, F. (1932) Z. Phys., 35, 172.  
(1932) Ergb. Exakt. Naturwiss., 11, 641.

- Kokosh, G.V. and Sinani, S.S. (1960) Fiz. Tverdogo. Tela., 2, No.6, 1118.
- Kolomiets, B.T. and Goryunova, N.A. (1955) Z. Tech. Fiz., 25, No.6, 984 (In Russian).
- Kolomiets, B.T., Lyubin, V.M. and Tarkhin, D.V. (1959 A) Fiz. Tverdogo. Tela., 1, No.6, 899.
- Kolomiets, B.T. and Zeinally, A. Kh. (1959 B) Fiz. Tverdogo. Tela., 1, No.6, 979.
- Kosevich, V.M. (1961) Kristallografiya (U.S.S.R.), 6, No.3, 475 (In Russian).
- Kossel, W. (1927) Nachr. Ges. Weiss. Göttingen, 135;  
(1928) Quantentheorie und Chemie, p.46, Leipzig.
- Krebs, H., Schultze-Gebhardt, F. and Thees, R. (1955) Z. anorg. Chem., 232, 177.
- Kurov, G.A. and Pinsker, Z.G. (1956) Kristallografiya, 1, No.4, 407.
- Lavrentev, F.F., Soifer, L.M. and Startsev, V.I. (1960) Soviet Physics-Crystallography, U.S.A., 5, No.3, 449.
- Lu, S.S. and Chang, Y.L. (1941) Proc. Phys. Soc., 53, 517.
- Makedonskii, V.L. and Pustovoit, A.K. (1963) Fiz. Tverdogo. Tela. (U.S.S.R.), 4, No.8, 1490 (English Translation).
- van der Merwe, J.H. (1964) "Single Crystal Films"  
Ed. Francombe, M.H. and Sato, H., Pergamon Press.
- Mesnard, G., Uzan, R. and Vicario, E. (1964) Rev. Opt. (France), 43, No.6, 273.
- Mooser, E. and Pearson, W.B. (1957) J. Electronics, 2, No.4, 406.
- Mugge, O. (1903) News. Jahrb. Min. Beil-Bd, 16, 335.
- Natta, G. and Baccaredda, M. (1933) Z. Krist., 85, 271.
- Palatnik, L.S. and Kosevich, V.M. (1960 A) Kristallografiya, 3, No.6, 716 (English Trans.);  
(1960B) Kristallografiya, 4, No.5, 633. (English Trans.).
- Pandya, N.S. and Balsubramanian, A.P. (1963) Indian J. Pure and Appl. Phys., 1, No.7, 266.

- Pashley, D.W. (1956) *Phil. Mag.*, 5(Suppl.), 173.
- Piggott, M.R. and Wilman, H. (1958) *Acta Cryst.*, 11, 93.
- Pinsker, Z.G. (1953) "Electron Diffraction" Butterworth, London.
- Pinsker, Z.G., Semiletov, S.A. and Belova, E.N. (1956) *Dokl. Acad. Nauk. S.S.S.R.*, 106, No.6, 1003.
- Raether, H. (1951) *Erg. Exakt. Naturav.*, 24, 54;  
(1957) *Handbuch der Physik* (Ed. S. Flugge) 32, 443,  
(Berlin, Göttingen, Heidelberg:Springer-Verlag).
- Ramazanov, K.A. (1961) *Fiz. Tverdogo. Tela* (U.S.S.R.),  
3, No.8, 2259.
- Rhodin, T.N. and Walton, D. (1964) "Single Crystal Films"  
Ed. Francombe, M.H. and Sato, H. Pergamon Press.
- Rodot, H. and Weill, M.G. (1960) *J. Phys. Radium* (France),  
21, No.5, 502.
- Royer, L. (1928) *Bull. Soc. Franc. Min.*, 51, 7.
- Ruedl, E. (1959) *Vacuum*, 7, No.8, 56.
- Sawaki, T. (1958) *Sci. of Light* (Japan), 7, No.1, 18.
- Schneider, (1853) *Ann. Phys. Chem.*, 88, 55;  
(1898) *J. Pr. Chem.*, 58, 562.
- Schulz, L.G. (1951 a) *J. Chem. Phys.*, 19, 504.  
(1951 b) *Acta Crysta.*, 4, 437.
- Schumb, W.C. and Rittner, R.S. (1943) *J. Am. Chem. Soc.*,  
65, 1055.
- Sella, C., Miloche, M. and Dugue, M. (1964) *Electron  
Microscopy, A Publication of the Czechoslovak Academy  
of Sciences.*
- Semiletov, S.A. (1956) *Kristallografiya*, 1, 403.
- Semiletov, S.A. (1957) *J. Sci. & Ind. Res.*, 16A, 377.
- Shimaushi, M. (1960) *Sci. of Light* (Japan), 9, No.3, 109.
- Short, M.A. and Schott, J.J. (1965) *J. Appl. Phy.* (U.S.A.),  
36, No.2, 659.
- Sillen, L.G. (1937) *Arkiv. Kemi. Mineral Geol.*, 12A,  
No.18, 1.



- Skubenko, A.F. (1960) *Ukranian Fiz. Zh. (U.S.S.R.)*, 5, No.6, 781.
- Smith, G.E. and Wolfe, R. (1962) *J. Appl. Phys. (U.S.A.)*, 33, No.3, 841.
- Soifer, L.M. and Startsev, V.I. (1960) *Dokl. Acad. Nauk. S.S.S.R.*, 134, No.4, 795.
- Stoyanova, I.G. (1956) *Dokl. Akad. Nauk. S.S.S.R.*, 106, No.3, 437.
- Stranski, I.N. (1928) *Z. Phys. Chem.*, 136, 259;  
(1949) *Disc. Faraday Soc.*, No.5(Crystal Growth) p.13.
- Swanson, H.E., Fuyat, R.K. and Ugrinic, G.M. (1955) *Nat. Bur. Standards, Circular 539*, 4, 33.
- Takagi, M. (1956) *J. Phy. Soc. Japan*, 11, No.4, 396.
- Tanatar, S.M. (1901) *Zeit. Anorg. Chem.*, 27, 304 & 437.
- Tanuma, S. (1959) *J. Phys. Soc. (Japan)*, 14, No.9, 1246.
- Tatarinova, L.I. (1960) *Kristallografiya*, 4, No.5, 637.  
(English Trans.).
- Thomson, G.P. (1928) *Proc. Roy. Soc.*, A117, 600;  
(1928) *Proc. Roy. Soc.*, 119, 651.
- Thomson, G.P. and Cochrane, W. (1939) "The Theory and Practice of Electron Diffraction" London, Macmillan.
- Tideswell, N.W., Kruse, F.H. and McCullough, D.J. (1957) *Acta Cryst.*, 10, 99.
- Treubert, F. and Venino, L. (1914) *Z. anorg. Chem.*, 53, 564.
- Trzebiaowski, W. and Bryjak, E. (1938) *Z. anorg. Chem.*, 238, 255.
- Tutor, A.E.H. (1926) "Crystalline Form and Chemical Constitution" London.
- Vainshtein, B.K. (1964) "Structure Analysis by Electron Diffraction" Pergamon Press, N.Y.
- Volmer, M. (1939) "Kinetik der Phasenbildung", Steinkopff, Dresden und Leipzig.
- Wallerant, F. (1902) *Bull. Soc. Franc. Min.*, 25, 180.

- Wilman, H. (1943a) Proc. Phys. Soc. (London), 60, 341;  
(1943b) Proc. Phys. Soc. (London), 61, 416.  
(1949) Research, 2, 352.  
(1952) Acta Cryst., 5, 782.
- Wilman, H. and Evans, D.M. (1952) Acta Cryst., 5, 731.
- Wright, D.A. (1953) Nature, London, 181, 34.
- Wulff, G. (1901) Z. Kristallogr., 34, 29.
- Wyckoff, R.W.G. (1931) "Structure of Crystals" New York;  
(1935) *ibid*;  
(1964) *ibid*, (Second Edition) p. 27,  
Interscience Publishers.
- Zavyalova, A.A., Pinsker, Z.G. and Imamov, R.M. (1964)  
Kristallografiya (U.S.S.R.), 9, No.6, 857 (In Russian);  
(1965) Kristallografiya (U.S.S.R.), 10, No.4, 480  
(In Russian).
- Zorll, U. (1954) Z. Phys., 139, No.5, 649.
-